



University of
Stavanger

FACULTY OF SCIENCE AND TECHNOLOGY

MASTER'S THESIS

Study program/Specialization: Petroleum Engineering/Drilling Technology	Spring semester, 2018 Open
Author: Tofig Zeynalov	<u>Tofig</u> (Signature of author)
Supervisor(s): Mesfin Belayneh	
Title of master's thesis: <i>Effect of Boron nitride (BN) and surface modified BN on the properties of laboratory water-based drilling fluid formulated in Duovis/XG polymers: Experimental and Simulation studies.</i>	
Credits (ECTS): 30	
Keywords: <i>Drilling fluid</i> <i>Boron Nitride nanoparticle</i> <i>Duovis</i> <i>Xanthan Gum</i> <i>Grafting</i> <i>Tribology</i> <i>Viscoelasticity</i>	Number of pages: 138 + Supplemental material/other: 16 Stavanger, 15/06/2018

ACKNOWLEDGMENT.

I would like to seize this opportunity to express my gratitude to those who supported and motivated me throughout this project. First of all, I want to thank Professor Mesfin Agonafir Belayneh for his supervision and guidance at each stage of the work. You have always had your door open for the students regardless of the time. Your attention and dedication pushed me so many times when I needed it the most. I can genuinely say that this project could not have been implemented without your knowledge and awareness.

My gratitude is also extended to the administration of the University of Stavanger for providing their facilities for the involved experimental and simulation studies.

Last but not least, I would like to thank my family and my friends for their moral support. Special gratitude is expressed to my friend Steinar Aarnes who has been with me from the very beginning of the project and put his valuable insight and recommendations, which have improved the quality of this paper.

ABSTRACT.

Properly designed drilling fluid is one of the key factors for efficient and safe drilling operations. Oil-based muds (OBMs) are more extensively used to drill in deeper and harsher environments, where the fluid stability and properties are of major importance. However, economic and environmental considerations limit competitiveness of OBMs. Consequently, there is a current demand to customize the properties of water-based mud by introducing innovative additives.

Due to unique mechanical, chemical, thermal and tribological features, nanoparticles revolutionized the number of conventional technologies of energy industries including Petroleum industry. Among other contributions to the upstream domain, the nano-sized particles can enhance drilling fluid properties and hence reduce problems associated with excessive torque and drag, insufficient hole cleaning, borehole instability and fluid loss.

The thesis evaluates the performance of micro-sized (150-300nm) Boron nitride (BN) particles in the laboratory formulated WBM. The effect of mentioned additives on the drilling fluid was examined in the dry state as well as in oil grafted condition and coupled with oil lubricant. Results obtained from the experimental and simulation investigation are highlighted as:

- ❖ 0.03 wt.% of dry BN reduced the coefficient of friction (CoF) of Duovis-based fluid by 24%.
- ❖ 0.2 wt.% of grafted BN reduced CoF of Xanthan Gum (XG)-based fluid by 44%.
- ❖ 0.3 wt. % of BN along with a lubricant reduced the CoF of XG-based fluid by 54%.
- ❖ 0.3 wt.% of BN along with a lubricant improved the lubricity of the Duovis-based fluid containing 0.02 wt.% of MWCNT-OH by 53%.
- ❖ Grafted BN and BN along with a lubricant increased the plastic viscosity.
- ❖ BN along with a lubricant at the concentration of 0.3 wt.% reduced filtrate volume by 12%.
- ❖ Sonication had an adverse effect on the lubricating properties of nanofluids.
- ❖ High pH yielded lower coefficient of friction of the nanofluids.
- ❖ The addition of 0.3 wt.% of dry BN in the Duovis-based fluid reduced the pressure loss in circulating loop by average 32%.
- ❖ The addition of 0.3 wt.% of BN along with a lubricant in XG-based fluid allowed to extend the well length by 18%.
- ❖ The addition of 0.2 wt.% of grafted BN Duovis-based fluid decreased the flow rate required for cuttings carriage in the horizontal section by 31%.

Contents

ACKNOWLEDGMENT.....	2
ABSTRACT.....	3
LIST OF FIGURES.....	8
LIST OF TABLES.	10
NOMENCLATURE.	11
1. INTRODUCTION.....	13
1.1. Background.....	13
1.2. Problem formulation.....	15
1.3. Scope and objective.	15
1.4. Research methods.....	16
2. THEORY.	17
2.1. Fluid Rheology.	17
2.1.1. Rheological models.....	19
2.1.1.1. Newtonian Fluid.	19
2.1.1.2. Non-Newtonian Fluids.....	20
2.1.1.2.1. Bingham Plastic Model.....	22
2.1.1.2.2. Power Law Model.....	23
2.1.1.2.3. Herschel-Bulkley model.....	24
2.1.1.2.4. Robertson-Stiff model.....	24
2.1.1.2.5. Unified Model.	25
2.2. Viscoelasticity.	26
2.2.1. Oscillatory amplitude sweep test.	29
2.3. Drill string mechanics.	30
2.3.1. Torque.....	31
2.3.2. Drag.....	32
2.4. Hydraulics model.	32
3. LITERATURE STUDY.	36
3.1. Nanoparticles.....	36
3.1.1. Application of Nanoparticles in Petroleum Industry.	36
3.1.1.1. Exploration.	37
3.1.1.2. Production.....	37
3.1.1.3. Reservoir characterization.....	38
3.1.1.4. Drilling Fluids.	38
3.1.1.5. Refining and processing.....	41
3.2. Chemicals ingredients used in this thesis.	41
3.2.1. Nanoparticles.....	41

3.2.1.1.	Nano boron nitride	41
3.2.1.2.	Nano boron nitride grafted with oil.	43
3.2.1.3.	Hydroxyl functionalized multi-walled carbon nanotube (MWCNT-OH).	43
3.2.2.	Bentonite.	45
3.2.3.	Polymers.	47
3.2.3.1.	Duo-Vis.	48
3.2.3.2.	Xanthan Gum.....	48
3.2.4.	KCl salt.....	49
4.	EXPERIMENTAL STUDY.....	50
4.1.	Effect of dry BN powder in Duovis polymer.....	50
4.1.1.	Drilling fluid formulation.....	50
4.1.2.	Lubricity.	51
4.1.3.	Rheology.	53
4.1.4.	Filtration and pH.	55
4.2.	Effect of oil grafted BN in Duovis polymer system.....	57
4.2.1.	Drilling fluid formulation.....	57
4.2.2.	Lubricity.	58
4.2.3.	Rheology.	59
4.2.4.	Filtration and pH.	61
4.3.	Effect of BN/lubricant in Duovis polymer.....	62
4.3.1.	Drilling fluid formulation.....	62
4.3.2.	Lubricity.	63
4.3.3.	Rheology.	64
4.3.4.	Filtration and pH.	66
4.4.	Effect of Dry BN powder in Xanthan gum polymer.	67
4.4.1.	Drilling fluid formulation.....	67
4.4.2.	Lubricity.	67
4.4.3.	Rheology.	68
4.4.4.	Filtration and pH.	70
4.5.	Effect of oil grafted BN in XG polymer system.....	71
4.5.1.	Drilling fluid formulation.....	71
4.5.2.	Coefficient of friction.	72
4.5.3.	Rheology.	72
4.5.4.	Filtration and pH.	74
4.6.	Effect of BN/lubricant in Xanthan gum polymer.....	75
4.6.1.	Drilling fluid formulation.....	75
4.6.2.	Lubricity.	76
4.6.3.	Rheology.	76
4.6.4.	Filtration and pH.	78
4.7.	Effect of nanocomposite (MWCNT-OH + BN/lubricant) in Duovis system.	79
4.8.	Effect of mixing and pH on the lubricity.	81
4.8.1.	Effect of mixing.	81
4.8.2.	Effect of pH.	82

4.9.	Effect of temperature on the rheology of BN nanoparticle treated fluids.	83
4.10.	Viscoelasticity.....	85
4.10.1.	Oscillatory amplitude sweep test for Duovis-based fluids.....	87
4.10.2.	Oscillatory amplitude sweep test for XG-based fluid.	89
5.	SIMULATION STUDY.....	91
5.1.	Rheological modeling.....	91
5.1.1.	Rheological modeling of the Duovis-based fluids.	92
5.1.1.1.	Reference fluid (Duovis)	92
5.1.1.2.	Reference fluid (Duovis) + 0.03 wt.% dry BN.....	94
5.1.1.3.	Reference fluid (Duovis) + 0.2 wt.% grafted BN.	95
5.1.1.4.	Reference fluid (Duovis) + 0.16 wt.% BN/lubricant.	95
5.1.1.5.	Reference fluid (Duovis) + 0.3 wt.% BN/lubricant.	96
5.1.1.6.	Model matching and comparison.....	96
5.1.1.7.	Effect of nano-additives in Duovis system on the rheological parameters.	97
5.1.2.	Rheological modeling of the XG based fluids.....	99
5.1.2.1.	Model matching and comparison.....	100
5.1.2.2.	Effect of nano-additives on the rheological parameters (XG system).....	100
5.2.	Toque and drag simulation.	103
5.2.1.	Simulation setup.	104
5.2.2.	Simulation example.	105
5.2.3.	Simulation result.....	107
5.3.	Hydraulics simulation.....	109
5.3.1.	Simulation setup.	109
5.3.2.	Hydraulic simulation of the Duovis based fluids.....	109
5.3.3.	Hydraulic simulation of the XG based fluids.	111
5.4.	Hole cleaning simulation.	112
5.4.1.	Simulation setup.....	113
5.4.2.	Simulation result.....	113
6.	RESULTS SUMMARY AND DISCUSSION.....	115
6.1.	Effect of dry BN particles.	115
6.1.1.	Dry BN in Duovis biopolymer system.....	115
6.1.1.1.	Dry BN in XG system.	117
6.1.2.	Comparative study of the systems.....	119
6.2.	Effect of grafted BN particles.....	121
6.2.1.	Grafted BN in Duovis system.	121
6.2.2.	Grafted BN in XG system.....	122
6.2.3.	Comparative study of the systems.....	124
6.3.	Effect of BN particles in the presence of a lubricant.	126
6.3.1.	BN/lubricant in Duovis system.....	126
6.3.2.	BN/lubricant in XG system.	127
6.3.3.	Comparative study of the systems.....	129
6.4.	Effect of a nanocomposite.....	130

6.5. Effect of mixing and pH on lubricity.	131
6.6. Effect of temperature on rheology.....	131
7. CONCLUSION.....	133
REFERENCES.....	135
APPENDIX A: Photographs from grafting procedure.	139
APPENDIX B: Amplitude Sweep Measurements of drilling fluids.....	140
APPENDIX C: Effect of temperature on the rheology of drilling fluids.	144
APPENDIX D: Rheological modelling.....	148
APPENDIX E: Setup for Torque and Drag simulations.	152

LIST OF FIGURES.

Figure 1-1: Research methodology	16
Figure 2-1: The Two-Plates-Model to illustrate the velocity gradient [16]	17
Figure 2-2: Illustration of typical rheological behavior of fluids	19
Figure 2-3: Viscosity profile of Newtonian Fluid [19]	20
Figure 2-4: Time-independent rheological behavior.....	21
Figure 2-5: Time-dependent rheological behavior.....	21
Figure 2-6: Viscosity profile of non-Newtonian fluid [25]	22
Figure 2-7: Illustration of the Two-Plates-Model for the oscillatory test (Redrawn from Mezger (2006) [16])	27
Figure 2-8 Plot of the stress and strain curves versus time (Redrawn from Mezger (2006) [16]).....	27
Figure 2-9: Common output from the stress amplitude sweep test showing gel-like behavior.....	30
Figure 2-10: Loads on the segmented drill string (Redrawn from[33]).....	31
Figure 2-11: Frictional pressure losses in circulating system	33
Figure 3-1: (a) SEM image of BN; (b) Structure models of hexagonal BN, rhombohedral BN, wurtzite BN, cubic BN	42
Figure 3-2: Dispersion of Boron nitride nanoparticles [63].....	42
Figure 3-3: (a) BN-Oil sonication; (b) Centrifuge used for BN cleaning.....	43
Figure 3-4: (a) SEM image of MWCNT; (b) structure of MWCNT-OH	44
Figure 3-5: Different types of platelets and bonding between them [69]	46
Figure 3-6: Arrangement mechanism of clay particles [69]	46
Figure 3-7: Polymer structure	48
Figure 3-8: Molecular structure of XG	49
Figure 4-1: CMI tribometer at UiS	52
Figure 4-2: Effect of dry BN (in Duovis) on the coefficient of friction.....	53
Figure 4-3: Effect of dry BN (in Duovis) on the viscometer readings	54
Figure 4-4: Effect of dry BN (in Duovis) on the Bingham parameters.....	54
Figure 4-5: Effect of dry BN (in Duovis) on the Power Law parameters	55
Figure 4-6: Low-pressure filter press.....	56
Figure 4-7: pH meter	57
Figure 4-8: Effect of grafted BN (in Duovis) on the coefficient of friction	59
Figure 4-9: Effect of grafted BN (in Duovis) on the viscometer readings.....	60
Figure 4-10: Effect of grafted BN (in Duovis) on the Bingham parameters	60
Figure 4-11: Effect of grafted BN (in Duovis) on the Power Law parameters.....	61
Figure 4-12: Effect of BN/lubricant (in Duovis) on the coefficient of friction.....	64
Figure 4-13: Effect of BN/lubricant (in Duovis) on the viscometer response	65
Figure 4-14: Effect of BN/lubricant (in Duovis) on the Bingham parameters.....	65
Figure 4-15: Effect of BN/lubricant (in Duovis) on the Power Law parameters.....	66
Figure 4-16: Effect of dry BN (in XG) on the coefficient of friction	68
Figure 4-17: Effect of dry BN (in XG) on the viscometer response	69
Figure 4-18: Effect of dry BN (in Duovis) on the Bingham parameters.....	69
Figure 4-19: Effect of dry BN (in XG) on the Power Law parameters.....	70
Figure 4-20: Effect of grafted BN (in XG) on the coefficient of friction.....	72
Figure 4-21: Effect of grafted BN (in XG) on the viscometer readings.....	73

Figure 4-22: Effect of grafted BN (in XG) on the Bingham parameters.....	73
Figure 4-23: Effect of grafted BN (in XG) on the Power Law parameters	74
Figure 4-24: Effect of BN/lubricant (in XG) on the coefficient of friction	76
Figure 4-25: Effect of BN/lubricant (in XG) on the viscometer response.....	77
Figure 4-26: Effect of BN/lubricant (in XG) on the Bingham parameters	77
Figure 4-27: Effect of BN/lubricant (in XG) on the Power Law parameters	78
Figure 4-28: Effect of MWCNT-OH (in Duovis) on the coefficient of friction.....	79
Figure 4-29: Effect of nanocomposite (in Duovis) on the coefficient of friction.....	80
Figure 4-30: Effect of mixing on the coefficient of friction	82
Figure 4-31: Effect of pH on the coefficient of friction	82
Figure 4-32: Viscometer along with the heating cup	83
Figure 4-33: Effect of temperature on the viscometer readings of the nano-containing fluid	84
Figure 4-34: Effect of temperature on the Bingham parameters	84
Figure 4-35: Effect of temperature on the Power Law parameters.....	85
Figure 4-36: Rheometer	87
Figure 4-37: Plot of amplitude sweep measurements for the base fluid (Duovis)	88
Figure 4-38: Effect of the nano-additives on the flow point (Duovis).....	88
Figure 4-39: Plot of amplitude sweep measurements for the base fluid (XG).....	89
Figure 4-40: Effect of the nano-additives on the flow point (XG)	90
Figure 5-1: Modelled trend-lines along with measured data for the Base fluid (Duovis).....	93
Figure 5-2: Modelled trend-lines along with measured data for the “Base fluid + 0.03 wt.% dry BN” (Duovis).....	94
Figure 5-3: Deviation of the rheological models from the measured data (Duovis-based samples)....	96
Figure 5-4: Deviation of the rheological models from the measured data (XG-based samples).....	100
Figure 5-5: Well setup for the Torque&Drag simulations	104
Figure 5-6: Drag loads and limits for the “Base fluid” and the “Base fluid + 0.3 wt.% BN/lub”	106
Figure 5-7: Torque loads and limits for the “Base fluid” and the “Base fluid + 0.3 wt.% BN/lub”	106
Figure 5-8: Stresses and limits for the “Base fluid” and the “Base fluid + 0.3 wt.% BN/lub”	107
Figure 5-9: Effect of nano-additives on the simulated well length (Duovis).....	108
Figure 5-10: Effect of nano-additives on the simulated well length (XG)	108
Figure 5-11: Effect of nano-additives (in Duovis) on the pressure loss.....	110
Figure 5-12: Effect of nano-additives (in Duovis) on the ECD	110
Figure 5-13: Effect of nano-additives (in XG) on the pressure loss	111
Figure 5-14: Effect of nano-additives (in XG) on the ECD	112
Figure 5-15: Simulation setup for the hole cleaning simulations.....	113
Figure 5-16: Effect of nano-additives (in Duovis) on the minimum flow rate for cuttings transport .	114

LIST OF TABLES.

Table 2.1: Behavior classification from oscillatory test [16]	29
Table 2.2: Summary of equations used in the Unified model [37]	35
Table 3.1: Chemical composition of commercial bentonites [73]	45
Table 4.1: Formulation of drilling fluids containing dry BN (in Duovis)	51
Table 4.2: Effect of dry BN (in Duovis) on the filtration	56
Table 4.3 Effect of dry BN (in Duovis) on the pH.....	57
Table 4.4: Formulation of drilling fluids containing grafted BN (in Duovis).....	58
Table 4.5: Effect of grafted BN (in Duovis) on the filtration.....	61
Table 4.6: Effect of dry BN (in Duovis) on the pH.....	62
Table 4.7: Formulation of drilling fluids containing BN along with oil (in Duovis).....	63
Table 4.8: Effect of BN/lub (in Duovis) on the filtration.....	66
Table 4.9: Effect of BN/lub (in Duovis) on the pH	67
Table 4.10: Formulation of drilling fluids containing dry BN (in XG).....	67
Table 4.11: Effect of dry BN (in XG) on the filtration	70
Table 4.12: Effect of dry BN (in XG) on the pH.....	71
Table 4.13: Formulation of drilling fluids containing grafted BN (in XG)	71
Table 4.14: Effect of grafted BN (in XG) on the filtration	74
Table 4.15: Effect of grafted BN (in XG) on the pH	75
Table 4.16: Formulation of drilling fluids containing BN/lub (in XG)	75
Table 4.17: Effect of BN/lub (in XG) on the filtration	78
Table 4.18: Effect of BN/lub (in XG) on the pH.....	79
Table 4.19: Drilling fluids used for viscoelasticity measurements	86
Table 5.1: Duovis-based drilling fluids used for rheological modelling.....	92
Table 5.2: Modelled equations for the Base fluid (Duovis).....	93
Table 5.3: Modelled equations for the “Base fluid + 0.03 wt.% dry BN” (Duovis).....	94
Table 5.4: Modelled equations for the “Base fluid + 0.2 wt.% grafted BN” (Duovis)	95
Table 5.5: Modelled equations for the “Base fluid + 0.16 wt.% BN/lub” (Duovis)	95
Table 5.6: Modelled equations for the “Base fluid + 0.3 wt.% BN/lub” (Duovis)	96
Table 5.7: Rheological modelling summary of the Duovis-based fluids.....	97
Table 5.8: XG-based drilling fluids used for rheological modelling	99
Table 5.9: Rheological modelling summary of the XG-based fluids.....	101

NOMENCLATURE.

Acronyms

<i>API</i>	American Petroleum Institute
<i>BF</i>	Base Fluid
<i>BN</i>	Boron Nitride
<i>CMC</i>	Carboxymethyl Cellulose Sodium
<i>COF</i>	Coefficient Of Friction
<i>CT</i>	Computerized Tomography
<i>ECD</i>	Equivalent Circulation Density
<i>EOR</i>	Enhanced Oil Recovery
<i>GTL</i>	Gas-to-Liquids
<i>KSO</i>	Kapok Seeds Oil
<i>LSYS</i>	Lower Shear Yield Stress
<i>LVER</i>	Linear Viscoelastic Range
<i>MD</i>	Measured Depth
<i>MW</i>	Mud Weight
<i>MWCNT</i>	Multiwall Carbon Nanotube
<i>NP</i>	Nano Particle
<i>OBM</i>	Oil-Based Mud
<i>PV</i>	Plastic Viscosity
<i>RPM</i>	Rotation Per Minute
<i>SEM</i>	Scanning Electron Microscope
<i>TVD</i>	True Vertical Depth
<i>VES</i>	Viscoelastic Surfactant
<i>WAG</i>	Water Alternating Gas
<i>WBM</i>	Water-Based Mud
<i>XG</i>	Xanthan Gum
<i>YS</i>	Yield Stress

Variables

<i>A, B, C</i>	Parameters of the Robertson-Stiff model
<i>d</i>	Outer diameter of the drill string
<i>D</i>	Diameter of the wellbore

f	Friction factor
F_i	Axial load per segment
G'	Storage modulus
G''	Loss modulus
k	Consistency index
n	Flow behavior index
N_i	Normal force
N_{Re}	Reynolds number
P_p	Pump pressure
r	Rotation radius
T_i	Torsional load per segment
$\Delta P_{annulus}$	Friction pressure loss in annulus
ΔP_b	Friction pressure loss across bit
ΔP_{fadc}	Friction pressure loss in annulus around drill collar
ΔP_{fadb}	Friction pressure loss in annulus around drill pipe
ΔP_{fdc}	Friction pressure loss inside drill collar
ΔP_{fdp}	Friction pressure loss inside drill pipe
ΔP_{fs}	Friction pressure loss in surface connections
ΔS	Length of segment
θ	Well inclination
φ	Azimuth
μ	Coefficient of friction
ρ	Mud density
ω_i	Weight per segment
β	Buoyancy factor
$\theta_{600,300,6,3}$	Viscometer readings at 600/300/6/3 RPMs
τ	Shear stress
τ_o	Yield stress of Herschel Bulkley model
τ_y	Yield stress of Unified model
γ	Shear strain
δ	Loss angle
μ_p	Plastic viscosity

1. INTRODUCTION.

This thesis aims to evaluate the effect of nanoparticles on properties of water-based drilling fluid. The paramount goal of the study was to enhance the characteristics of the fluid system by introducing nano-sized additives. The performance of the fluids was characterized through experimental study where lubricity, rheology, filtrate volume, pH and viscoelasticity were measured and compared to the nano-free system. Furthermore, the best fluid systems, regarding tribology and rheology, were selected and evaluated through a performance simulation study, which covers rheological modeling, drill string mechanics and hydraulic simulations.

1.1. Background.

Drilling fluids are a vital part of the well construction phase, in which that fluid is pumped from the surface, down the drill string exiting at the bit and back to the surface through the annular space [1]. Drilling fluids are composed of natural and artificial chemicals such as viscosifiers, weighing additives, fluid loss and swelling control additives. The composition of the mud should be adequately designed and formulated to perform effectively under certain well conditions [2]. The primary functions of drilling fluids can be addressed as [3]:

- Bring cuttings from bottom to surface.
- Maintain well pressures.
- Cool and lubricate the drill bit.
- Support the stability of the walls in a wellbore until casing is run or completion equipment is set.
- Minimize the damage of producing zones.
- Transmit hydraulic power to the downhole tools and bit.
- Control corrosion.
- Transmit the signal containing information about the formation.

To fit the purpose, drilling fluids are required to possess particular rheological and lubricating properties, adequately prevent fluid loss, exhibit stable behavior under extreme temperature

and pressure conditions, prevent fluid contamination and comply with HSE requirements [3] [4].

Drilling fluids are commonly categorized as either water-based mud (WBM) or oil-based mud (OBM), according to their foundation [2]. WBM is the most broadly used system (applied in approximately 80% of all wells worldwide [5]) owing to cost availability and environmental friendliness. On the other hand, OBMs are more sustainable to high pressure and high temperature conditions, where WBM can break down and eventually cause viscosity reduction and the decline in fluid loss control [6]. Other advantages of OBM can be mentioned as shale stability, faster penetration rates, maintaining the hole in gauge and superior corrosion protection. In addition, oil-based mud possesses high lubricating properties what minimize the possibility of differential sticking and can potentially increase the length of the wellbore due to reduced torque and drag [6]. At the same time, there are some environmental and economic limitations, which make the utilization of OBM not always feasible. High initial cost and restrictions associated with cuttings discharge and disposal of mud itself led to rising demand for WBM utilization in applications where OBM was previously more preferential [7].

In the last few years, there has been a growing interest in the development and implementation of additives to enhance the properties of water-based mud and develop a fluid which is capable of fulfilling the same characteristics and reliability as oil-based mud does; without compromising environmental concerns [8].

Nanotechnology is a revolutionary concept presented in the Twenty-first century that has been qualified to improve the properties of materials in many fields. Due to the size ranges from 1 to 100 nm, nanoparticles demonstrate particular and novel characteristics [9]. Introducing of nanoparticles to the petroleum industry is considered as a promising application to solve a number of problems in areas such as exploration, drilling, production, EOR, refining and distribution [10]. In the field of drilling fluids, nanotechnology is capable of improving lubricating properties, strengthen the wellbore, reduce the fluid loss, stabilize shale formations, enhance filtrate characteristics at HP/HT conditions [11], [12], [13], [14], [15].

This research is intended to design and provide a comprehensive characterization of nano-enhanced water-based drilling fluid. The effect of Boron nitride nanoparticles on the mud

design was examined in the commercially affordable form as well as in the presence of a lubricant. Furthermore, a novel method was used to functionalize the BN nano powder. This approach holds a promise of being able to improve the lubricating and rheological effect of conventional BN. The properties of the formulated nanofluids were assessed through experimental and simulation studies. The study is to propose the concentration of certain type nanoparticles alone or with accompanying substance that has the ability to perform at conditions where usage of oil-based mud was previously feasible.

1.2. Problem formulation.

As mentioned earlier, the performance of OBM is superior except with the cost and environmental issues. Moreover, nanotechnology showed remarkable results in EOR, cementing and drilling operations, what has attracted much attention from the oil industry. Nanotechnology is therefore believed to have a great potential in solving conventional technology related challenges. The Boron nitride nanoparticles are documented to be a lubricant for solids in contact. This thesis investigates the effect of BN in water-based drilling fluids. The primary issues to be addressed were:

- ✓ Effect of commercial Boron nitride nanoparticles.
- ✓ Effect of grafted BN nanoparticles.
- ✓ Effect of BN nanoparticles together with a lubricant.
- ✓ Compare the performance of aforementioned additives in the fluids with Duovis polymer and Xanthan gum polymer.

1.3. Scope and objective.

The paramount objective of this thesis is to evaluate the performance of Boron nitride nanoparticles on the properties of the water-based mud as well as to find a method to reinforce the impact. The scope of the work includes following activities:

- Review of the theory, which underlies experimental and simulation studies.
- Literature study of the nanoparticles, their application in the petroleum industry and chemical constituent making up the tested drilling fluids.

- Experimental work to investigate the effect of dry BN, grafted BN and BN with oil on the properties of a conventional laboratory formulated water-based mud.
- Simulation study to assess the performance of the most appealing samples.

1.4. Research methods.

Flowchart 1-1 summarizes the methodology of this research. The first part includes the review of the theory for the drilling fluids analysis, introduction to the Nanotechnology, possible applications of it in the Petroleum sector and description of the chemicals making up the experimental samples. The second part implies the experiments to assess the effect of nano-additives on the formulated drilling fluids. Whilst, the last section contains the performance simulation study.

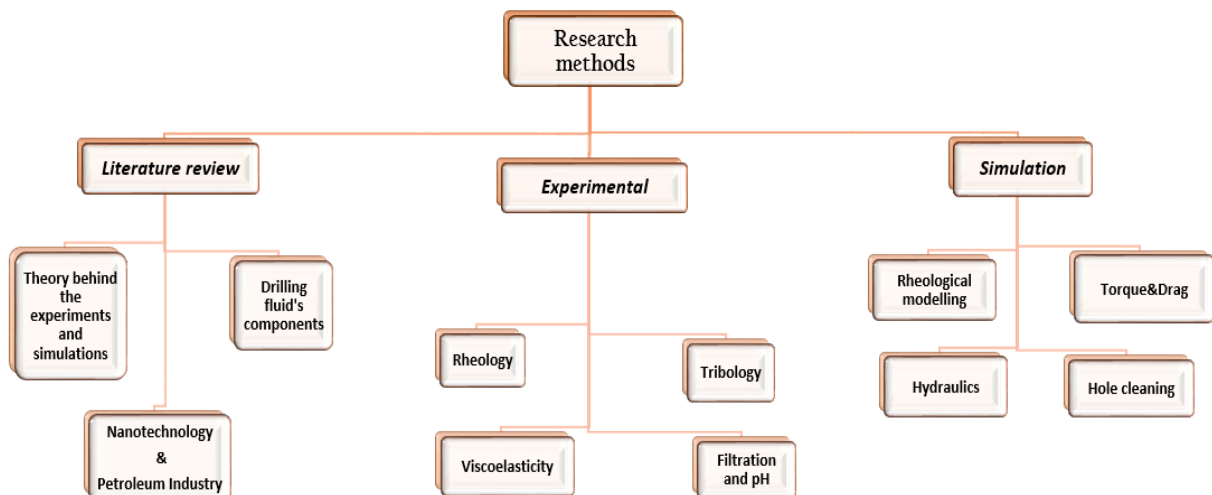


Figure 1-1: Research methodology

2. THEORY.

This chapter outlines the theory used to analyze the experimental data presented in **Chapter 4** as well as interpret the results of simulations in **Chapter 5**.

2.1. Fluid Rheology.

Rheology is a term used to define the flow behavior of liquids as well as deformation behavior of solids. These two physical concepts are referred to the same branch of science because many materials start to flow under high deformation caused by shear forces [16]. Prediction of the right rheological properties is crucial for drilling fluid. An appropriately selected rheological model accurately evaluates wellbore hydraulics, characterizes a flow regime under a variety of conditions, estimate swab and surge pressure, estimate the efficiency of hole cleaning, calculate the settling velocity of cuttings [17], [18].

The Two-Plates-Model (**Figure 2-1**) can be deployed for the better understanding of fundamental rheological parameters. Assumptions behind the model [16]:

- The upper plate with surface area A is moving with velocity V under applied force F
- The lower plate is stationary
- The distance between plates h
- The fluid shows adhesion to plates without wall-slip effect
- The flow is laminar

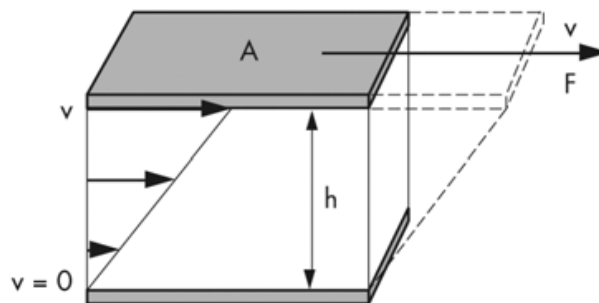


Figure 2-1: The Two-Plates-Model to illustrate the velocity gradient [16]

Shear stress (τ). The shear stress is defined as an applied force acting per unit surface area.

$$\tau = \frac{F}{A} \quad (2.1)$$

The unit of the shear stress is [Pa], (“Pascal”). However, in the industry often used [lbf/100 ft²]

Shear rate (γ). The shear rate is the gradient of velocity, i.e. change in velocity (dv) between two moving layers per difference in distance between that layers (dh). Mathematically it can be presented as:

$$\gamma = \frac{dv}{dh} \quad (2.2)$$

The unit of the shear rate is [1/s] or [s⁻¹].

Viscosity. Viscosity is a rheological term used to define resistance of a fluid to flow. The origin of the resistance is the internal forces between the molecules of the liquid. The small particles in the fluid move relative to each other and this movement always leads to internal friction. In addition, there are some other mechanical and electrostatic forces involved in a process. Hence, any fluid generates a certain resistance to flow, which is regarded as viscosity. For drilling fluids, this parameter is not constant but is the function of temperature, pressure, time and shear stress [16].

Plastic viscosity (μ_p). The plastic viscosity (PV) is a component of the fluid resistance emerged solely due to mechanical friction. This friction is caused by solid-to-solid, solid-to-fluid and fluid-to-fluid interactions. The PV is dependent on the number of solid particles in the fluid system, their size, distribution and shape [19]. The unit of PV is centipoise [cP].

Yield stress (τ_y). The yield stress (YS) is a component of flow resistance occurred due to electrochemical forces. High YS value is associated with strong intermolecular forces. The yield stress presents a minimum value of applied pressure to launch the flow. The field unit is [lbs/100ft²] [20].

Gel strength (τ_g). The gel strength presents electrochemical forces within the system when the sample is at rest. This property is essential for the drilling fluid since the gel strength determines the ability of the mud to hold the cuttings in suspension when the pumps are turned off. The fluid with adequately designed gel structure minimizes lost circulation issues [21].

2.1.1. Rheological models.

Rheological behavior of the fluids is categorized into two basic type, namely *Newtonian* and *non-Newtonian*. There are several models proposed in the literature to delineate the rheology of non-Newtonian fluids. Some of those models along with the Newtonian model are depicted in **Figure 2-2**.

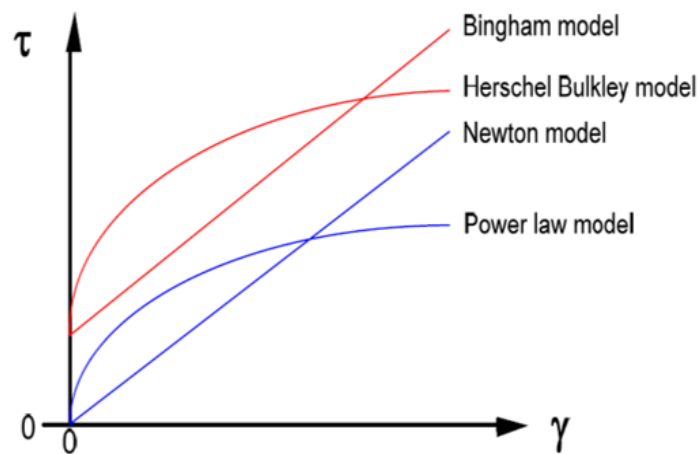


Figure 2-2: Illustration of typical rheological behavior of fluids

2.1.1.1. Newtonian Fluid.

A Newtonian model describes the fluids, which exhibit the linear relationship between shear rate and shear stress. The flow behavior is determined by a single term – viscosity, which remains constant for a set temperature and pressure, regardless of applied shear rate. Common Newtonian fluids can be listed as water, gases and light oils. The equation below expresses the rheological behavior of Newtonian fluids [19]:

$$\tau = \mu\gamma \quad (2.3)$$

Where:

- γ = shear rate
- τ = shear stress.
- μ = viscosity, which is determined from the slope of the shear stress - shear rate graph as illustrated in **Figure 2-3**.

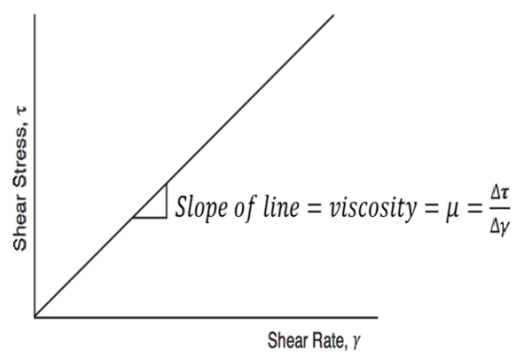


Figure 2-3: Viscosity profile of Newtonian Fluid [19]

2.1.1.2. Non-Newtonian Fluids.

Behavior of the fluid, which does not exhibit constant viscosity, is described by the non-Newtonian model. The viscous properties of non-Newtonian fluids are a function of shear stress and/or the prevailing shear rate or shear history. The rheological behavior of Non-Newtonian Fluids can be either time-dependent or time-independent.

The Non-Newtonian fluids, which do not have a memory of their past history (time-independent), can be categorized regarding dependency of the viscous parameter on the shear rate (**Figure 2-4**). The class of fluids, which shows a decrease of apparent viscosity with increasing shear rate, is categorized as *pseudoplastic* or *shear-thinning*. The fluids are classified as being *dilatant* or *shear-thickening* if increased shear rate yields an increase of apparent viscosity [22].

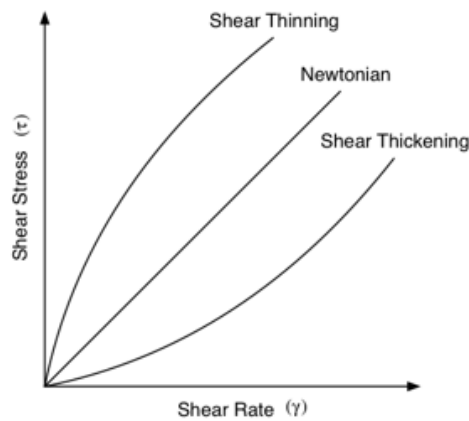


Figure 2-4: Time-independent rheological behavior

The time-dependent Non-Newtonian Fluids can be divided into two types, depending on the response over a period of time when the sample is sheared at a constant rate (**Figure 2-5**). When the apparent viscosity of the fluid decreases with time, the fluid is categorized as *thixotropic*. On the other hand, the behavior is termed as *negative thixotropy* or *rheopectic*, when apparent viscosity becomes higher with time [23]. Cement and most of the drilling fluids are examples of Non-Newtonian fluid and mainly exhibit thixotropic and shear-thinning behavior [24].

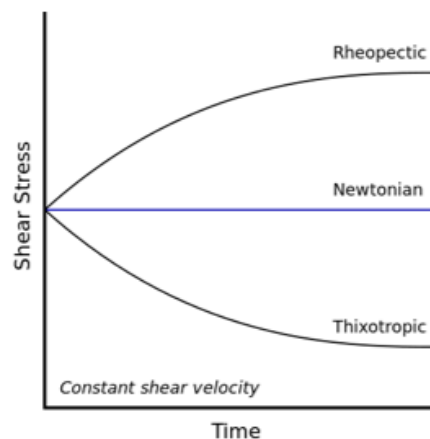


Figure 2-5: Time-dependent rheological behavior

Nevertheless, for Non-Newtonian Fluids, there exist a section at high shear rates (*“Upper Newtonian region”*) and low shear rates (*“Lower Newtonian region”*) (**Figure 2-6**) whereby viscosity does not depend or depends insignificantly on shear rate, and a region of strong dependency between those sections [25].

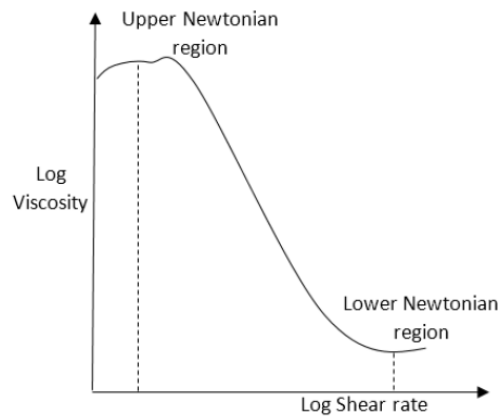


Figure 2-6: Viscosity profile of non-Newtonian fluid [25]

The following models are the most suitable to describe the rheological behavior of non-Newtonian fluids:

1. Bingham Plastic
2. Power Law
3. Herschel-Bulkley model
4. Robertson-Stiff model
5. Unified model

2.1.1.2.1. Bingham Plastic Model.

This model assumes minimum shear stress, defined as yield point (τ_y), which needs to be surpassed to launch the flow. Beyond this point the behavior is in accordance with Newtonian fluid, i.e. shear stress and shear rate are directly proportional, with the constant of proportionality known as the plastic viscosity, μ_p . The model can be represented as [17]:

$$\tau = \tau_y + \mu_p \cdot \gamma \quad (2.4)$$

The plastic viscosity (μ_p) and yield stress (τ_y) are obtained from viscometer readings using following equations:

$$\mu_p = PV[cP] = \theta_{600} - \theta_{300} \quad (2.5)$$

$$\tau_y = YS[lbf/100sqft] = \theta_{300} - \mu_p = 2 \cdot \theta_{300} - \theta_{600} \quad (2.6)$$

2.1.1.2.2. Power Law Model.

The Power Law or the Ostwald-de Waele model is a two-parameter model that describes a fluid without yield stress. It assumes that the flow initiates immediately after the shear stress has been applied. Mathematically model can be expressed as [17]:

$$\tau = k \cdot \gamma^n \quad (2.7)$$

Where, the viscosity index is replaced by the coefficient of consistency, k [lbf·sec ^{n} /100ft²]; and shear thinning tendency is expressed by flow behavior index, n [25]. The parameters can be calculated from the linearized general equation, which takes the following form:

$$\log \tau = \log k + n \cdot \log \gamma \quad (2.8)$$

Where n is measured from the slope and k is intercept.

These parameters can also be estimated from the Fann viscometer data using the following equations:

$$n = 3.32 \cdot \log \left(\frac{\theta_{600}}{\theta_{300}} \right) \quad (2.9)$$

$$k = \frac{\tau}{\gamma^n} = \frac{\theta_{600}}{1022^n} \quad (2.10)$$

Almost all non-Newtonian fluids are shear thinning ($n < 1$) meaning that effective viscosity decreases with the growth of shear rate. However, for some concentrated suspensions, effective viscosity increases with increasing shear rate. As mentioned earlier, they are regarded as shear thickening and can be distinguished by flow behavior index larger than one ($n > 1$). When $n = 1$, the liquid behavior corresponds to the Newtonian fluid [26],[27].

The Power Law model does not take into account the yield stress what adds more uncertainties in rheological calculations of a real fluid [17].

2.1.1.2.3. Herschel-Bulkley model.

The Herschel-Bulkley (H-B) model is a three-parameter model, which is yielded Power Law model. Drilling fluid have yield stress, and exhibits shear thinning behavior. Therefore, H-B model describes the drilling fluid behavior better than the Power Law and the Bingham plastic models. Mathematically the model is given as [28]:

$$\tau = \tau_o + k \cdot \gamma^n \quad (2.11)$$

The k and n parameters can be measured by converting **Equation 2.11** into the logarithmic form (**Equation 2.12**) and plotting $\log(\tau - \tau_o)$ versus $\log \gamma$ what gives a straight line with intercept $\log k$ and slope n [25].

$$\log(\tau - \tau_o) = \log k + n \cdot \log \gamma \quad (2.12)$$

The yield stress is calculated from the equation below [29]:

$$\tau_o = \frac{\tau^{*2} - \tau_{min} \cdot \tau_{max}}{2\tau^* - \tau_{min} - \tau_{max}} \quad (2.13)$$

Where τ^* is linearly interpolated from the corresponding shear rate value, γ^* :

$$\gamma^* = \sqrt{\gamma_{min} \cdot \gamma_{max}} \quad (2.14)$$

2.1.1.2.4. Robertson-Stiff model.

The Robertson-Stiff model adequately characterizes the rheological behavior of the most drilling fluids and cement slurries; however, it is not widely used in the industry due to complexity. The model is represented by the equation below [30]:

$$\tau = A \cdot (\gamma + C)^B \quad (2.15)$$

The parameters A and B can be regarded as similar to the parameters k and n of Power Law model. The term $(\gamma + C)$ is addressed as “effective shear rate”; where the C parameter is considered to be a correction factor to the shear rate and obtained from the equation below:

$$C = \frac{\gamma_{min} \cdot \gamma_{max} - \gamma^{*2}}{2 \cdot \gamma^* - \gamma_{min} - \gamma_{max}} \quad (2.16)$$

Where γ^* is the shear rate value, which corresponds to the geometric mean of shear stress, τ^* :

$$\tau^* = \sqrt{\tau_{min} \cdot \tau_{max}} \quad (2.17)$$

The modified version of **Equation 2.15** is given as:

$$\log \tau = \log A + B \cdot \log(\gamma + C) \quad (2.18)$$

The abovementioned equation is simplified by replacing $\log(\gamma + C)$ and $\log \tau$ with X and Y respectively, which yields:

$$Y = \log A + B \cdot X \quad (2.19)$$

Thereby, the remaining two parameters (A and B) are read from X vs. Y plot. The obtained straight line has a slope equal to B parameter, whereas A is an intercept [29].

2.1.1.2.5. Unified Model.

This model is an advanced combination of Power Law model what, in its turn, is the determination of the Herschel-Bulkley as well, but the difference between those two is in the estimation of k , n parameters and minimum stress to launch a flow. The general form of the model is [28]:

$$\tau = \tau_{yl} + k \cdot \gamma^n \quad (2.20)$$

Where τ_{yl} is termed as lower shear yield stress and can be computed as:

$$\tau_{yl} = (2 \cdot \theta_3 - \theta_6) \cdot 1.066 \quad (2.21)$$

The k and n parameters are calculated differently for the annular and pipe flow:

$$n_p = 3.32 \cdot \log \left(\frac{2 \cdot \mu_p + \tau_y}{\mu_p + \tau_y} \right) \quad (2.22)$$

$$k_p = 1.066 \cdot \left(\frac{\mu_p + \tau_y}{511^{n_p}} \right) \quad (2.23)$$

Pipe flow

$$n_a = 3.32 \cdot \log \left(\frac{2 \cdot \mu_p + \tau_y - \tau_o}{\mu_p + \tau_y - \tau_o} \right) \quad (2.24)$$

$$k_a = 1.066 \cdot \left(\frac{\mu_p + \tau_y - \tau_o}{511^{n_a}} \right) \quad (2.25)$$

Annular flow

2.2. Viscoelasticity.

This section introduces the general theory of viscoelasticity what will be beneficial for the data interpretation during the experimental study.

Viscoelasticity is the feature of matter, which shows both viscous and elastic properties when exposed to deformation under applied stress. Drilling fluids are categorized as time-dependent and viscoelastic materials. Although during normal operations, the viscous component prevails over the elastic, under infinitesimal deformation, the gel structure exhibits viscoelastic properties. Therefore, the viscous models, like Power Law, Herschel–Bulkley and Unified, may not cover all range of strain, and a viscoelastic model should be implemented for proper evaluation of gel strength and structure, barite sag, solid suspension [21].

The viscoelastic behavior of materials can be assessed by implementing the oscillatory tests (**Figure 2-7**). The fundamentals behind these tests can be explained based on Two-Plates-Model where the specimen is placed between the lower stationary plate and the upper plate, which produces oscillatory motion, thereby inducing shear in the sample [16].

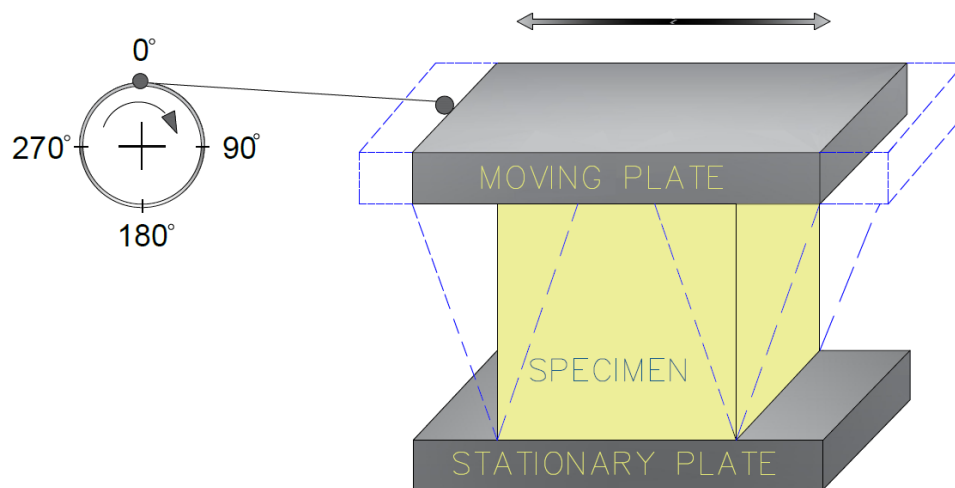


Figure 2-7: Illustration of the Two-Plates-Model for the oscillatory test (Redrawn from Mezger (2006) [16])

During the test, the applied shear causes the sinusoidal deformation, and arising stress in a sample is measured. The figure below depicts stress (τ) and strain (γ) curves plotted against time. The lag time between sine curves is regarded as the phase shift angle or loss angle (δ) [16].

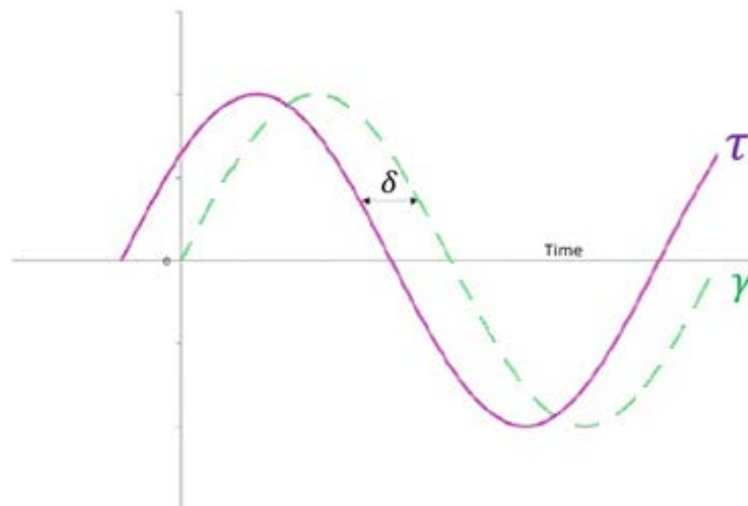


Figure 2-8 Plot of the stress and strain curves versus time (Redrawn from Mezger (2006) [16])

The following equations are used to calculate shear strain and shear stress [21]:

$$\gamma(t) = \gamma_o \sin(\omega t) \quad (2.26)$$

$$\tau(t) = \tau_o \sin(\omega t + \delta) \quad (2.27)$$

$$\tau(t) = \tau_o [\sin(\omega t) \cos \delta + \cos(\omega t) \sin(\delta)] \quad (2.28)$$

$$\tau(t) = \gamma_o \left[\left(\frac{\tau_o}{\gamma_o} \cos \delta \right) \sin(\omega t) + \left(\frac{\tau_o}{\gamma_o} \sin \delta \right) \cos(\omega t) \right] \quad (2.29)$$

$$\tau(t) = [G' \sin(\omega t) + G'' \cos(\omega t)] \quad (2.30)$$

The shear storage modulus (G') measures the ability of a test sample to store the deformation energy and quantifies the elastic behavior of the specimen. On the other hand, the loss modulus (G'') measures the deformation energy and quantifies the viscous behavior [16] :

$$G' = \frac{\tau_o}{\gamma_o} \cos \delta \quad (2.31)$$

$$G'' = \frac{\tau_o}{\gamma_o} \sin \delta \quad (2.32)$$

The ratio of the viscous component and the elastic component is called the loss factor or damping factor ($\tan \delta$) and defined as:

$$\tan \delta = \left(\frac{G''}{G'} \right) \quad (2.33)$$

The loss angle (δ) can be obtained by modifying abovementioned equation:

$$\delta = \tan^{-1} \left(\frac{G''}{G'} \right) \quad (2.34)$$

For viscoelastic materials, the loss angle ranges between 0° (perfectly elastic material) and 90° (perfectly viscous material). At the point where the shear storage modulus and the loss modulus are equal ($\delta = 45^\circ$), the material has the even fractions of viscous and elastic properties. This is the transition point or may also be termed as flow point [16]. **Table 2.1** outlines the behavior characterization of liquids according to the viscoelastic response.

The ideal-viscous flow behavior	The behavior of a viscoelastic liquid	The viscoelastic behavior showing 50/50 ratio of the viscous and elastic portions	The behavior of viscoelastic gel or solid	The ideal-elastic deformation behavior
$\delta = 90^\circ$	$90^\circ > \delta > 45^\circ$	$\delta = 45^\circ$	$45^\circ > \delta > 0^\circ$	$\delta = 0^\circ$
$\tan \delta \rightarrow \infty$	$\tan \delta > 1$	$\tan \delta = 1$	$\tan \delta < 1$	$\tan \delta \rightarrow 0$
$G' \rightarrow 0$	$G'' > G'$	$G' = G''$	$G' > G''$	$G'' \rightarrow 0$

Table 2.1: Behavior classification from oscillatory test [16]

There are several available techniques to perform an oscillatory test, such as amplitude sweep test, frequency sweep test, time sweep test, temperature sweep test. However, in this thesis, the drilling fluid is subjected only to the oscillatory amplitude sweep test.

2.2.1. Oscillatory amplitude sweep test.

The amplitude sweep test is performed at a ramping amplitude of oscillation whilst holding the frequency and the temperature constant. **Figure 2-9** shows the typical output curves from the viscoelastic test of the fluids showing gel-like character. One can distinguish the low shear strain region where the storage and loss modulus exhibits unaltered behavior at different levels. This region is given as straight horizontal lines on the graph and called linear viscoelastic range (LVER). The gradually increased strain results in deviation of these lines from horizontal, and the stress associated with this point is termed as the shear yield stress (τ_y). The point where the lines cross each other ($G' = G''$) is a flow point (τ_{fp}), beyond which the behavior is dominated by viscous forces [16].

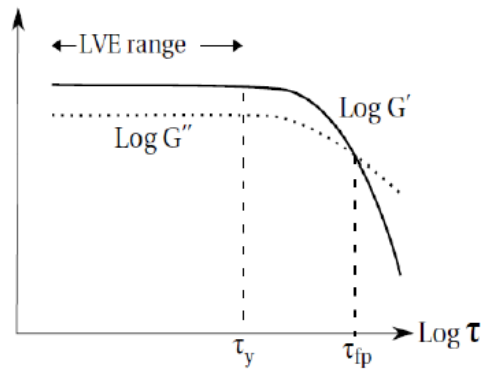


Figure 2-9: Common output from the stress amplitude sweep test showing gel-like behavior.

2.3. Drill string mechanics.

Drill string loads are one of the critical limitations for wellbore trajectory and length. Torque and drag loads are a crucial consideration prior to any drilling operations, which assess the possibility to reach the desired target successfully.

A thorough investigation of torque and drag is an essential basis for well trajectory optimization, calculating the possible well length, selecting the rig with proper hoisting and rotating capabilities, etc. Various reasons can lead to excessive torque and drag, some of which can be listed as differential sticking, tight hole conditions, insufficient hole cleaning leading to cuttings build up, high sliding wellbore friction [19], [31]. However, in the wells, which do not experience any problems related to the hole condition, the sliding friction appears to be the primary source of excessive torque and drag. The sliding friction coefficient is a function of friction force and the normal contact force. In practice, this factor depends on the material and structure of contacting surfaces, as well as on lubrication degree between them [32]. Thus, one of the fundamental functions of drilling mud identified as a reduction of friction to avoid excessive torque and drag, and minimize the wear of equipment [19].

In this section, a general theory of torque and drag will be presented, which underlies further simulation studies. The most popular models for torque and drag prediction consider a division of a drill string into small segments, as shown in the figure below. Each segment is exposed to axial and torsional loads at the ends and transmits increments of these loads to the upper segment, as calculation goes from bottom to the top [19].

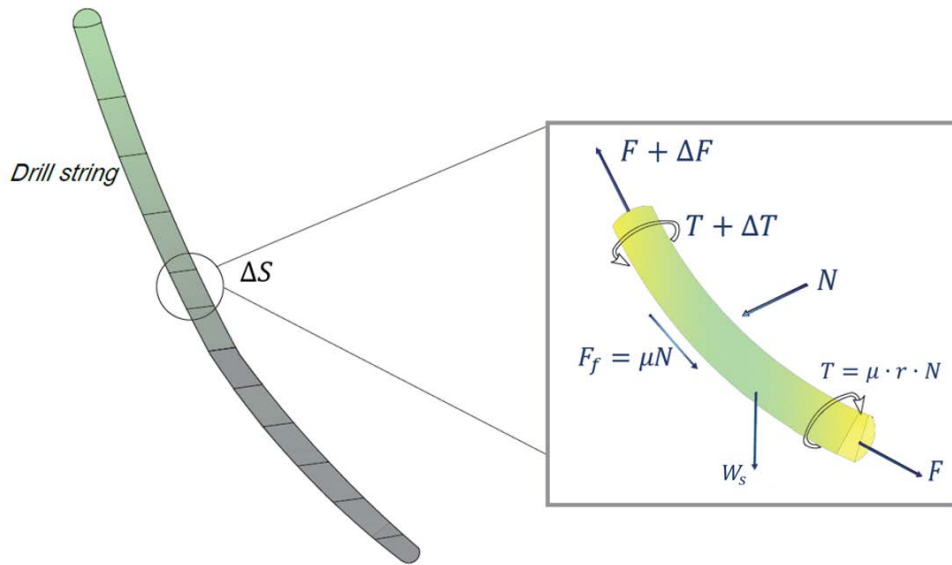


Figure 2-10: Loads on the segmented drill string (Redrawn from[33])

2.3.1. Torque.

Torque is a rotational force required to twist a body. In drilling, torque may be defined as a moment applied to the pipe to transmit rotation to the drill bit. Besides insignificant loss due to viscous forces in drilling fluid, there would not be any torque loss in a perfectly vertical well where there is no contact between the drill string and the surface of formation or casing. On the other hand, in inclined wells, the drill pipe can partially or fully lie on the borehole wall causing great frictional forces. In this case, the torque loss is noticeably high and can seriously affect the drilling program [31].

The value of the torque is affected by rotation radius, normal force over the pipe and coefficient of friction. The increment of each segment to overall torque can be estimated as [34]:

$$\Delta T = \mu_t N_i r \Delta S \quad (2.35)$$

Where:

- μ_t = coefficient of friction
- N_i = normal force
- r = rotation radius
- ΔS = change in length

The torque loss per unit length for buckled and non-buckled string is given as [33]:

$$T_{i+1} = T_i + \sum_{i=1}^n \mu_t r_i N_i (S_{i+1} - S_i) \quad (2.36)$$

2.3.2. Drag.

Drag is defined as the cumulative axial force needed to run the drill string in or out of the hole. Generally, this force is parallel to the gravitational force of the string and depends on the static weight, friction-drag force and direction of the motion. The drag force is given by the following equation [33]:

$$F_{i+1} = F_i + \sum_{i=1}^n \left[\beta \omega_i \cos \left(\frac{\theta_{i+1} + \theta_i}{2} \right) \pm \mu_i N_i \right] (S_{i+1} - S_i) \quad (2.38)$$

Where, F_i is a weight on bit applied on the lowest segment; μ is coefficient of friction; β is buoyancy factor; ω_i is a weight of each segment and N_i is a contact force.

High drag and high torque are associated with each other and normally occurs simultaneously. As was mentioned earlier, the root of excessive torque and drag is considered to be the troublesome wellbore. However, if a good wellbore condition is considered, the origin of excessive torque and drag will be sliding friction, which, in turn, is affected by the normal contact force and coefficient of friction. Therefore, one of the driving forces behind this thesis was to improve the frictional characteristics of drilling muds.

2.4. Hydraulics model.

Drilling hydraulics is mainly associated with the pressure exerted by the drilling mud on different components of the system while circulating. The magnitude of pressure induced by a mud depends on the true depth, fluid characteristics, borehole geometry and whether the liquid in the system is in dynamic or static condition [35].

When the drilling mud is in the static condition, the hydrostatic weight of the fluid column (often termed as bottom hole pressure) is the only component that creates a pressure against the formation. However, while circulating, the fluid generates dynamic friction acting against the direction of the flow and creating additional effective pressure in the annulus. This

pressure increment can be regarded in terms of mud weight and resulted effective density is called equivalent circulating density (ECD) [36]:

$$ECD = MW + \frac{\Delta P_{annulus}}{0.052 \cdot TVD}; \quad [ppg] = [ppg] + \frac{[psi]}{[ft]} \quad (2.39)$$

Or

$$ECD = MW + \frac{\Delta P_{annulus}}{0.0981 \cdot TVD}; \quad [sg] = [sg] + \frac{[bar]}{[m]} \quad (2.40)$$

Where

- $\Delta P_{annulus}$ = pressure drop in the annulus,
- MW = static mud weight and
- TVD = true vertical depth to the point of interest.

The wellbore annulus is not the single part of a circulation system where pressure drops occur, even though it is the only component used for ECD calculations. For a visual representation of main components where losses occur, the reader is referred to **Figure 2-11**.

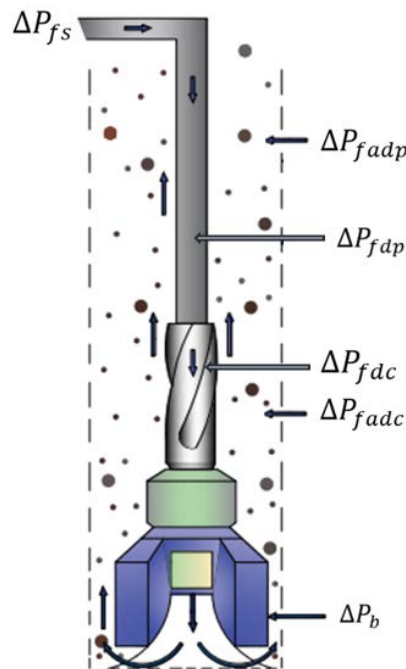


Figure 2-11: Frictional pressure losses in circulating system

In circulation loop, the pump is to overcome frictional drops in the whole drilling arrangement, and the total pump pressure (P_p) is defined as the sum of friction pressure loss, which is given as [19]:

$$P_p = \Delta P_{fs} + \Delta P_{fdp} + \Delta P_{fdc} + \Delta P_b + \Delta P_{fadc} + \Delta P_{fadp} \quad (2.41)$$

Where:

- ΔP_{fs} = friction pressure loss in surface connections
- ΔP_{fdp} = friction pressure loss inside a drill pipe
- ΔP_{fdc} = friction pressure loss inside a drill collar
- ΔP_b = friction pressure loss across a bit
- ΔP_{fadc} = friction pressure loss in the annulus around a drill collar
- ΔP_{fadp} = friction pressure loss in the annulus around a drill pipe

The performance of formulated fluids, in terms of pump pressure and equivalent circulating density, has been evaluated in the simulation part. Despite the diversity of hydraulic models available in the literature, the Unified model was chosen for the study. A reference point in this choice was the study carried out by *Sadigov* [37] who performed the analysis of field and experimental records and showed that Unified model complies better with the measured data. A summary of equations used in the selected model is given in the table below.

Unified model	
Pipe Flow	Annular flow
$\mu_p = R_{600} - R_{300} \cdot [cP] \quad \tau_y = R_{300} - \mu_p \cdot [lbf/100ft^2] \quad \tau_0 = 1.066 \cdot (2 \cdot R_3 - R_6)$	
$n_p = 3.32 \cdot \log\left(\frac{2 \cdot \mu_p + \tau_y}{\mu_p + \tau_y}\right)$	$n_a = 3.32 \cdot \log\left(\frac{2 \cdot \mu_p + \tau_y - \tau_0}{\mu_p + \tau_y - \tau_0}\right)$
$k_p = 1.066 \left(\frac{\mu_p + \tau_y}{511^{n_p}}\right)$	$k_a = 1.066 \left(\frac{\mu_p + \tau_y - \tau_0}{511^{n_a}}\right)$ $k = [lbf \cdot sec^n/100ft^2]$
$G = \left(\frac{(3 - \alpha)n + 1}{(4 - \alpha)n}\right) \cdot \left(1 + \frac{\alpha}{2}\right)$	
$\alpha = 1$ for pipe	$\alpha = 1$ for annuli
$v_p = \frac{24.51 \cdot q}{D_p^2}$	$v_a = \frac{24.51 \cdot q}{D_2^2 - D_1^2}$ $v = [ft/min]$
$\gamma_w = \frac{1.6 \cdot G \cdot v}{D_R} = [sec^{-1}]$	
$\tau_w = \left[\left(\frac{4 - \alpha}{3 - \alpha}\right)^n \tau_0 + (k \cdot \gamma_w^n)\right] = [lbf/100ft^2]$	
$N_{Re} = \frac{\rho \cdot v_p^2}{19.36 \cdot \tau_w}$	$N_{Re} = \frac{\rho \cdot v_a^2}{19.36 \cdot \tau_w}$
$f_{laminar} = \frac{16}{N_{Re}}$ $f_{transient} = \frac{16 \cdot N_{Re}}{(3470 - 1370 \cdot n_p)^2}$ $f_{turbulent} = \frac{a}{N_{Re}^b}$ $a = \frac{\log(n) + 3.93}{50} \quad b = \frac{1.75 - \log(n)}{7}$	$f_{laminar} = \frac{24}{N_{Re}}$ $f_{transient} = \frac{16 \cdot N_{Re}}{(3470 - 1370 \cdot n_a)^2}$ $f_{turbulent} = \frac{a}{N_{Re}^b}$ $a = \frac{\log(n) + 3.93}{50} \quad b = \frac{1.75 - \log(n)}{7}$
$f_{partial} = (f_{transient}^{-8} + f_{turbulent}^{-8})^{-1/8}$	
$f_p = (f_{partial}^{12} + f_{laminar}^{12})^{1/12}$	$f_a = (f_{partial}^{12} + f_{laminar}^{12})^{1/12}$
$\left(\frac{dp}{dL}\right) = 1.076 \cdot \frac{f_p \cdot v_p^2 \cdot \rho}{10^5 \cdot D_p} = [psi/ft]$ $\Delta p = \left(\frac{dp}{dL}\right) \cdot \Delta L = [psi]$	$\left(\frac{dp}{dL}\right) = 1.076 \cdot \frac{f_a \cdot v_a^2 \cdot \rho}{10^5 \cdot (D_2 - D_1)} = [psi/ft]$ $\Delta p = \left(\frac{dp}{dL}\right) \cdot \Delta L = [psi]$
$\Delta p_{Nozzles} = \frac{156 \cdot \rho \cdot q^2}{(D_{N1}^2 - D_{N2}^2 - D_{N3}^2)^2} = [psi]$	

Table 2.2: Summary of equations used in the Unified model [37]

3. LITERATURE STUDY.

In this chapter, an overview of nanoparticles, their application in the petroleum industry and brief information about the chemical components making up the experimental drilling fluids are given.

3.1. Nanoparticles.

Nanoparticles (NPs) are microscopic materials with a size diapason from 1 to 100 nm. Due to the nano dimensions and the ability to control their behavior, these particles allow to produce the new generation of lightweight materials with ultrahigh strength, improved mechanical, thermal, electronic, optical and magnetic properties [38]. The scale of NPs is in the contiguous area between the clusters and the macroscopic materials. Thus, they exhibit one of a kind effects, such as surface effect, small size effect and quanta size effect, rather than directly exhibit atomic and macroscopic properties [39]. Consequently, nanomaterials possess unique characteristics and have become a field of keen interest for scientific study and commercial exploration [40].

NPs can exist in the form of crystals, powders or clusters and classified based on morphology, size and chemical properties. Some of the most popular categories based on physical and chemical properties can be listed as carbon-based NPs, metal NPs, ceramics NPs, semiconductor NPs, polymeric NPs and lipid-based NPs [41].

In recent years, the application of NPs has gained instant popularity in different fields such as aerospace, medicine, manufacturing and materials, refining, electronics, photography and energy industries. Nanoscience and nanotechnologies have enormous potential in future technologies and are attracting significant and rising investments from governments and industrial companies all over the world [38], [42], [43].

3.1.1. Application of Nanoparticles in Petroleum Industry.

Nanotechnology has found its application in almost all branches of industry, from consumer electronics to healthcare and telecommunications. Even though nanoparticles are not a novel product and have been used for many years in different sectors, many nanomaterial-based products are still in the investigation and lab developmental phase and newly found field

application in oil and gas activities. In recent past, a large number of research and studies have been conducted and proved that nanomaterial-based products can facilitate more efficient, cost-effective and environmentally friendly operations of the petroleum industry [42],[44]. In this section, some applications of nanotechnology in different areas of oil and gas sector will be discussed.

3.1.1.1. Exploration.

As the oil and gas reservoirs becoming shrink and mature, there is a need to conduct exploration activities in more hostile and deep environments. Nanoparticles have superior optical, magnetic and electrical properties, what turns them into an excellent material to implement in nanosensors and imaging contrast agents [45]. A new generation of nanosensors, called “nanodust,” has been deployed in pore space to improve reservoir characterization, fluid-flow monitoring and fluid type recognition [46]. Hyperpolarized silicon NPs are a modern tool for measuring and imaging, claimed by *Song and Marcus (2007)* [47]. Nano-based Computerized Tomography (CT) is able to reflect the tight gas sands, tight shales, and tight carbonates formations where the pore structure is below the “vision” of micro-CT. Moreover, nanomaterials can be applied for geothermal production, due to the high thermal conductivity of nanoparticles [10].

3.1.1.2. Production.

Advantages of nanotechnology during the production phase of the well have been studied by different scientists. *Bhatia and Chacko (2011)* proposed utilization of nanoparticles for recovery of gas from hydrate. They reported that injection of air-suspended self-heating Ni-Fe nanoparticles, at very low concentrations, increases the temperature of formation by 42°C, what leads to decomposition of water cage and release of methane [48]. *Huang et al. (2008)* studied the effect of nanoparticles in the stimulation operation. The results showed that nanoparticles along with conventional viscoelastic surfactant (VES) stabilized fluid viscosity at high temperatures, decrease fluid loss and improve fluid efficiency. Due to nanometer size, nanoparticle modified VES fluid efficiently and entirely cleans up and flows back through pore throat without any damage [49]. Another application of nanotechnology in this stage of well life can be described as protection of production tubing against scale deposition, which is

performed by creating a hydrophobic nano-surface using nano-silicate particles. This surface effectively increases contact angle for water, what reduces the probability of scale formation significantly [50].

3.1.1.3. Reservoir characterization.

The advantage of nanotechnology in enhanced oil recovery (EOR) becoming an important topic, as reservoirs moving towards depletion. Nanoparticles can affect the properties of the reservoir by improvement of surface tension as well as reserves themselves. The viscosity of injected liquid often is lower than the viscosity of the displaced oil. Injection of nanoparticles along with conventional fluid can set the viscosity of the mixture to the desired level, improving by thus the mobility [10]. *Ogolo et al. (2012)* analyzed the application of nano-sized particles of magnesium oxide, aluminum oxide, zinc oxide, zirconium oxide, tin oxide, nickel oxide, hydrophobic silica oxide, silica oxide treated with silane and silica oxide with regard to EOR. The study showed that diesel as a base fluid along with above-mentioned NPs proved to be a valuable nano-agent for enhanced oil recovery, which reduces viscosity and interfacial tension and modifies permeability [51]. *Moradi B. et al. (2015)* carried out an experimental work to see how silica nanoparticles can affect the performance of water alternating gas (WAG) in terms of EOR. The results revealed 20% improvement in recovery factor in comparison with conventional WAG method. The increase of recovery can be regarded in terms of wettability. It was documented that silica NPs altered the wettability of the bulk from oil-wet to water-wet what influence the recovery [52].

3.1.1.4. Drilling Fluids.

Drilling fluid is considered as a crucial aspect of smooth and efficient drilling activities. Performing these operations in previously unreachable locations, under severe temperature and pressure conditions became possible nowadays due to improved characteristics of drilling fluids. Water-based muds are more popular because of being less expensive and less hazardous to the natural environment as compared to oil-based or synthetic-based muds. Nevertheless, the properties of water-based muds are impaired strongly under harsh conditions, and there is a demand to improve characteristics and enhance their usage at new

locations by adding new-generation additives [53]. This section contains a review of some papers where different nanoparticles were used to improve the performance of drilling fluids.

Caldarola et al. (2016) studied the use of barite nanoparticles in water-based drilling fluids and how it can affect the potential horizontal penetration. They conducted the lubricity test of three different mixtures, two of them containing 3 wt.% barite nanoparticles made by different means and one base fluid. Nanofluid prepared through a chemical reaction exhibited better performance in terms of friction as compared to the sample generated using mechanical ball-grinder. Considering the pulling out load with the base fluid as maximum available capacity, it was found that horizontal section could be prolonged to 1124 meters using the mechanically synthesized nanoparticles, while the extension of the well was 1841 meter when the chemical barite NPs were used. Moreover, it was reported an average decrease of rotational torque by 34% and 15% for the fluid with Chemical NPs and Mechanical NPs, respectively. The paper concluded that usage of nanoparticles in WBM could generate a smooth nanofilm on the surface of the metal what decreases the friction. As a result, the reservoir may be penetrated deeper, and better drainage strategy can be achieved, as well as reduction of applied torque leads to decrease in tubular wear [54].

Aforementioned nanoparticles were investigated by *Cedola et al. (2016)* regarding the effect on the loss gradient. In-situ stresses were recreated by hydraulic fracturing cell where the core samples placed and sealed by a rubber sleeve. The fluid was injected in 2 cycles with a ten-minute lag between allowing the fracture to be sealed. The pressure variation curve was plotted against the time curve for each liquid, and readings of breakdown pressure and reopening pressure were documented. Examination of the data revealed that the breakdown pressure for the three cases was about the same value; however, reopening pressure of the sample tested with the fluid containing mechanically generated nano barite was 13% as much as the sample tested with the base fluid. The mud with chemically created particles did not show any vast improvement in fracture sealing ability. The paper found out that by adding barite nanoparticles the number of casing strings may be lessened since there would be a larger area for a casing program; fractures get sealed better allowing more substantial pressures without reopening the crack [55].

Iron oxide (Fe_2O_3) and silica (SiO_2) nanoparticles at different concentrations were also added to the water-based drilling fluid to examine the rheology and the properties of filter cakes at different temperature conditions. Rheological measurements for the fluids containing different concentrations of iron oxide demonstrated that increased amount of these nanoparticles leads to increased yield stress compared to the base fluid; however, this effect is more significant at high temperatures. Besides, samples containing Fe_2O_3 nanoparticles diminished the fluid loss, even at the weak concentration of 0.5% wt. On the other hand, silica nanoparticles added to the mud exhibited an unstable behavior regarding the yield stress fluctuations and had an adverse effect on filtration characteristics [56].

Another iron oxide's nanoparticles, magnetite Fe_3O_4 , were used as an additive to the bentonite-based fluid by Z.Vryzas *et al.* (2016). The study revealed that the experimental fluid with nanoparticles concentration of 0.5% by weight showed a linear relationship between yields stress and temperature, up to 250°F. Apparent viscosity showed growth with the increased temperature in the whole diapason of shear rates. Nanofluid conserved good rheological characteristics at high temperature, what is opposite to the base fluid, and exhibited a significant decline in fluid loss. Use of Fe_3O_4 nano-additives proved to be favorable at HP/HT in terms of filtration losses and ability to create a fine filter cake [53].

Y. Kang *et al.* (2016) studied the effect of silica nanoparticles on a shale wellbore strengthening both for oil-based mud (OBM) and water-based mud (WBM). The research comprised three separate tests, namely spontaneous imbibition, swelling rate and acoustic transit time. It was documented the significant reduction in imbibition amount and swelling rate when WBM was used. They also observed a decline in Young's-modulus reduction of shale caused by filtrate invasion, what indicates that using WBM in combination with silica nanoparticles can strengthen the shale formations and lower wellbore instability issues. On the other hand, the observations for OBM in combination with these nanoparticles were counterproductive, showing negative results concerning filtration, crack propagation and lower Young's modulus of formation as compared to the base fluid. The reason for such phenomena was the better dispersion of particles in WBM and easy plugging of pore throats what prevents filtrate invasion into the formation [57].

3.1.1.5. Refining and processing.

The refining and petrochemical processes are the first areas where nanotechnology has found its practical application and contributed significantly for almost 100 years. Nano-based filters have the ability to exempt a vapor from toxic matters such as oxides of sulfur and nitrogen, related acids and acid anhydrates as well as release mercury from soil and water [46]. A new generation of nanomembranes provides the means for improved separation of tight gas from gasses, removal of metal grains from heavy oil, and GTL (gas-to-liquids) production [45]. Nanocatalyst allowed for the possibility to facilitate difficult transportation and handling of dense and viscous substances such as bitumen and heavy crude oil, by introducing an on-site upgrading [58]. Currently, there is a high focus on designing and development of nanocatalyst for on-site field upgrading in combination with hydrogen/methane production [59].

3.2. Chemicals ingredients used in this thesis.

This section presents the review of chemical components used to prepare experimental drilling fluid. The fluid used in this thesis contains fresh water, nanoparticles, bentonite, polymers and salt.

3.2.1. Nanoparticles.

3.2.1.1. Nano boron nitride.

The crystal structure of boron nitride (BN) is very similar to diamond, graphite, fullerene and other carbon materials. Due to superior properties such as heat resistance, high oxidation resistance, corrosion resistance, low coefficient of thermal expansion and friction reduction abilities, boron nitride found its application in different fields of industry, science and technology. They are considered as potential material for electronic devices, insulator lubricants, gas storage materials, nanocables, heat resistant semiconductors [60], [61].

As can be seen from the SEM image (**Figure 3-1 (a)**), the size range of BN varies from 150 nm to 300 nm. The crystalline structure of these particles can be listed as hexagonal-BN, cubic-BN, BN-nanotubes, rhombohedral-BN, wurtzite-BN and BN-cages [62].

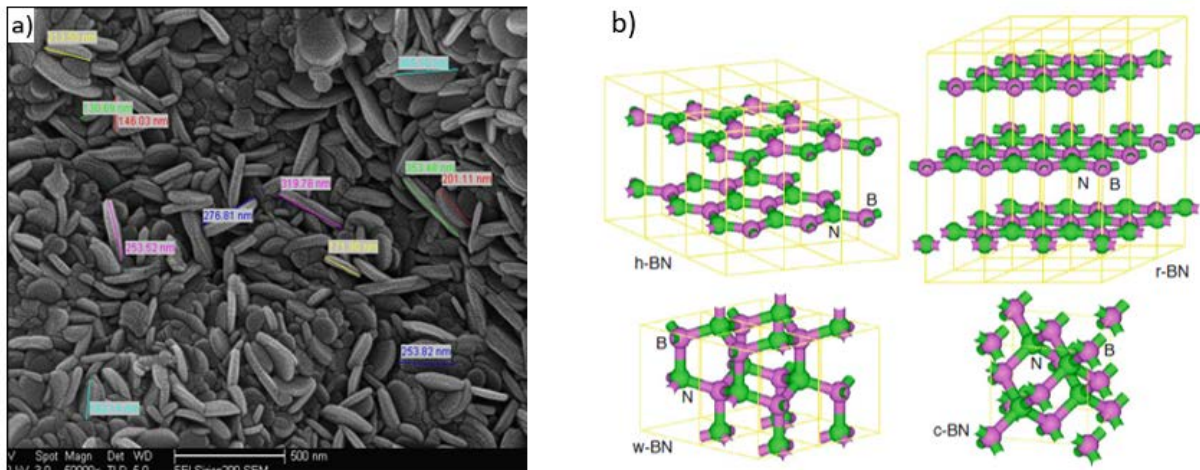


Figure 3-1: (a) SEM image of BN; (b) Structure models of hexagonal BN, rhombohedral BN, wurtzite BN, cubic BN

Several papers reported excellent tribological properties of BN powder nano-additives, thereby, mentioned nanoparticles seem to be an appealing additive to a drilling fluid capable of serving as a lubricity agent. At the University of Stavanger, *Awais et al. (2018)* have tested the performance of BN in CMC polymer. Results showed that the addition of 0.0095% by weight BN reduced the friction coefficient with 37% [63]. In the thesis work, the performance of dry BN nano-powder was experimentally investigated in Duovis and Xanthan gum polymers based drilling fluids. Moreover, there was an intention to enhance the effect of BN nanoparticles by grafting with oil since the first dry BN trial in the selected polymers was not satisfactory. The idea of grafting procedure was obtained from the ongoing PhD work, and the process of grafting was accomplished together with my supervisor.

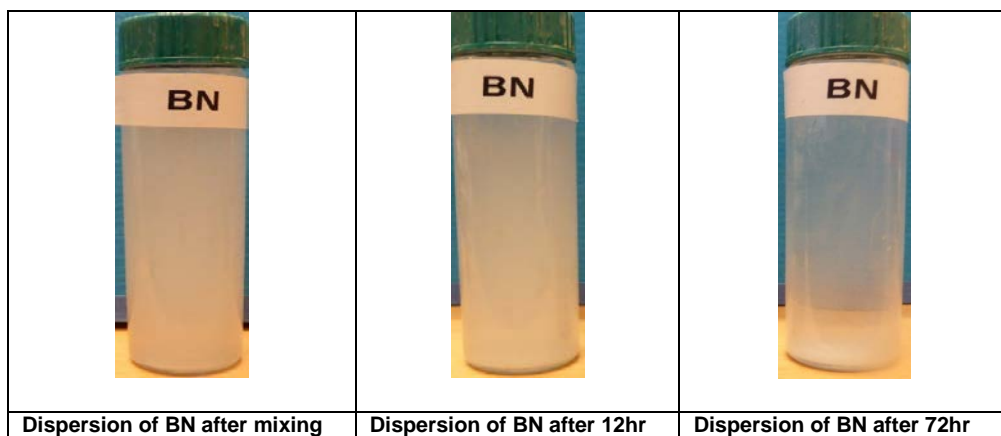


Figure 3-2: Dispersion of Boron nitride nanoparticles [63]

3.2.1.2. Nano boron nitride grafted with oil.

As mentioned earlier, in addition to dry BN, an attempt was made to modify the surface chemistry of BN nanopowder. The grafting was carried out with the environmentally friendly oil with the objective of reinforcing the lubricity effect. The procedure of grafting consisted of several steps. First, 8g of dry BN nanoparticles were mechanically mixed with 250 ml of oil. Afterwards, the mixture was sonicated for 1:30hr (**Figure 3-3 (a)**). The procedure was followed by the washing and drying of the mixture. During the washing process, the suspension was mixed with acetone and centrifuged twice at 3000 RPM to separate different phases according to their densities (**Figure 3-3 (b)**). After centrifugation, the oil phases have been poured out. Then, the solution was again centrifuged with distilled water to clean out the residual oil. Finally, wet nanoparticles were poured on the flat surface and kept at room temperature to let the liquid to evaporate. The condition of the particles was assessed by visual inspection, and the particles were collected when they lost its moisture. It took a couple of days to get dry nanoparticles. Associated photographs can be find in **Appendix A**.

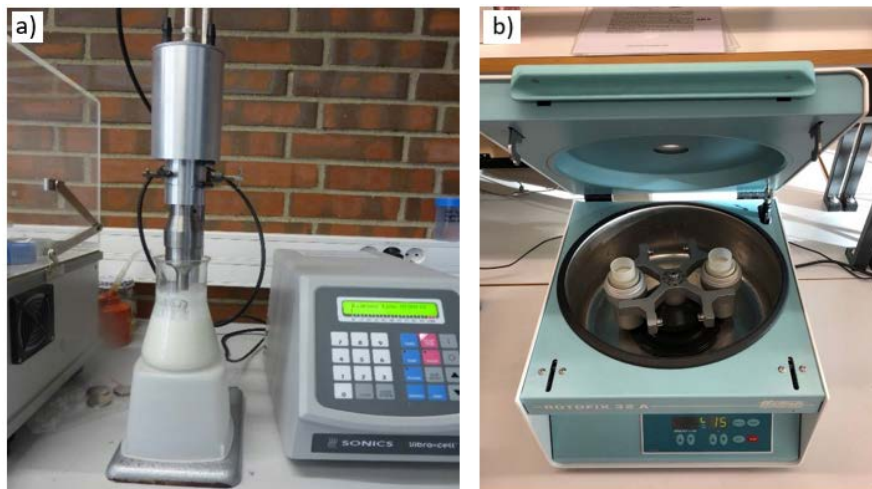


Figure 3-3: (a) BN-Oil sonication; (b) Centrifuge used for BN cleaning

3.2.1.3. Hydroxyl functionalized multi-walled carbon nanotube (MWCNT-OH).

Multi-walled carbon nanotubes (MWCNT) belong to the carbon nanotube (CNT) family of nanomaterials. The structure of MWCNT consists of multiple graphite layers, which are rolled up to form a tubular shape [64]. CNTs find their application in different fields of the industry due to valuable properties such that tensile strength, elastic modulus, electrical and thermal conductivity [65].

Ultrasonication is considered as the most effective and conventional method for better dispersion of CNTs in a mixture. However, this often results in particles split up resulting in deterioration of electrical and physical properties. The defects of sonication can be reduced by surface modification (functionalization) of nanotubes [66].

Functionalized multi-walled carbon nanotubes are used in petroleum industry, especially in cementing operations. They have been proven to be capable of developing strength cement [67]. Rheological effect of functionalized MWCNTs in water-based mud was described by *Abduo et al. (2016)*. Generally, the shear stress of MWCNT's containing mud increased compared to the conventional WBM. The viscosity of the drilling fluid showed directional proportionality to the concentration of these particles, i.e. increased concentration of nanoparticles led to increased viscosity [7]. This type of response is common for the nanofluids can be explained in such a way that high concentration of particles creates agglomeration in the system. Therefore, a greater force required to disperse the agglomeration resulting in higher internal shear stress in nanofluid what leads to increased viscosity [68].

In one of the frictional experiments performed in this thesis, hydroxyl functionalized multi-walled carbon nanotubes (MWCNT-OH) were used as a basic chemical during the formulation of the reference fluid. Then Boron nitride particles along with a lubricant were added ex-situ to evaluate the performance of these nanoparticles' composition. **Figure 3-4** shows the transmission electron microscopy of MWCNT and the structure hydroxyl (–OH) functionalized MWCNT.

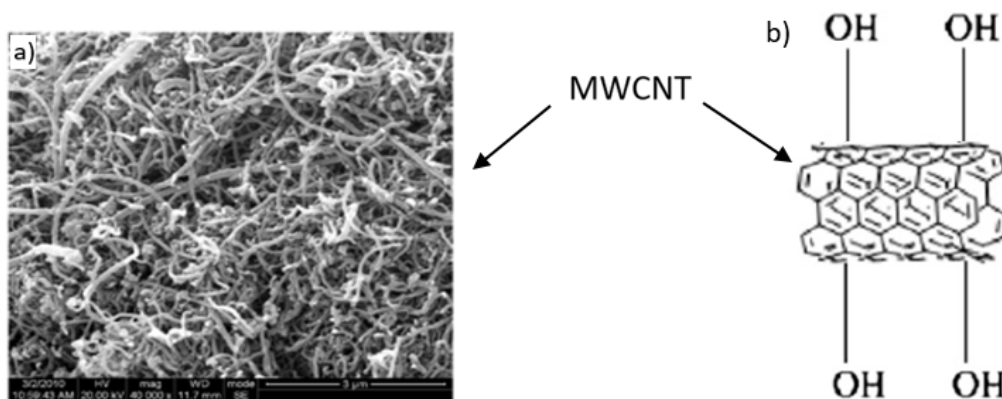


Figure 3-4: (a) SEM image of MWCNT; (b) structure of MWCNT-OH

3.2.2. Bentonite.

Bentonite is termed as any clay where smectite, usually montmorillonite, prevails the physical properties [69]. The primary functions of bentonite in water-based drilling muds are to increase the viscosity of suspension and to decrease fluid loss [19]. Bentonites can be split into two categories depending on swelling rate when getting in contact with water. The first category contains Na^+ as exchangeable ion and has an extensive absorption capacity, great swelling properties and remains in suspension without settling down for a quite long time, while the second group of bentonites does not swell at all and fall out of thin water dispersion. This group contains Ca^+ as the exchangeable ion and does not absorb any water [70].

A drilling class bentonite should readily disperse in water to contribute to thixotropic or shear thinning properties with adequate gel strength and low fluid loss. If the characteristics of raw bentonite are insufficient, it can be improved by ion exchange or adding an extender [71]. For example, the blending of sheared and dried bentonite with sodium carbonate will improve suspending and swelling properties. Acid treatment modifies the specific surface while quaternary ammonia compounds can improve organophilic properties [72].

Structure and composition.

As noted above, the dominant mineral in bentonite is montmorillonite, which gives the unique properties to the drilling fluid; however, the percentage of chemicals can vary greatly. **Table 3.1** presents chemical composition of commercial bentonites available in different regions:

Chemical composition in %			
	Wyoming "Volclay"	Panther Creek Mississippi	Ponza, Italy
Silica, SiO_2	64.32	64.00	67.42
Alumina, Al_2O_3	20.74	17.10	15.83
Ferric oxide, Fe_2O_3	3.03	} 4.70 {	0.88
Ferrous oxide, FeO	0.46		-
Titanium dioxide, TiO_2	0.14	1.50	-
Lime, CaO	0.50	3.80	2.64
Magnesia, MgO	2.30	0.50	1.09
Potash, K_2O	0.39	0.20	} 1.09
Soda, Na_2O	2.59	-	
Phosphoric anhydride, P_2O_5	0.01	-	-
Sulfuric anhydride, SO_3	0.35	0.20	0.01
Other minor constituents	0.01	8.00	-
Combined water	5.14	64.00	10.88

Table 3.1: Chemical composition of commercial bentonites [73]

Most of the clay minerals containing smectite group have the similar structure. Their flakes are made up of microscopic crystal platelets, which are arranged face to face. Each platelet consists of either octahedral sheet or tetrahedral sheet, which are tied to each other by covalent bonds through shared oxygen atoms as shown in **Figure 3-5**.

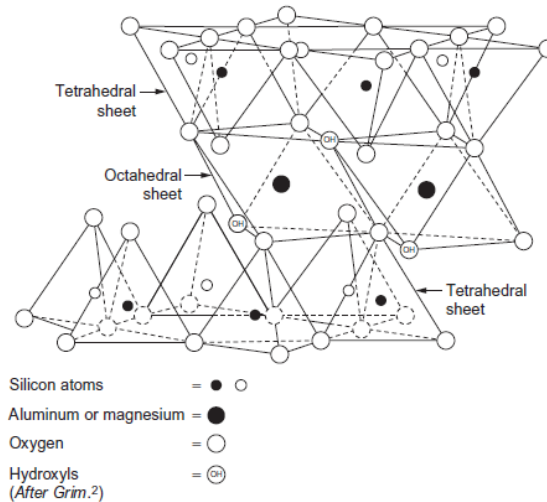


Figure 3-5: Different types of platelets and bonding between them [69]

Particle association.

The particle arrangement of clay minerals significantly influence the fluid properties such as viscosity, yield point and the filtrate loss [74]. There is four common disposition of clay particles which are described below and shown in **Figure 3-6**.

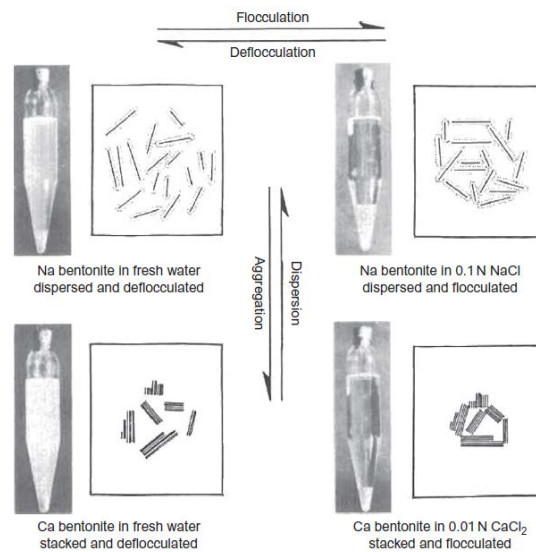


Figure 3-6: Arrangement mechanism of clay particles [69]

Deflocculated system.

When the particle arrangement is governed by repulsive forces, the system is called deflocculated. Such system can be achieved if the constituent particles have the same charge or if the particles were neutralized and dispersed by chemicals. The alkalinity of the system can create a net negative charge. The yield point and filtrate loss of deflocculated system are small.

Flocculated system.

A system is considered to be flocculated when net forces between the particles are attractive. The particles are grouped and coupled to each other either end to end or end to the surface, building a three-dimensional system. In such bentonite system, the viscosity and filtrate loss will be high.

Dispersed system.

When the particles in the system are separated and exist in the form of an individual unit or a small group, the system is dispersed. The pH of the solution govern the charge of particles. The arrangement of particles in a dispersed system can be both flocculated and deflocculated.

Aggregated system.

In this system, the crystals are bound to each other and create aggregates. When the clay is wetted, the sheets making up the platelets will split up causing an increase in viscosity.

3.2.3. Polymers.

A polymer is a chemical molecule where small and identical units, monomers, are joined together and repeated [75]. The progress of polymer chemistry diversified their application in drilling mud. Some examples of polymers and their function are listed below [76], [77]:

- Polysaccharide derivatives to control filtration
- Partially hydrolyzed polyacrylamides to encapsulation wellbore walls
- Xanthan gum to viscosify the fluid
- Carboxymethyl Cellulose Sodium (CMC) to control fluid loss and increase the viscosity

Other functions of polymers can be indicated as keeping mud stabilized at high temperatures, enhancing the yield of clay, flocculating or deflocculating some solids [19]. The structure of the polymers is shown in **Figure 3-7**.

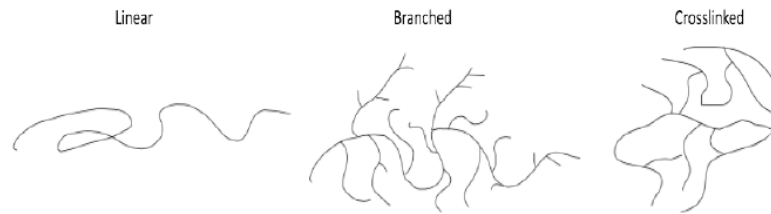


Figure 3-7: Polymer structure

The performance of selected nanoparticles will be examined both in Duovis polymer and Xanthan Gum polymer. Based on the experimental and simulation study, it will be concluded how the polymers can alter the properties of the nano-containing fluid.

3.2.3.1. Duo-Vis.

Duo-Vis is a dispersible biopolymer with high molecular weight. This polymer used in water-based mud to viscosify the system for improved cutting transport and better suspension. Duo-Vis affects the rheology of the drilling fluid making it highly shear-thinning and thixotropic to refine hydraulics. One of the disadvantages of Duo-Vis is susceptibility to bacterial degradation, which can be avoided by adding a biocide to the mixture.

3.2.3.2. Xanthan Gum.

Xanthan gum (XG) is a water-soluble microbial exo-polysaccharide derived from the bacterium *Xanthomonas campestris* [78]. Due to superior properties such as high viscosity at low concentrations, stability at the temperature and PH variations, non-toxicity, XG are broadly used in agriculture, nutrition products, pharmaceuticals, household and industry [79], [80]. In drilling fluids, Xanthan gum is used to increase viscosity, provide better suspension of drilling cuttings and stabilized the mud against the salt [76], [78]. It is most commonly applied in high salt environments, where bentonite is not capable to viscosify the mud [76]. The molecular structure of XG can be described as repeating monomer. Each monomer comprises two linearly connected backbones, which are very similar to the ring of glucose. Every other backbone has a trisaccharide side chain. The side chain is made of three rings: mannose

acetate connected to the backbone, terminal mannose in the tail and glucuronic acid salt between them. The graphical illustration is shown in **Figure 3-8**.

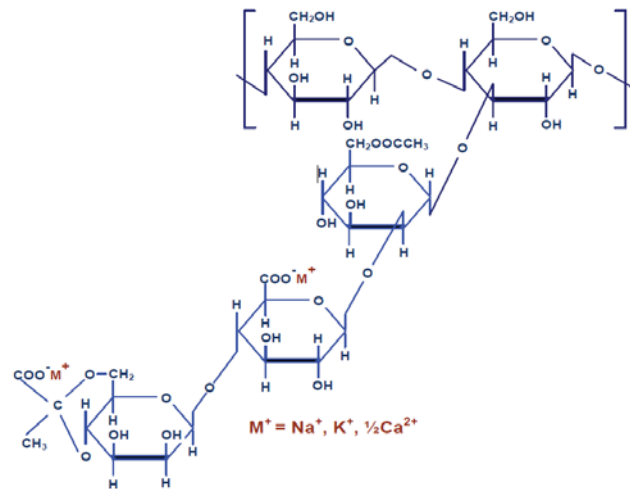


Figure 3-8: Molecular structure of XG

The main advantage of such structure is that hydrogen bonds, connecting the rings, are easily broken under high shear making the fluid thin. It gives low viscosities in bit nozzles, resulting in increased penetration rate. On the other hand, when the shear rate drops, the proper annular viscosity ensure proper hole cleaning [76].

3.2.4. KCl salt.

Potassium chloride (KCl) is a soluble salt, which is used in water-based drilling muds to maintain the stability of water-sensitive shale regions. Prior to the revealing the effect of potassium salts on shale formations, oil-based muds were suggested to drill such sections [81]. Theoretical and experimental studies showed that potassium ions at proper concentrations used in WBM are incredibly efficient in environments where there might be problems associated with swelling or dispersive tendencies of clay [82].

The process of shale inhibition is generated due to molecules exchange. The mechanism of KCl protection against shale inhibition can be explained as follows: positively charged potassium ions (K⁺) are attracted by the negatively charged clay surface. After the ions fit in the tiny spaces between platelets, they are held together, preventing invasion of water molecules [83].

4. EXPERIMENTAL STUDY.

Several different mixtures of weighted water-based drilling fluid were formulated and tested to investigate the effect of nano-sized additives. The chemical components making up the drilling muds were presented in **Chapter 3**.

The primary objective of the research was to improve the properties of conventional water-based drilling fluid by introducing nanoparticles to the system. The experimental fluids were characterized with regard to rheological properties, coefficient of friction, filtration, pH and viscoelasticity. Lastly, the parameters of formulated fluids were used as input data for simulation setup to assess the performance regarding the important drilling functions.

In this thesis work, the experimental fluids were formulated using two different polymers, namely Duovis and Xanthan gum. At first, the screening test was performed to establish the most attractive concentration of nano-additives, capable of reducing the friction. Further characterization was based on these results. The mass ratio between water, bentonite, polymers and salt has been established by previous students [84].

4.1. Effect of dry BN powder in Duovis polymer.

This section presents the performance of the commercial dry Boron nitride nanoparticles. Nanofluids were formulated in the Duovis-based fluid and tested with the wide range of BN concentrations.

4.1.1. Drilling fluid formulation.

The experimental fluids were prepared and further tested to see how different chemical compounds can affect each other and determine the best system regarding interested parameters. Salt was added to improve inhibitive properties, polymers were used to viscosify the system, and bentonite for filtrate loss and viscosity. The components of experimental fluids and their functions were discussed thoroughly in **Section §3.2**. The mud systems were formulated in the following sequence:

- 1) Water
- 2) Salt

- 3) Polymer
- 4) Nano-additives
- 5) Bentonite

The weight of each chemical was measured with precision balance according to the required concentration. The suspensions were mixed using Hamilton beach mixer with different rotation speeds until it became smooth. It is of great significance to add polymers carefully; otherwise, they would agglomerate and form lumps. After thorough mixing, the fluid system was allowed to age for 48 hours before carrying out any experiments to ensure the proper bentonite swelling.

The base fluid did not contain any nanoparticles and served as a reference to calculate the relative changes of tested and simulated parameters. The concentration of nanoparticles was gradually increased from fluid to fluid; however, other chemical compounds have the same weight as in reference liquid.

	<i>Base fluid</i>	<i>Base fluid + 0.01 wt.%</i>	<i>Base fluid + 0.02 wt.%</i>	<i>Base fluid + 0.03 wt.%</i>	<i>Base fluid + 0.04 wt.%</i>	<i>Base fluid + 0.3 wt.%</i>
Water	500 g	500 g	500 g	500 g	500 g	500 g
Bentonite	25 g	25 g	25 g	25 g	25 g	25 g
KCl	5 g	5 g	5 g	5 g	5 g	5 g
Duovis	0.5 g	0.5 g	0.5 g	0.5 g	0.5 g	0.5 g
BN (dry)	0	0.05 g	0.1 g	0.15 g	0.2 g	1.5 g

Table 4.1: Formulation of drilling fluids containing dry BN (in Duovis)

4.1.2. Lubricity.

The tribological behavior of the fluids was studied using pin-on-disc tribometer from CMI instruments (**Figure 4-1**). The equipment cooperates with the computer software showing instant and average friction factors between the rotating disc and steel ball on the end of tribometer arm. The rotating radius has been altered to catch the whole spectrum of possible friction values with 5N normal force applied to the arm. The experimental muds were tested at constant room temperature and constant rotation speed.

Each fluid sample was tested three times to eliminate uncertainties in the measurements and get an averaged value. Prior to conducting any test, it is essential to fill the cup with sufficient amount of tested fluid, ensure clear surface and inspect the condition of a steel ball and rotating disc. If the rubbing elements were damaged, the computer would fail to show the correct friction result. One should keep in mind that during this thesis work, the balls from different companies were used and the data could be compared only to the fluids from the same batch, but not to the fluids from other experiments.



Figure 4-1: CMI tribometer at UiS

Figure 4-2 outlines friction measurements of five fluids containing dry BN nanoparticles along with the reference system. The graph exhibits the mean values calculated from the several tests for each fluid. The left axis represents average values of friction coefficient, whereas the right one shows the change relative to the reference fluid in percentage.

The results from these experiments showed that increasing concentration of BN nanoparticles does not show a constant decrease in a friction factor. The fluids with low concentrations of BN (0.01 wt.% and 0.02 wt.%) showed around 8 percent friction reduction. The lowest friction value was observed for a sample with 0.03 percent weight of dry BN, which corresponds to 23.6% reduction in comparison with the reference fluid. An interesting observation was made

for the fluid with 0.04 wt.% of given nano. There was a sharp rise in the friction factor compared to the fluid with slightly smaller concentration. The lubricity coefficient was approximately the same as for the base fluid. In order to verify the validity of the data, the fluid with the equal weight ratio of components was prepared and tested once more. The new experiments showed the same average value. To study the effect of high concentrations, the amount of BN particles was significantly raised up to 0.3 wt.%; however, the friction improvement was 12.1% what is still not the best result documented in the batch.

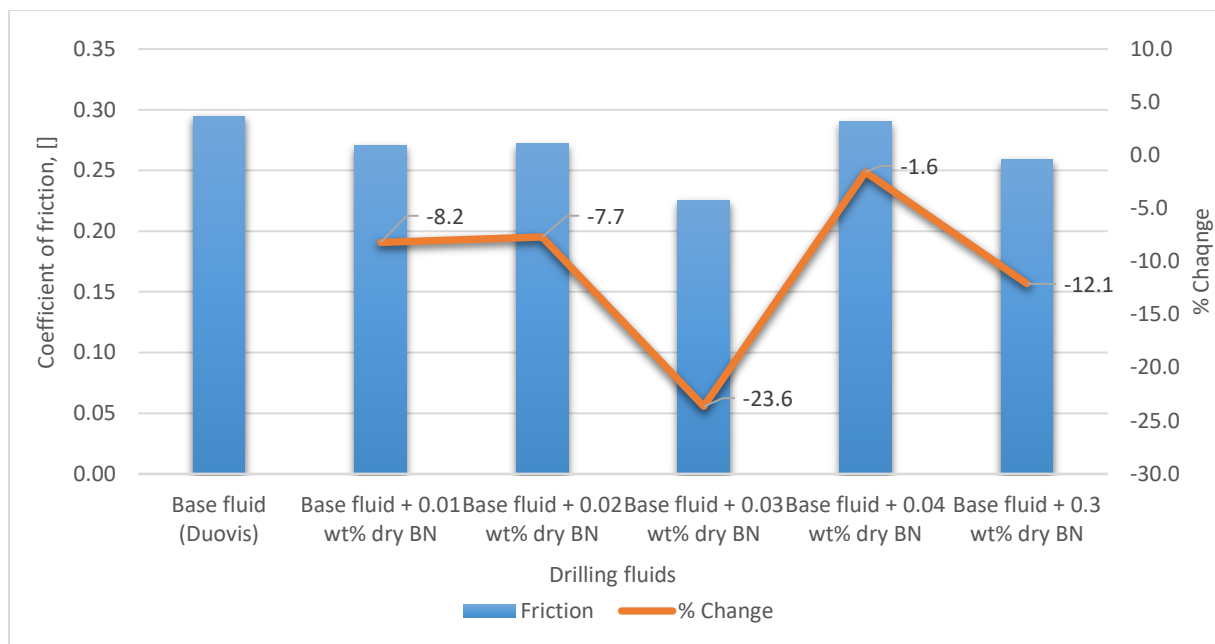


Figure 4-2: Effect of dry BN (in Duovis) on the coefficient of friction

4.1.3. Rheology.

The rheological test was conducted using a Fann-35 viscometer with a rotating cylinder, which allows to take the readings at 600, 300, 200, 100, 60, 30, 6 and 3 RPM. Before any measurements, the fluid samples were mixed for 2 minutes to ensure even particle distribution. The rheological test was performed at room temperature.

For the visual representation of the dependence of the rheology on the presence of BN nanoparticles, the reader is referred to **Figure 4-3**. The minor changes were observed for all nano-treated drilling fluids as compared to the base system. The curves exhibited inconsistent behavior and intersected each other. The line corresponding for the rheological data of the

fluid with 0.3% BN particles showed the lowest readings at slow rotation speed; however, at high RPM, the shear stress had the maximum values among all the tested fluids.

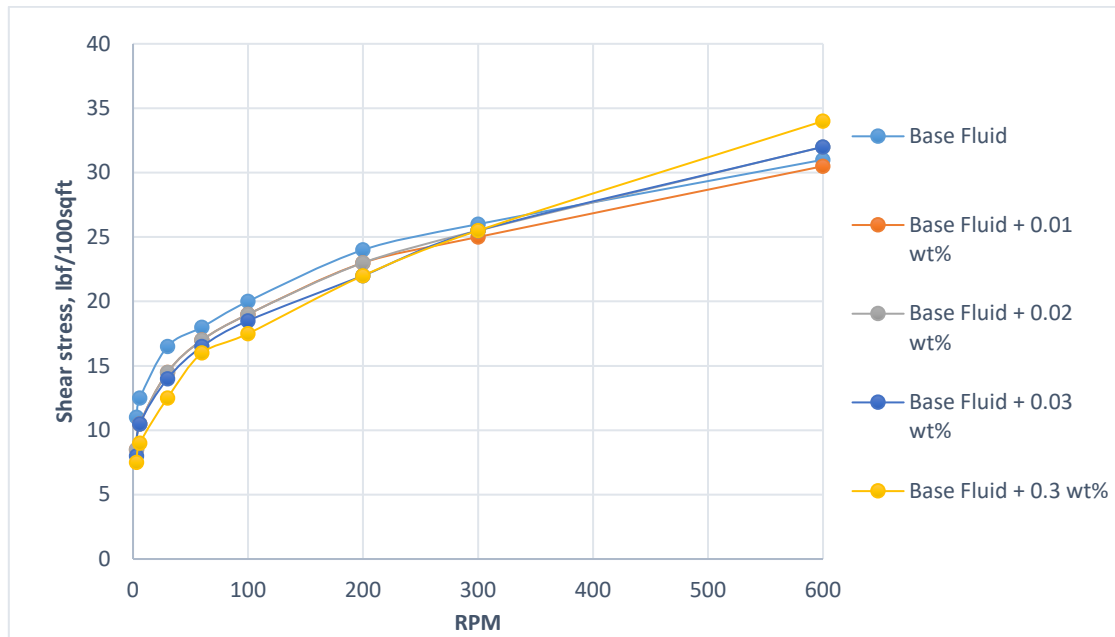


Figure 4-3: Effect of dry BN (in Duovis) on the viscometer readings

Further examination was conducted by calculating and plotting the Bingham and Power Law parameters, which are shown in **Figure 4-4** and **Figure 4-5**.

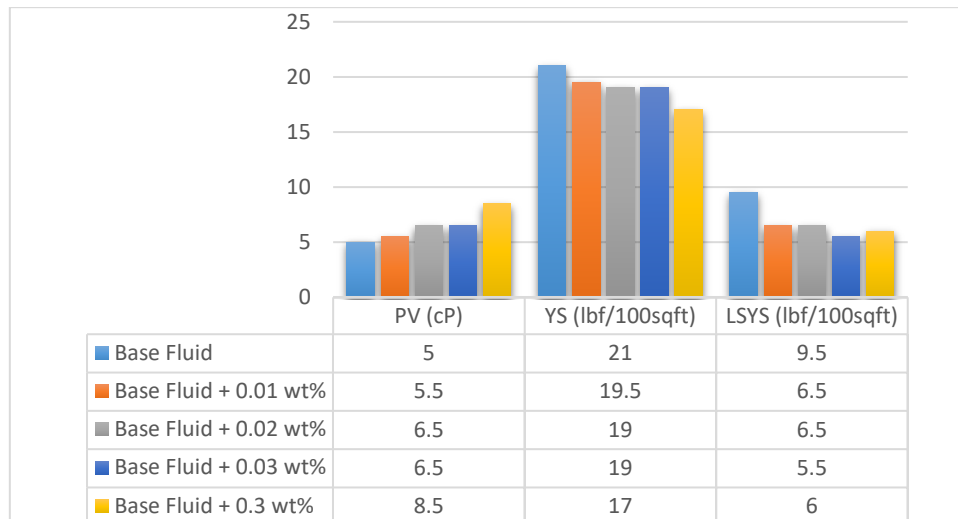


Figure 4-4: Effect of dry BN (in Duovis) on the Bingham parameters

As shown in **Figure 4-4**, the Bingham parameters were affected by the presence of the nano-additives. The plastic viscosity was directly proportional to the concentration of BN. On the

other hand, the increased weight ratio of nanoparticles reduced the yield stress. The same trend was observed for the lower shear yield stress (LSYS) values; however, there was a slight increase in the fluid with the highest concentration of 0.3 wt.%.

Figure 4-5 represents the alteration of Power Law parameters for the systems with the different weight percentage of BN in the system. The flow behavior index (n) was below 1.0 for all cases what depicts the shear thinning behavior of the fluids and drop of viscosity with the increased shear rate. The flow index exhibited a rise when the concentration of nanoparticles was increased. The most significant increase of 64% was observed for a system containing 0.3% BN particles. In contrast, consistency index (k) reduced with the increased amount of nanoparticles. 64% reduction was documented when the fluid was diluted with 0.3 wt.% of nano-BN. Lower consistency index describes a fluid with lower viscosity.

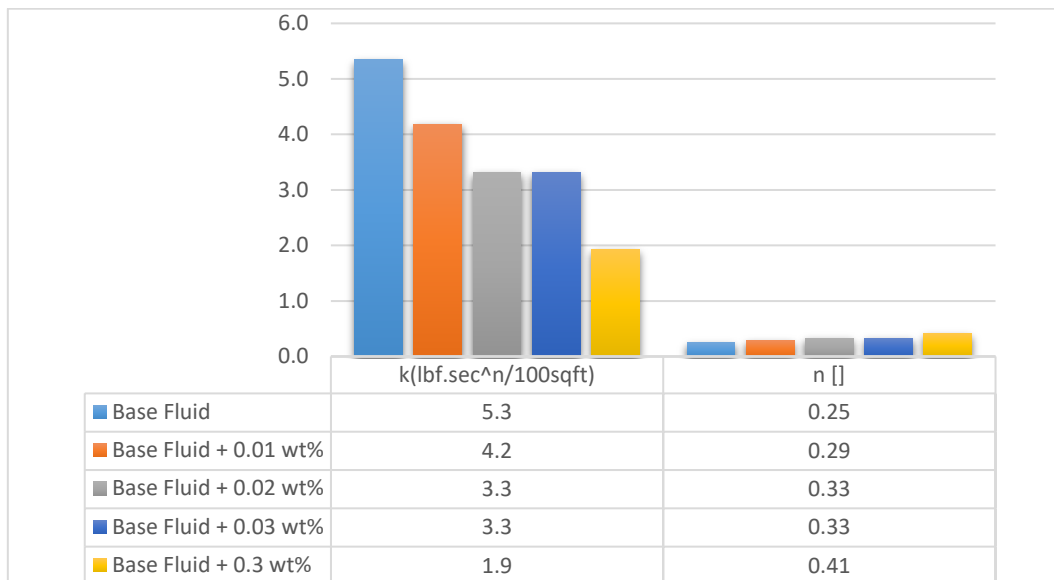


Figure 4-5: Effect of dry BN (in Duovis) on the Power Law parameters

4.1.4. Filtration and pH.

API static low-pressure filter press (**Figure 4-6**) was used to measure the filtrate loss of the samples and estimate the thickness of the filter cake. The equipment consisted of a cylinder, which was filled with an experimental fluid. The base of the cylinder was fitted with the sieve and paper filter. The pressure of 7 bar (100psi) was exerted to the top of the cylinder, and the

filtrate was gathered from the bottom. The filtrate was collected for 7.5 minutes, and the volume of loss was recorded.



Figure 4-6: Low-pressure filter press

Table 4.2 reports the filtrate values along with percentage change relative to the Base fluid. The filtrate loss increased for all the nano-enhanced drilling fluids, other than for the fluid with 0.03% BN, where the filtrate value remained equal to the reference. The most substantial increment of 33.3% was documented for the specimen with 0.3% additives. The remaining samples exhibited a slight increased up to 8.9%.

	<i>Base Fluid</i>	<i>Base Fluid + 0.01 wt.%</i>	<i>Base Fluid + 0.02 wt.%</i>	<i>Base Fluid + 0.03 wt.%</i>	<i>Base Fluid + 0.3 wt.%</i>
Filtrate (ml)	9	9.8	9.3	9	12
% Change		8.9%	3.3%	0.0%	33.3%

Table 4.2: Effect of dry BN (in Duovis) on the filtration

The pH of drilling fluids is an important parameter, which can influence the performance of filtration agents, affect corrosion rates, improve thermal stability, etc. The pH of the fluids can be determined either by the colorimetric method or electrometric method. In this thesis, the latest method was used as it is more accurate and reliable. The pH-meter is shown in **Figure 4-7**.

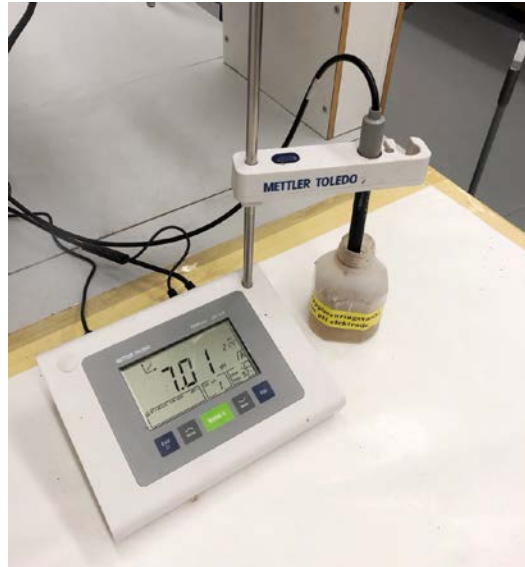


Figure 4-7: pH meter

The change in pH values was documented in **Table 4.3**. In general, there was a decreasing trend in pH of nano-containing fluids; however, the variations were barely noticeable (less than one percent). The fluid with 0.02 wt.% of dry BN nanoparticles did not show any deviation from the reference value.

	<i>Base Fluid</i>	<i>Base Fluid + 0.01 wt.%</i>	<i>Base Fluid + 0.02 wt.%</i>	<i>Base Fluid + 0.03 wt.%</i>	<i>Base Fluid + 0.3 wt.%</i>
pH	8.7	8.62	8.7	8.63	8.65
% Change		-0.9%	0.0%	-0.8%	-0.6%

Table 4.3 Effect of dry BN (in Duovis) on the pH

4.2. Effect of oil grafted BN in Duovis polymer system.

This subchapter analyzes the effect of oil grafted Boron nitride nanoparticles. The procedure of surface modification has been covered in **Section §3.2.1.2**.

4.2.1. Drilling fluid formulation.

In order to investigate the effect of modified nano-BN, four fluids along with the base fluid were formulated and tested. In this case, two fluids with low and two with relatively high concentrations were subjected to the analysis. The nanoparticles were added ex-situ meaning that first the reference fluid was prepared, and then the particles were mixed in the required

amount to get the desired concentration. The procedure and sequence of the mixing were the same as the one described in **Section §4.1.1**.

	Base fluid	Base fluid + 0.01 wt.%	Base fluid + 0.03 wt.%	Base fluid + 0.2 wt.%	Base fluid + 0.3 wt.%
Water	500 g	500 g	500 g	500 g	500 g
Bentonite	25 g	25 g	25 g	25 g	25 g
KCl	5 g	5 g	5 g	5 g	5 g
Duovis	0.5 g	0.5 g	0.5 g	0.5 g	0.5 g
Grafted BN	0	0.05 g	0.15 g	1.0 g	1.5 g

Table 4.4: Formulation of drilling fluids containing grafted BN (in Duovis)

4.2.2. Lubricity.

This section presents a friction analysis of the fluids containing different ratios of modified Boron nitride nano-additives. The friction values and changes relative to the base system are plotted in **Figure 4.8**. In general, the lubricating properties were enhanced with increasing concentration. A small volume of additives showed a minor improvement up to 13.1% (the fluid with 0.03 wt.% of modified BN). The presence of grafted BN at the concentration of 0.01% improved the lubricity by 9.7%.

The best lubricity value in the batch was observed for the fluid with 0.2 wt.% of grafted BN particles, which reduced the friction by 35.4% as compared to the base fluid. Further increase in percent weight of additives resulted in a deviation from the trend. The grafted BN at the concentration of 0.3% exhibited higher friction value than the previous result (28.4% reduction in comparison with the reference fluid).

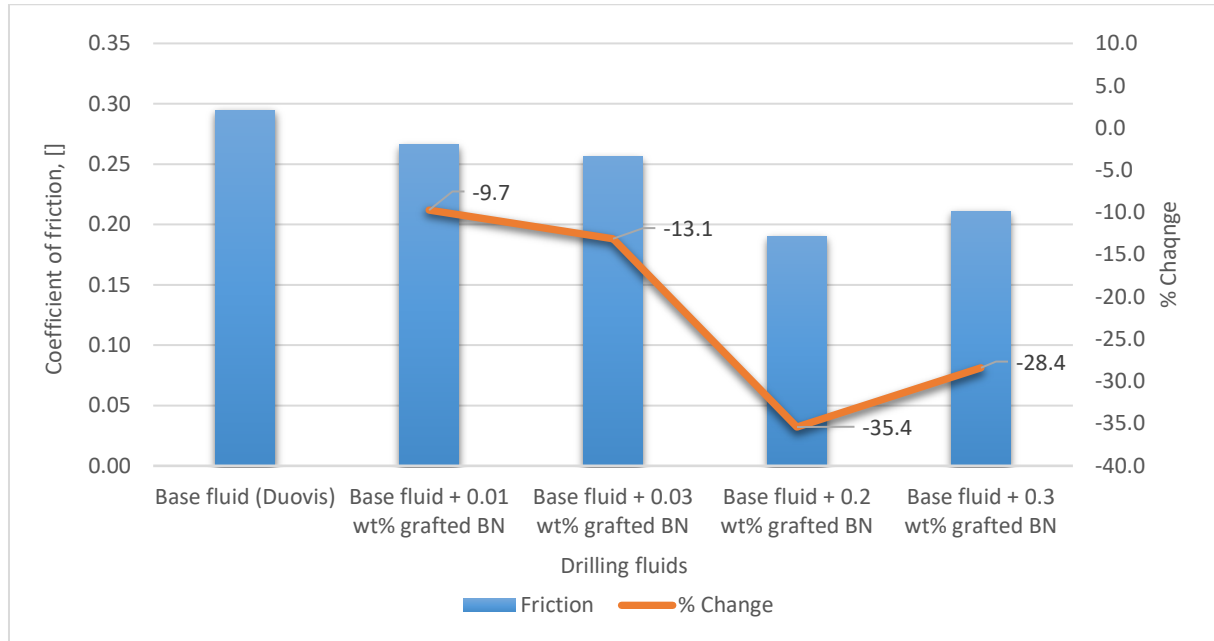


Figure 4-8: Effect of grafted BN (in Duovis) on the coefficient of friction

4.2.3. Rheology.

Figure 4-9 presents the viscometer response on the addition of grafted nanoparticles to the reference fluid. The visual inspection of the graph did not reveal any particular relationship between the concentration of the NPs and the viscometer readings. The lowest shear stress values were observed for the fluid with 0.01 wt.% of grafted BN; whereas, the pick readings were depicted by the fluid with 0.03 wt.% of additives. The sample containing 0.2 wt.% of additives yielded approximately similar shear stress values to the reference fluid; however, at high RPM the readings slightly deviated. The additives at the concentration of 0.3 wt.% increased the readings, which almost approached the maximum values in the spectrum.

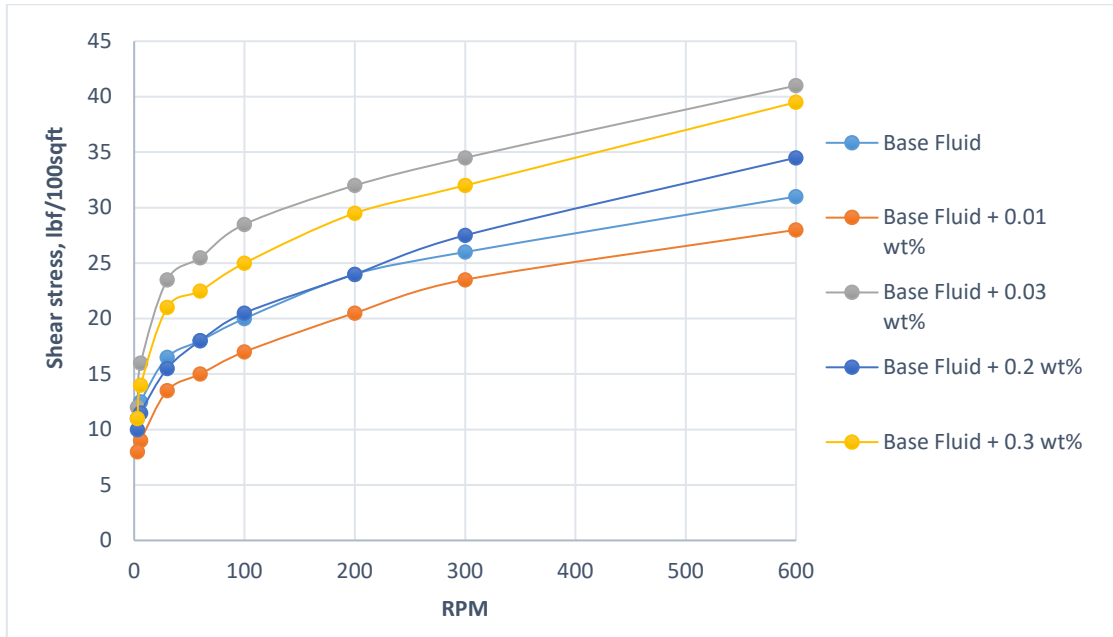


Figure 4-9: Effect of grafted BN (in Duovis) on the viscometer readings

Bar chart 4-10 illustrates the Bingham parameters calculated from the viscometer data. The lowest concentration of grafted BN particles slightly decreased the PV followed by the increasing trend for the higher concentrations. The yield stress value considerably fluctuated, exhibiting a pick value for the fluid with 0.03 wt.% and the minimum value for the fluid with 0.01 wt.% of known additives. The LSYS also behaved inconsistently; however, no severe variations were observed.

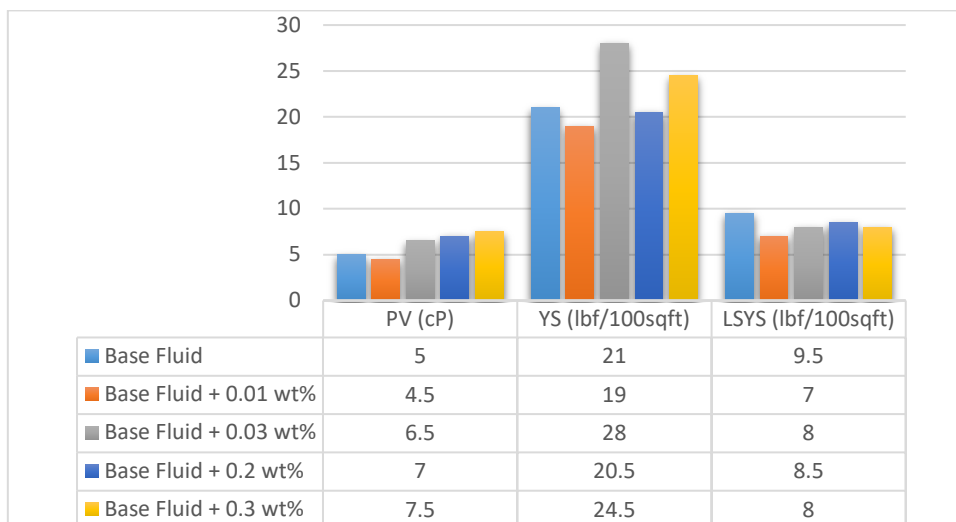


Figure 4-10: Effect of grafted BN (in Duovis) on the Bingham parameters

The Power Law parameters are summarized in **Figure 4-11**. The consistency index showed a random behavior without any relation to the percentage of additives. The maximum value was documented for the fluid at the concentration of 0.03% of grafted particles; whereas the fluid with 0.2 wt.% had the lowest *k*-value in the batch. The flow behavior index remained unchanged when the small amount of grafted BN was used; however, the increased weight of additives led to the rise in the flow index.

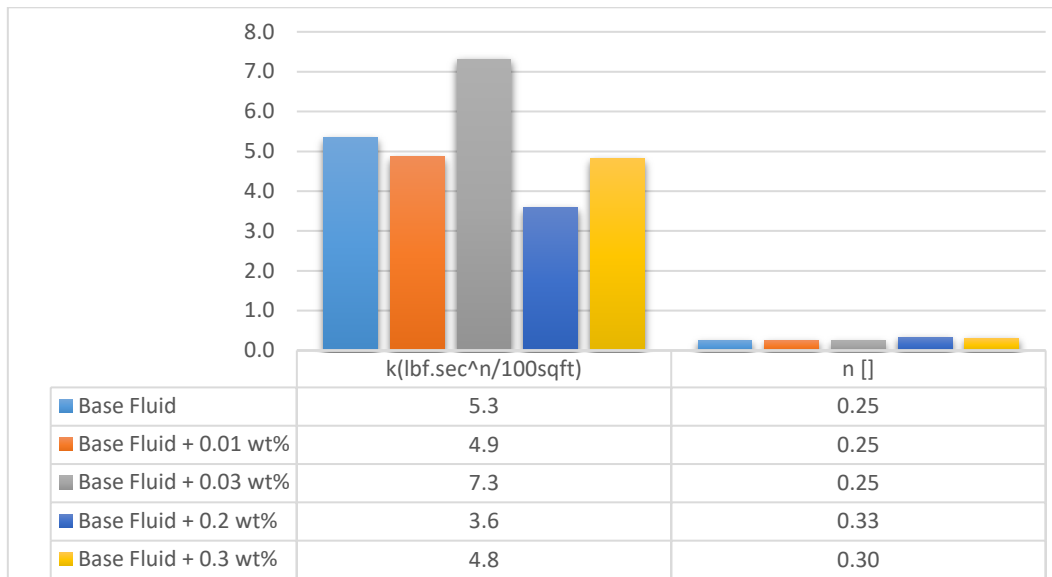


Figure 4-11: Effect of grafted BN (in Duovis) on the Power Law parameters

4.2.4. Filtration and pH.

The filtration characteristics of the drilling muds are depicted in the table below. The lowest concentration of grafted particles improved the filtrate loss by 4.4%; however, other concentrations revealed an increase of filtrate volume relative to the reference fluid. The maximum increment in the whole batch (7.8%) corresponded to the sample with 0.2 wt.% of modified BN.

	Base Fluid	Base Fluid + 0.01 wt.%	Base Fluid + 0.02 wt.%	Base Fluid + 0.2 wt.%	Base Fluid + 0.3 wt.%
Filtrate (ml)	9	8.6	9.5	9.7	9.5
% Change		-4.4%	5.6%	7.8%	5.6%

Table 4.5: Effect of grafted BN (in Duovis) on the filtration

Table 4.6 outlines the pH measurements of the fluids having modified BN nanoparticles as additives. Overall, the presence of grafted particles had a reducing tendency on the alkalinity of the mixtures. The most evident decrease of 2.8% was documented for the sample having BN-modified at the concentration of 0.02 wt.%. The remaining proportions barely affected the pH value or did not affect it at all.

	<i>Base Fluid</i>	<i>Base Fluid + 0.01 wt.%</i>	<i>Base Fluid + 0.02 wt.%</i>	<i>Base Fluid + 0.2 wt.%</i>	<i>Base Fluid + 0.3 wt.%</i>
pH	8.55	8.55	8.51	8.31	8.48
% Change		0.0%	-0.5%	-2.8%	-0.8%

Table 4.6: Effect of dry BN (in Duovis) on the pH

4.3. Effect of BN/lubricant in Duovis polymer.

In this section, the effect of Boron nitride nanoparticles was studied in the presence of a lubricant. *Mijić et al. (2017)* stated in their paper that addition of a small amount of oil together with SiO₂ and TiO₂ nanoparticles could improve lubricity performance of the fluid [85]. In their case, nanoparticles alone did not improve the friction regardless of their percentage in the base fluid. However, as was observed from the previous experiments, dry BN nanoparticles can improve lubricity up to 25%. Another observation the authors mentioned was increased plastic viscosity, yield point and gel strength when nanoparticles were added with the lubricant as compared to the muds containing only nanoparticles. The section covers the review of tribology, rheology, filtrate loss and pH measurements.

4.3.1. Drilling fluid formulation.

The experimental fluids were formulated with a wide concentrations range of BN nanoparticles mixed with oil. Oil was mixed with the nanoparticles using magnetic stirrer for 24 hours. There was not any certain ratio between oil and nanoparticles established; thereby it was not possible to calculate the separate mass percentage of nano-additives and oil in the suspension. The weight of BN/oil (BN/lub) mixture was counted to calculate the concentrations of the tested fluids. Seven base fluids were prepared first, then six of them were blended with the various amount of BN in oil. Duovis polymer was used in the formulation of this batch of experimental muds.

	Base fluid	Base fluid + 0.08 wt.%	Base fluid + 0.12 wt.%	Base fluid + 0.16 wt.%	Base fluid + 0.2 wt.%	Base fluid + 0.25 wt.%	Base fluid + 0.3 wt.%
Water	500 g	500 g	500 g	500 g	500 g	500 g	500 g
Bentonite	25 g	25 g	25 g	25 g	25 g	25 g	25 g
KCl	5 g	5 g	5 g	5 g	5 g	5 g	5 g
Duovis	0.5 g	0.5 g	0.5 g	0.5 g	0.5 g	0.5 g	0.5 g
BN/oil	0	0.4 g	0.6 g	0.8 g	1.0 g	1.25 g	1.5 g

Table 4.7: Formulation of drilling fluids containing BN along with oil (in Duovis)

4.3.2. Lubricity.

Figure 4-12 displays the mean values of tribometer readings for the fluids with BN nanoparticles mixed in lubricant. The change in friction coefficient relative to the base fluid was also plotted on this graph. Generally, there was reducing trend in friction coefficient when the concentration of BN in lubricant was increased. The 0.08 wt.% of BN/oil showed 22% friction reduction, what can be compared to the 0.03 wt.% of dry BN which showed about 25% reduction. Subsequent increase in concentration up to 0.2 wt.% showed only slight improvement in friction result. Presence of nano along with a lubricant at the concentration of 0.25% by weight reduced the friction by 39%. The friction coefficient had its lowest number for the sample with the highest concentration of additives (0.3 wt.%), which corresponded to 45% decrease in friction value. Comparing this value to the case where fluid was modified with dry BN particles, 0.3 wt.% of dry Boron nitride nanoparticles improved lubricity parameters by only 19%.

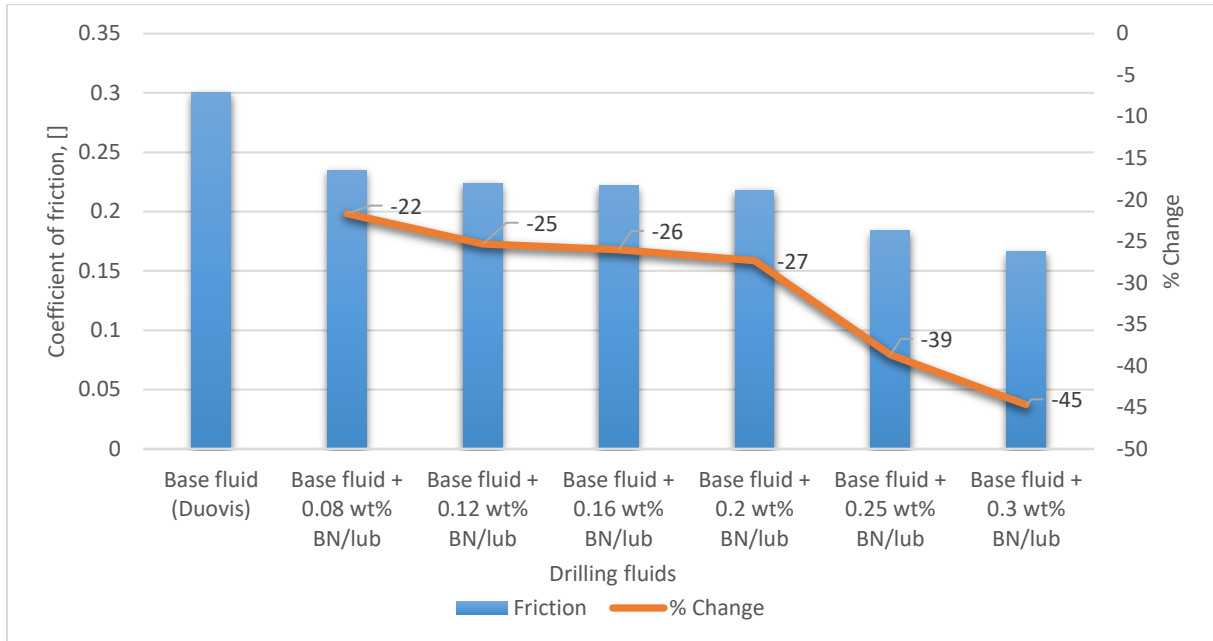


Figure 4-12: Effect of BN/lubricant (in Duovis) on the coefficient of friction

4.3.3. Rheology.

Consider **Figure 4-13**, which presents the rheological records for the fluids with lowest, highest and medium concentration of additives along with the data for the reference fluid. The overall observation can be made that increased concentration of Boron nitride nano-additives in oil led to the increased shear stress for all ranges of RPM. The fluids with the small weight of additives showed minor changes in the readings, whereas the highest concentration displayed a noticeable increment.

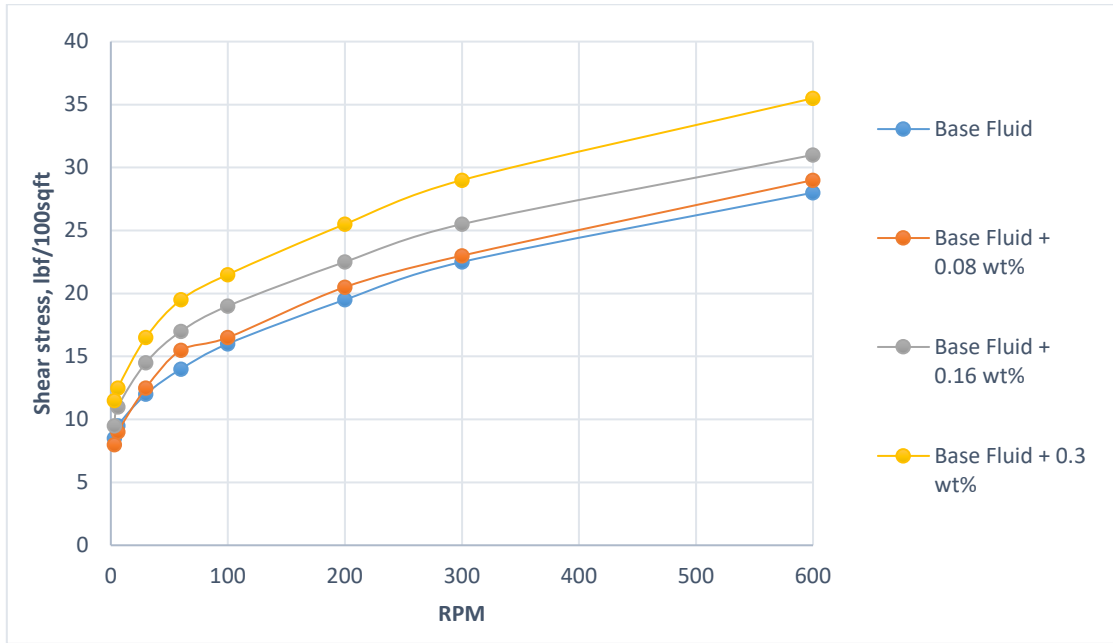


Figure 4-13: Effect of BN/lubricant (in Duovis) on the viscometer response

For further examination, the Bingham and Power Law parameters were calculated and plotted (Figure 4-14 and Figure 4-15).

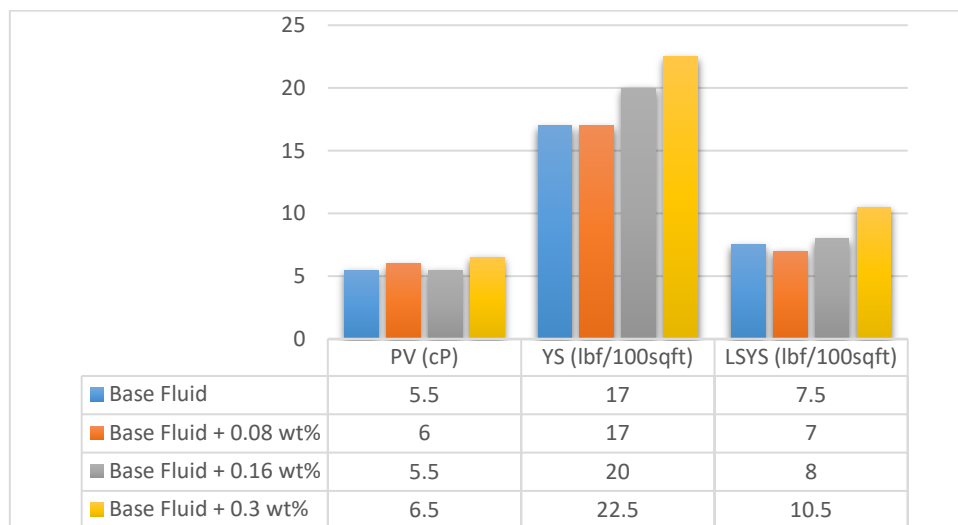


Figure 4-14: Effect of BN/lubricant (in Duovis) on the Bingham parameters

The Bingham parameters showed an increasing trend in plastic viscosity when the concentration increased, except for the fluid with 0.16% additives where PV was identical to the reference fluid. Regarding yield stress, the fluid with low content of BN in oil does not show any differences with the base fluid. On the other hand, the increased mass of selected

additives raised the YS of nanofluid from 17 lbf/100ft² up to 22.5 lbf/100ft². The value of the lower shear yield stress (LSYS) also rose when the weight of BN/lubricant was increased; however, the lowest concentration of nano/lubricant slightly decreased the parameter.

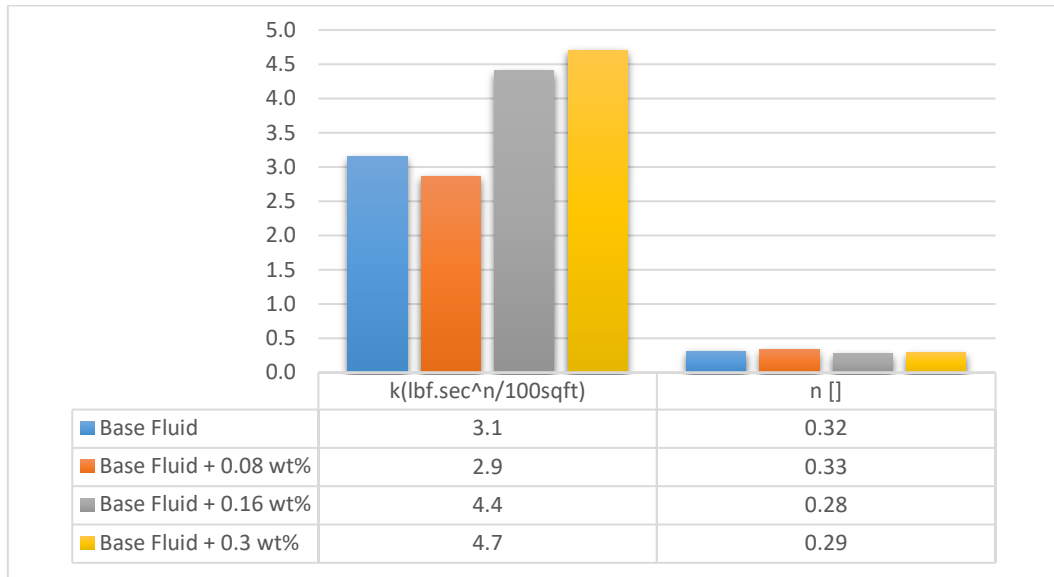


Figure 4-15: Effect of BN/lubricant (in Duovis) on the Power Law parameters

The consistency index slightly decreased when the base fluid was mixed with 0.08 wt.% of BN/lubricant. Higher concentrations showed a rise of *k*-value by average 47%. The response of the exponent law index on the presence of known additives was trivial, showing a maximum deviation of 12% for the fluid with 0.16 wt.% of BN/lubricant.

4.3.4. Filtration and pH.

Table 4.8 illustrates the effect of BN/lubricant mixture on filtrate loss. Low concentrations of additives did not affect the filtrate properties; while, the addition of BN in oil at the concentration of 0.3% by weight decreased filtrate loss by 11.8 percent.

	Base Fluid	Base Fluid + 0.08 wt.%	Base Fluid + 0.16 wt.%	Base Fluid + 0.3 wt.%
Filtrate (ml)	8.5	8.5	8.5	7.5
% Change		0.0%	0.0%	-11.8%

Table 4.8: Effect of BN/lub (in Duovis) on the filtration

The pH response on BN/lubricant additives is shown in **Table 4.9**. As concentration was increased, the pH value declined. The maximum fall of 3.6 was documented for the “Base Fluid + 0.3 wt.%”.

	Base Fluid	Base Fluid + 0.08 wt.%	Base Fluid + 0.16 wt.%	Base Fluid + 0.3 wt.%
pH	8.59	8.45	8.35	8.29
% Change		-1.6%	-2.8%	-3.6%

Table 4.9: Effect of BN/lub (in Duovis) on the pH

4.4. Effect of Dry BN powder in Xanthan gum polymer.

From this section onwards, the polymer making up the foundation for the experimental fluids was changed from Duovis to Xanthan gum. By doing this, it was investigated how the performance of given additives varies in the fluids with different polymers. This section covers the analysis of dry BN in said polymer. Nanoparticles were used mostly in low concentrations; however, one of the specimens was prepared with the high amount of BN.

4.4.1. Drilling fluid formulation.

The selection of nanoparticle’s concentration was based on the most appealing tribological results obtained from the experiments with the Duovis polymer. The mass ratio of water, bentonite and polymer was preserved, but the weight of KCl was halved. It was previously determined that such proportion of XG and KCl yields better stability of the fluid and reduce the water phase. **Table 4.10** illustrates the composition of experimental drilling fluids.

	Base fluid	Base fluid + 0.01 wt.%	Base fluid + 0.02 wt.%	Base fluid + 0.03 wt.%	Base fluid + 0.3 wt.%
Water	500 g	500 g	500 g	500 g	500 g
Bentonite	25 g	25 g	25 g	25 g	25 g
KCl	2.5 g	2.5 g	2.5 g	2.5 g	2.5 g
XG	0.5 g	0.5 g	0.5 g	0.5 g	0.5 g
BN (dry)	0	0.05 g	0.1 g	0.15 g	1.5 g

Table 4.10: Formulation of drilling fluids containing dry BN (in XG)

4.4.2. Lubricity.

The averaged readings from the tribology measurements along with the percentage change are shown in **Graph 4-16**. The friction coefficient decreased as the fluids were diluted with nanoparticles; however, the fluids with 0.01 wt.% and 0.02 wt.% of dry BN exhibited an insignificant drop. The maximum friction reduction of 16.9% was observed for the sample having 0.03 percent weight of nano-additives. When the BN nanoparticles were added at the highest concentration of 0.3 wt.%, the friction coefficient reduced by 10.3%.

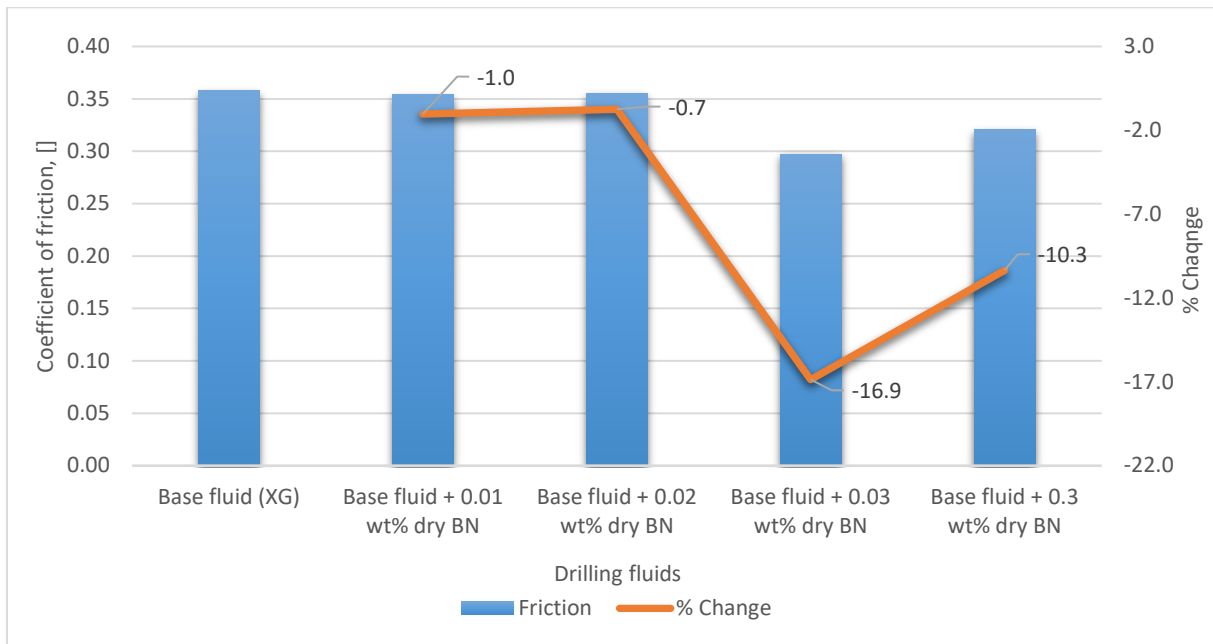


Figure 4-16: Effect of dry BN (in XG) on the coefficient of friction

4.4.3. Rheology.

The rheological data of the fluids formulated in this section was presented in **Graph 4-17**. The viscometer readings showed some changes of the nanoparticle-treated fluid as compared to the reference drilling mud. Shear stress values increased for all sample with nano-additives. For high RPM, the increase in readings was proportional to the concentration; however, at low RPM the fluid with 0.3% of nanoparticles exhibited the smallest shear stress value. The viscometer data was used to calculate Bingham and Power Law parameters. The parameters are plotted on **Figure 4-18** and **Figure 4-19**.

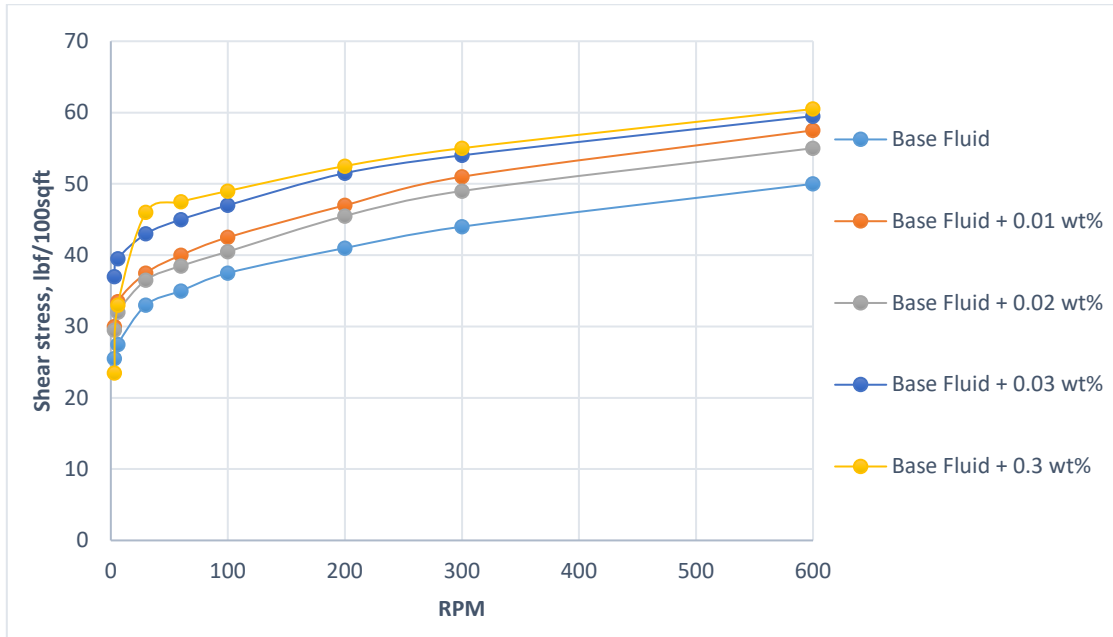


Figure 4-17: Effect of dry BN (in XG) on the viscometer response

Figure 4-18 presents the Bingham parameters of the fluid with dry BN particles is XG polymer. The PV of the fluid with 0.02 wt.% of additives was similar to the reference fluid. The system with 0.01 wt.% of BN showed an increase of 0.5 cP compared to the base mud; however, the fluids with the concentration higher than 0.02 wt.% showed a decrease in PV. The YS of all the nanofluids was higher than the value for the reference fluid. The LSYS of nano-treated fluids with the low concentration of particles showed an increasing trend; however, the LSYS parameter of the fluid with 0.3% BN dropped by 40% as compared to the base case.

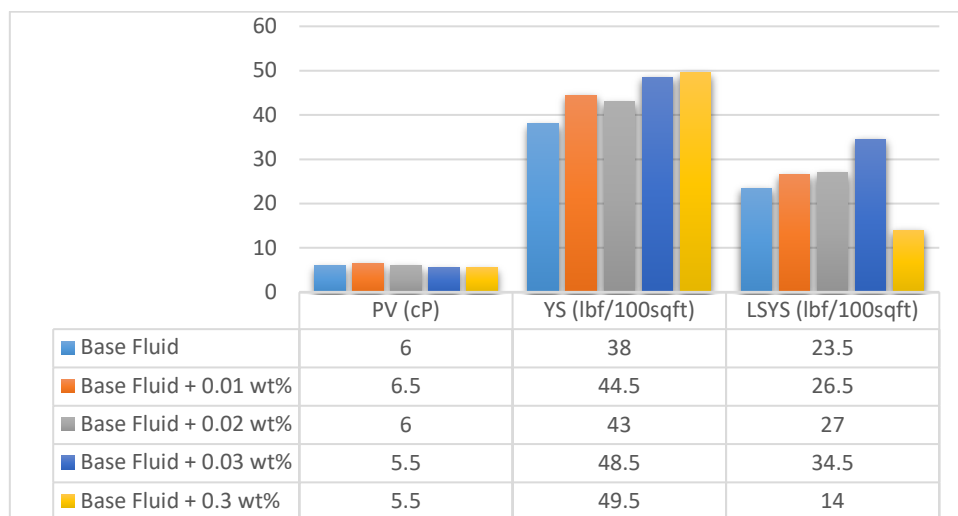


Figure 4-18: Effect of dry BN (in Duovis) on the Bingham parameters

The Power Law parameters (**Figure 4-19**) showed that consistency index went up for all the samples with BN compared to the reference fluid. The most noticeable growth was observed for the fluid with 0.3 wt.% of particles. The trend of the flow index was opposite, i.e., the values decreased for the nanofluids. The drop for the fluids having 0.01% and 0.02% BN was only 6%; however, the n -value reduced by 22% for the fluids with 0.03% and 0.3% BN.

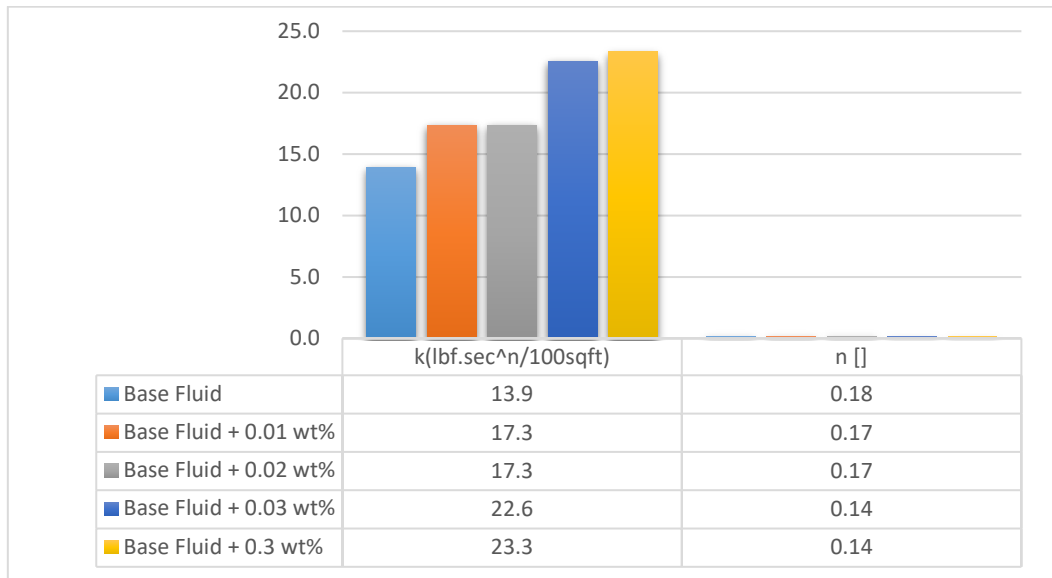


Figure 4-19: Effect of dry BN (in XG) on the Power Law parameters

4.4.4. Filtration and pH.

Table 4.11 shows the filtrate values for the experimental fluids and the percentage change relative to the reference sample. Filtrate decreased by 5.8% for the fluid at the concentration of 0.01% by weight. When the percent weight of nanoparticles was increased, the filtrate values showed increasing trend. The most prominent increment of 14.5% was observed for a sample with 0.3% of BN.

	Base Fluid	Base Fluid + 0.01 wt.%	Base Fluid + 0.02 wt.%	Base Fluid + 0.03 wt.%	Base Fluid + 0.3 wt.%
Filtrate (ml)	6.9	6.5	6.8	7.4	7.9
% Change		-5.8%	-1.4%	7.2%	14.5%

Table 4.11: Effect of dry BN (in XG) on the filtration

The pH readings along with variations relative to the reference were presented in **Table 4.12**. Generally, the addition of nanoparticles did not affect pH severely, and the values increased up to 0.7%; besides the fluid with 0.03% of nano-additives where pH decreased by 1.4%.

	Base Fluid	Base Fluid + 0.01 wt%	Base Fluid + 0.02 wt%	Base Fluid + 0.03 wt%	Base Fluid + 0.3 wt%
pH	8.48	8.48	8.49	8.36	8.54
% Change		0.0%	0.1%	-1.4%	0.7%

Table 4.12: Effect of dry BN (in XG) on the pH

4.5. Effect of oil grafted BN in XG polymer system.

This subchapter analysis the performance of oil grafted BN nanoparticles in the Xanthan gum system. The experiments in the Duovis-based drilling fluids illustrated that surface modified Boron nitride nanoparticles enhances the lubricating effect at high concentrations. The effect of additives on tribology and rheology as well as on filtration and alkalinity was examined in this study. Further viscoelasticity and simulation study has been carried out on the fluid with the best lubricating properties.

4.5.1. Drilling fluid formulation.

The percentage ratio of grafted nanoparticles was selected similarly to those tested in the Duovis polymer. This facilitated the comparison study between two systems. The nano-additives were introduced to the solution after the base fluid was prepared and aged. The matrix below depicts the formulation and the content of the experimental fluids.

	Base fluid	Base fluid + 0.01 wt.%	Base fluid + 0.03 wt.%	Base fluid + 0.2 wt.%	Base fluid + 0.3 wt.%
Water	500 g	500 g	500 g	500 g	500 g
Bentonite	25 g	25 g	25 g	25 g	25 g
KCl	5 g	5 g	5 g	5 g	5 g
XG	0.5 g	0.5 g	0.5 g	0.5 g	0.5 g
Grafted BN	0	0.05 g	0.15 g	1.0 g	1.5 g

Table 4.13: Formulation of drilling fluids containing grafted BN (in XG)

4.5.2. Coefficient of friction.

The mean values of the tribometer readings are summarized in **Figure 4-20**. The percentage change relative to the reference system was also included in the graph. The friction coefficient linearly dropped when the percent weight of nano-additives was increased. This trend was observed until the lowest friction value, which showed the system with 0.2 wt.% of BN grafted. At this point, the friction reduced by 43.9% compared to the base system. Higher addition of known particles did not show a decreasing trend. The fluid at the highest concentration of 0.3 wt.% showed a drop of friction coefficient by 33.7%. The minor improvement of 6% and 13% was noted for the systems containing grafted BN at 0.01 wt.% and 0.03 wt.% respectively.

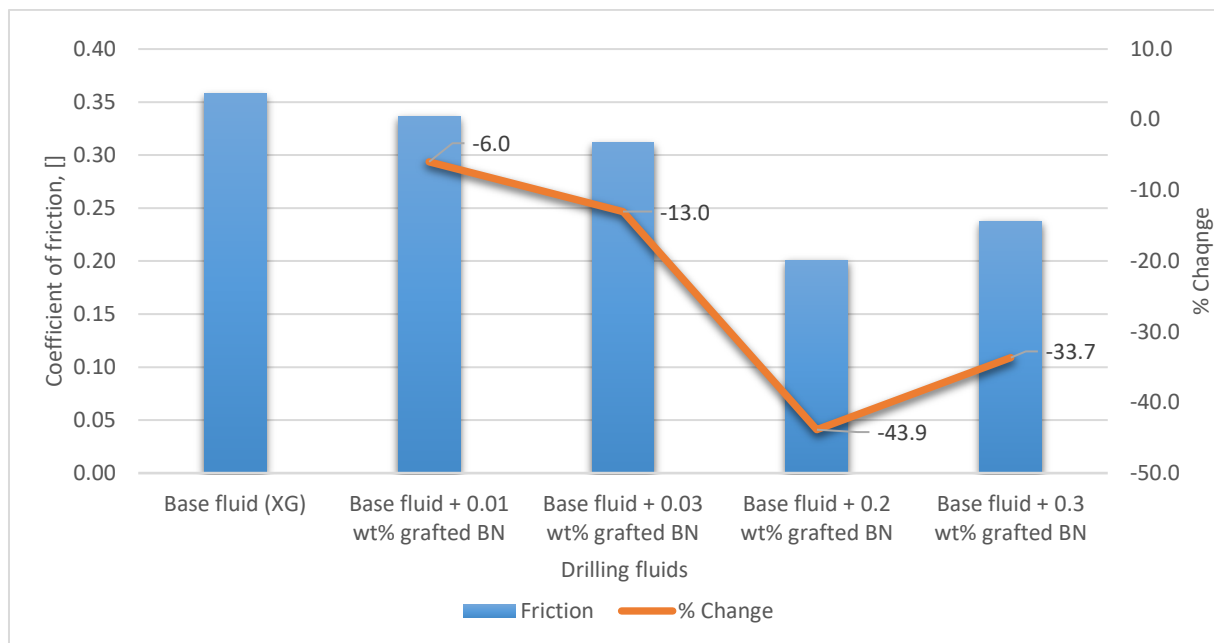


Figure 4-20: Effect of grafted BN (in XG) on the coefficient of friction

4.5.3. Rheology.

Figure 4-21 outlines the rheological response of the drilling fluids on the presence of grafted BN nanoparticles at various concentrations. Generally, the viscometer readings showed an increase for the nano-enhanced fluids as compared to the reference system. The readings surged when the base fluid was diluted with the little amount of BN grafted. However, the subsequent rise of concentration gradually decreased the shear stress values. Further insight was conducted by calculating and analyzing the Bingham and Power Law parameters.

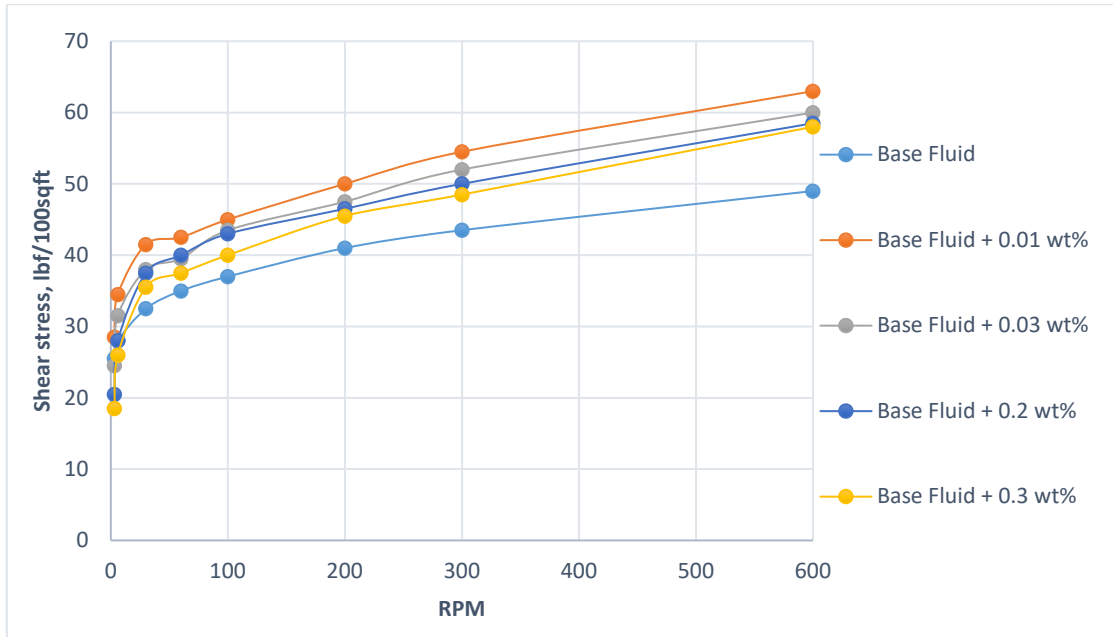


Figure 4-21: Effect of grafted BN (in XG) on the viscometer readings

As can be seen from **Figure 4-22**, the plastic viscosity and yield stress showed a step change when the grafted nanoparticles were added at the lowest concentration. Further increase of concentration resulted in a gradual decrease of the YS and a minor increase of PV. The LSYS had a decreasing trend and showed the lowest value for the fluid of 0.3 wt.% grafted BN.

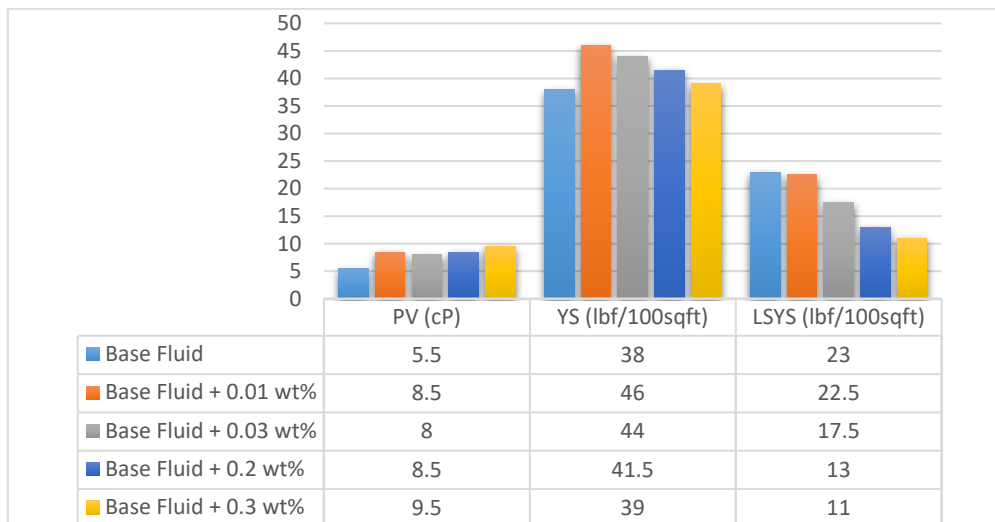


Figure 4-22: Effect of grafted BN (in XG) on the Bingham parameters

Chart 4-23 represents the effect of given additives on the Power Law parameters. There was observed a clear relationship between the parameters and the concentration. The k -value dropped progressively with increasing concentration. The most significant decline of

consistency index was documented as 35% for the fluid at saturation of 0.3% grafted BN. In contrast, the flow index rose linearly when more particles were introduced to the mixture. Again, the highest change (53%) was documented for the system with 0.3% of mentioned additives.

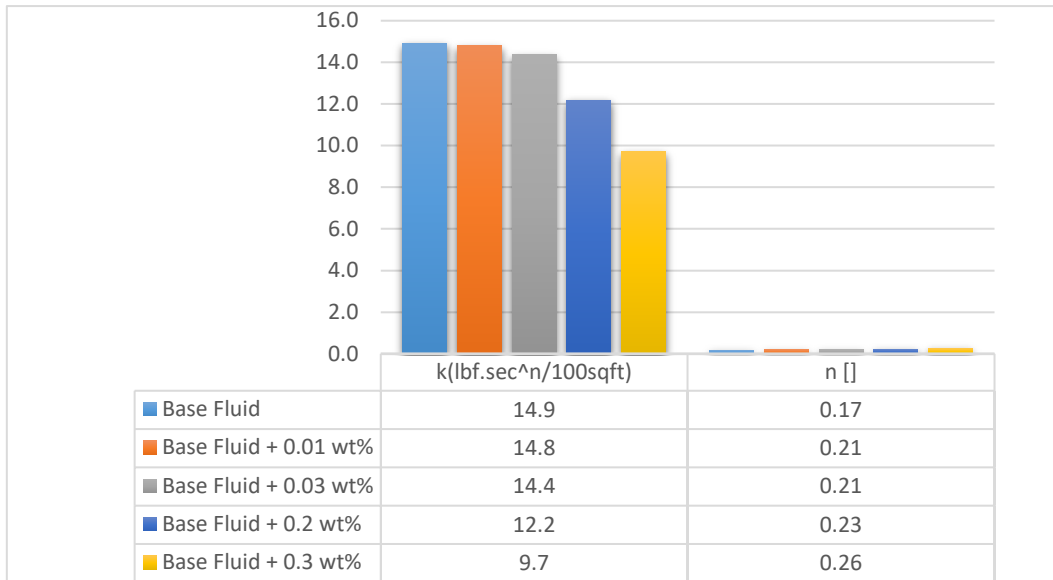


Figure 4-23: Effect of grafted BN (in XG) on the Power Law parameters

4.5.4. Filtration and pH.

Table 4.14 reflects the effect of grafted BN nanoparticles on the filtration properties of the drilling fluid. Similar to the case with Duovis polymer, the lowest concentration of known additives slightly improved filtration. However, the increased percent weight of particles uplifted the filtrate volume. The similar growth of 8.6% was noted for the fluids diluted with 0.2 wt.% and 0.3 wt.% of modified BN. The minor increase of 2.9% showed a system containing 0.02% of grafted BN.

	Base Fluid	Base Fluid + 0.01 wt.%	Base Fluid + 0.02 wt.%	Base Fluid + 0.2 wt.%	Base Fluid + 0.3 wt.%
Filtrate (ml)	7.0	6.8	7.2	7.6	7.6
% Change		-2.9%	2.9%	8.6%	8.6%

Table 4.14: Effect of grafted BN (in XG) on the filtration

The alkalinity of the experimental drilling fluids was presented in the table below. All the samples other than “Base fluid + 0.3 wt.% grafted BN” lowered the pH value as compared to

the reference fluid. However, the changes of the pH caused by the presence of nanoparticles did not exceed 2%.

	Base Fluid	Base Fluid + 0.01 wt.%	Base Fluid + 0.02 wt.%	Base Fluid + 0.2 wt.%	Base Fluid + 0.3 wt.%
pH	8.58	8.41	8.57	8.46	8.72
% Change		-2.0%	-0.1%	-1.4%	1.6%

Table 4.15: Effect of grafted BN (in XG) on the pH

4.6. Effect of BN/lubricant in Xanthan gum polymer.

According to the previous experiments with Duovis polymer, the best result concerning the lubricity can be achieved when BN nanoparticles are introduced into the system together with a lubricant. In this section, an attempt was made to check the performance of BN/lubricant mixture in the system having Xanthan gum (XG) as a polymer.

4.6.1. Drilling fluid formulation.

The procedure of preparation of BN/lubricant was similar to the one described before, i.e., the nanoparticles were added to the oil and mixed mechanically for 24 hours using magnetic stirrer. One should keep in mind that single concentrations of Boron nitride and lubricant could not be calculated since these two additives were mixed at approximate mass proportion. The most attractive results from the tribological tests with Duovis polymer served as the basis for the concentration selection for this fluid batch. Nano-BN mixed in lubricant was added to the mixture ex-situ. The composition and concentration of the tested fluid are shown in the table below.

	Base fluid	Base fluid + 0.12 wt%	Base fluid + 0.25 wt%	Base fluid + 0.3 wt%
Water	500 g	500 g	500 g	500 g
Bentonite	25 g	25 g	25 g	25 g
KCl	2.5 g	2.5 g	2.5 g	2.5 g
Xanthan gum	0.5 g	0.5 g	0.5 g	0.5 g
BN in lubricant	0	0.6 g	1.25 g	1.5 g

Table 4.16: Formulation of drilling fluids containing BN/lub (in XG)

4.6.2. Lubricity.

Figure 4-24 presents the tribological data of the fluids formulated in this section. As was mentioned earlier, the concentration of additives was chosen on the basis of the frictional readings from **Section §4.3.2**, where BN/lubricant was added to the base fluid with Duovis polymer. All the samples exhibited good results in terms of friction reduction. The effect was more significant when the concentration of the additives increased. The fluid with the lowest content of additives (0.12wt.%) showed 32% friction decrease; however, the best value of 54% lubricity improvement was recorded for the fluid with 0.3 wt.% percent weight of BN in lubricant.

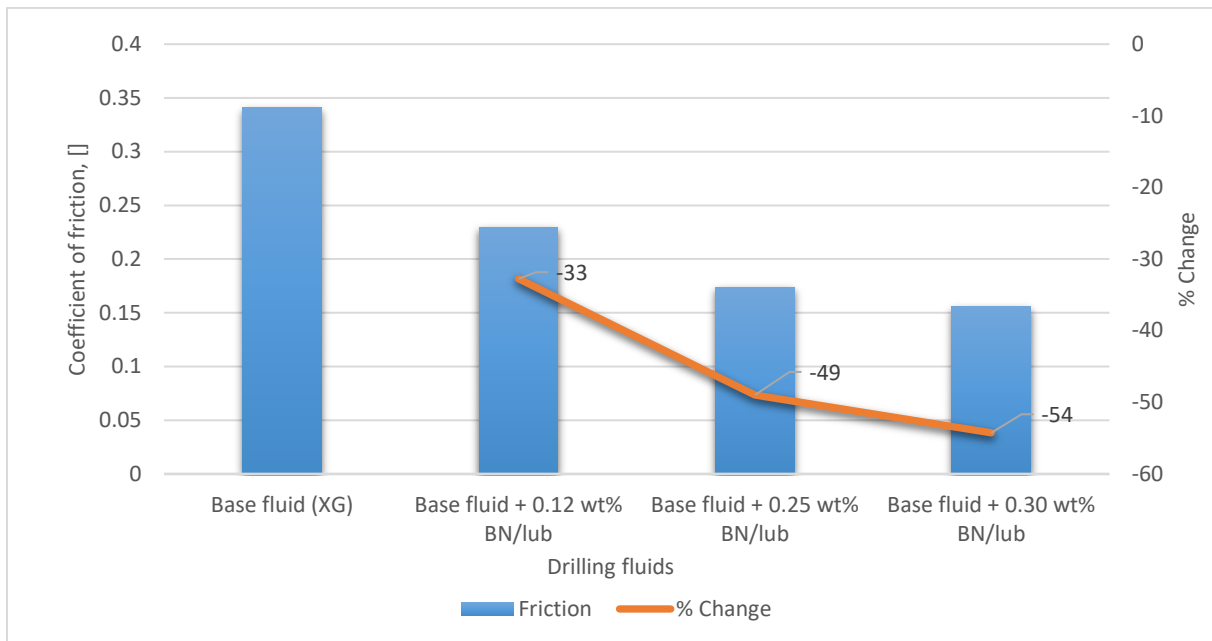


Figure 4-24: Effect of BN/lubricant (in XG) on the coefficient of friction

4.6.3. Rheology.

Figure 4-25 shows the viscometer data for the mixture of BN/lubricant and the base fluid. The readings revealed the consistent rise in shear stress values with increased concentration of BN/lubricant. There was a noticeable difference between the readings for the reference fluid and the fluids containing nano/lubricant. Calculating and analyzing Bingham and Power Law parameters allowed to study the rheological effect of additives more thoroughly (**Figure 4-26** and **Figure 4-27**).

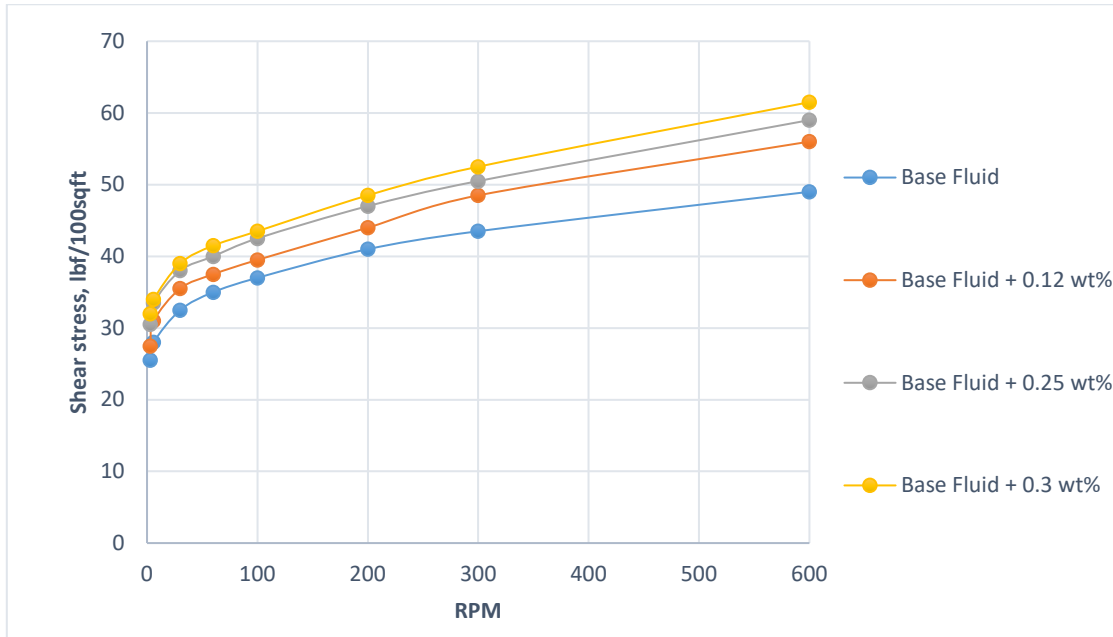


Figure 4-25: Effect of BN/lubricant (in XG) on the viscometer response

The Bingham parameters revealed a linear increase of PV, YS and LSYS for all the systems having BN/oil mixture as an additive. The most significant effect showed the highest concentration of additives. The addition of 0.3 wt.% of BN/oil increased the PV and YS by 63.6% and 30.4%, respectively. Yield stress value was less susceptible to the presence of BN/oil, showing a maximum rise of 14.5%.

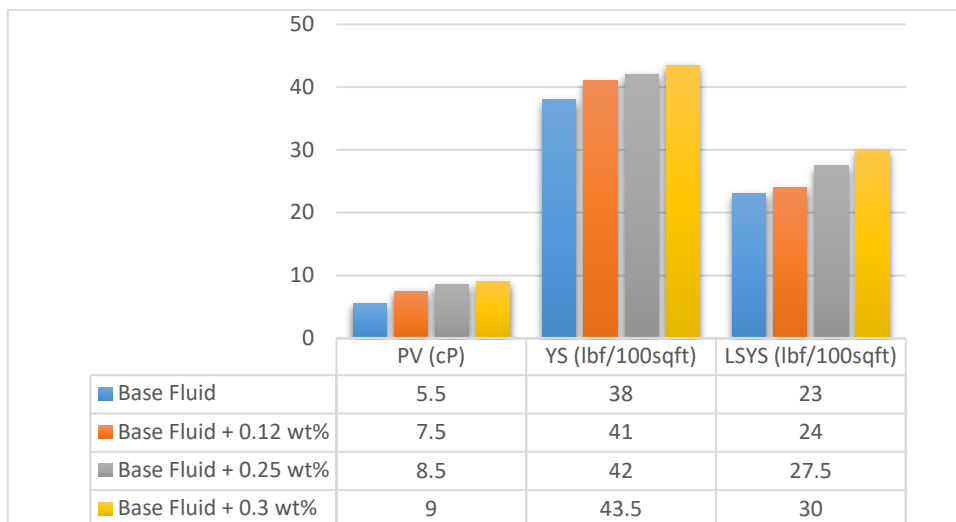


Figure 4-26: Effect of BN/lubricant (in XG) on the Bingham parameters

The consistency index values decreased for all samples with BN/oil additives as compared to the base fluid. The reduction was the most dramatic for the fluid with 0.25% of additives. This type of behavior was opposite as compared to the fluids with the same additives but having the Duovis as a polymer, where high concentration increased k -value. The flow index increased for all the systems in accordance with increased additive's weight; however, the fluids were still showing pseudo-plastic behavior.

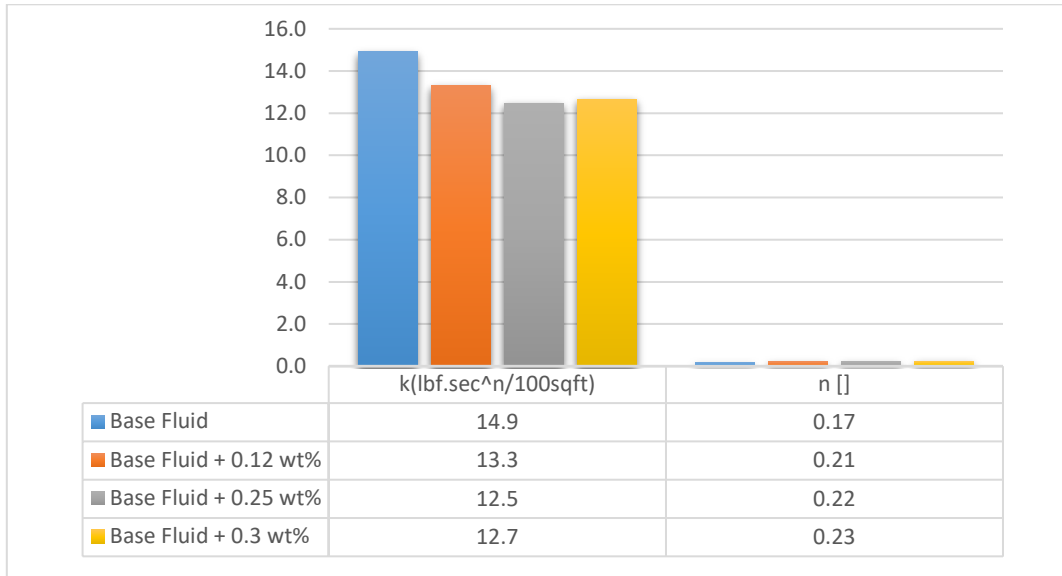


Figure 4-27: Effect of BN/lubricant (in XG) on the Power Law parameters

4.6.4. Filtration and pH.

The influence of BN/lubricant on the filtrate properties of Duovis-based fluid were presented in **Table 4.17**. In general, the additives at all concentrations increased the filtrate volume. The most significant effect showed the Nano/lubricant mixture at the concertation of 0.25% by weight. The system with 0.12 wt.% content of BN/oil exhibited a slight increase of 4.3%. The “Base fluid + 0.3 wt.%” percent weight of additives boosted the filtrate by 14.3%.

	Base Fluid	Base Fluid + 0.12 wt.%	Base Fluid + 0.25 wt.%	Base Fluid + 0.3 wt.%
Filtrate (ml)	7.0	7.3	8.7	8.0
% Change		4.3%	24.3%	14.3%

Table 4.17: Effect of BN/lub (in XG) on the filtration

Table 4.18 shows the dependency of pH on the presence of BN/lubricant mixture. pH value was not affected strongly by the presence of additives and showed slight changes from -0.7% to 1.2% only for the fluids with high concentration.

	<i>Base Fluid</i>	<i>Base Fluid + 0.12 wt.%</i>	<i>Base Fluid + 0.25 wt.%</i>	<i>Base Fluid + 0.3 wt.%</i>
pH	8.60	8.60	8.54	8.70
% Change		0.0	-0.7	1.2

Table 4.18: Effect of BN/lub (in XG) on the pH

4.7. Effect of nanocomposite (MWCNT-OH + BN/lubricant) in Duovis system.

The initial intention of this section was to test the effect of Hydroxyl functionalized multi-walled carbon nanotubes on the lubricating properties of the water-based mud. The fluids were formulated in the Duovis polymer following the same technique as described earlier. The screening study was performed to identify the most feasible concentration of MWCNT-OH capable of improving lubricity. However, the results (**Figure 4.28**) showed that the improvement was achieved only at high concentration. Moreover, the low addition of MWCNT-OH even deteriorated the original properties of the mud.

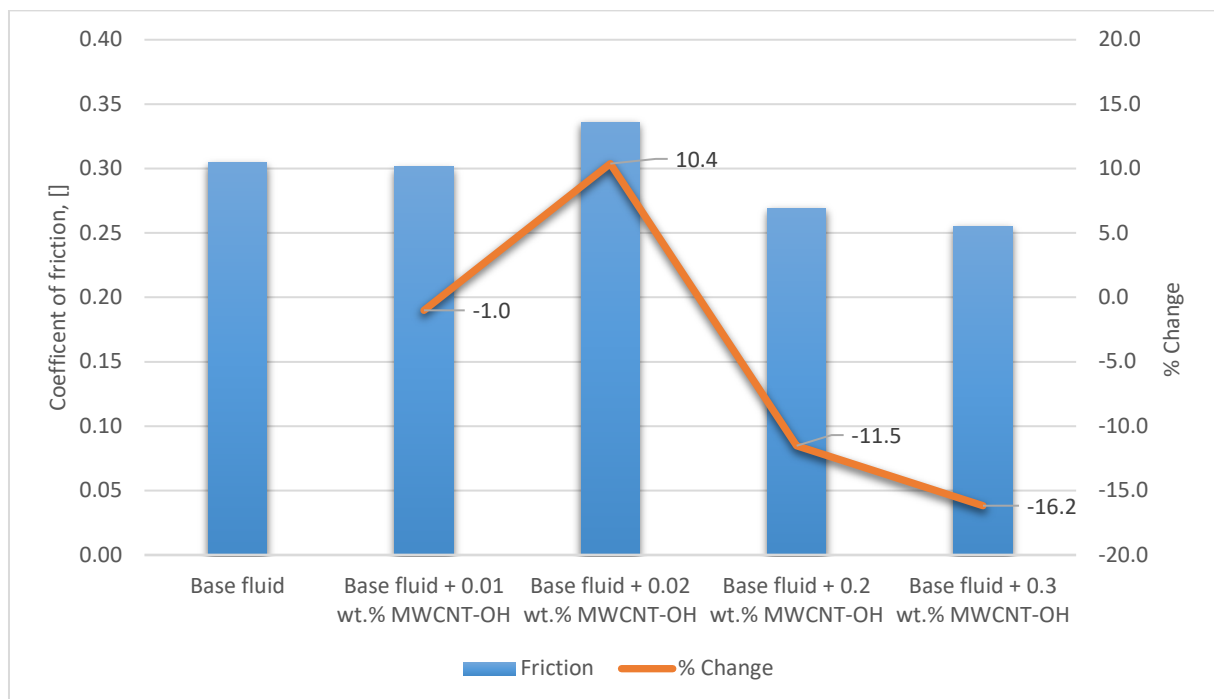


Figure 4-28: Effect of MWCNT-OH (in Duovis) on the coefficient of friction

The decision was made to take the specimen with the worst lubricating properties and combine with the BN nanoparticles mixed with a lubricant. The thinking behind that was to check the performance of the BN/lubricant additives in combination with other nanoparticles. The three samples with 0.02% MWCNT-OH were formulated, and later the BN/lubricant was added ex-situ.

It has been found that the addition of BN/lubricant to the system having the small concentration of 0.02% MWCNT-OH increased the lubricating properties of the fluid significantly. The graph below depicts the change in friction coefficient relative to the conventional drilling fluid as well as relative to the fluid already having the MWCNT-OH in the suspension. The presence of 0.14 wt.% BN/lubricant showed a decrease of around 30% relative to the fluid with a small amount of MWCNT-OH. The maximum friction reduction was observed when the “Base fluid + 0.02 wt.% MWCNT-OH” was diluted with 0.3 wt.% of BN/lubricant. This proportion yielded a drop more than half as compared to the system having MWCNT-OH nanoparticles as a single additive.

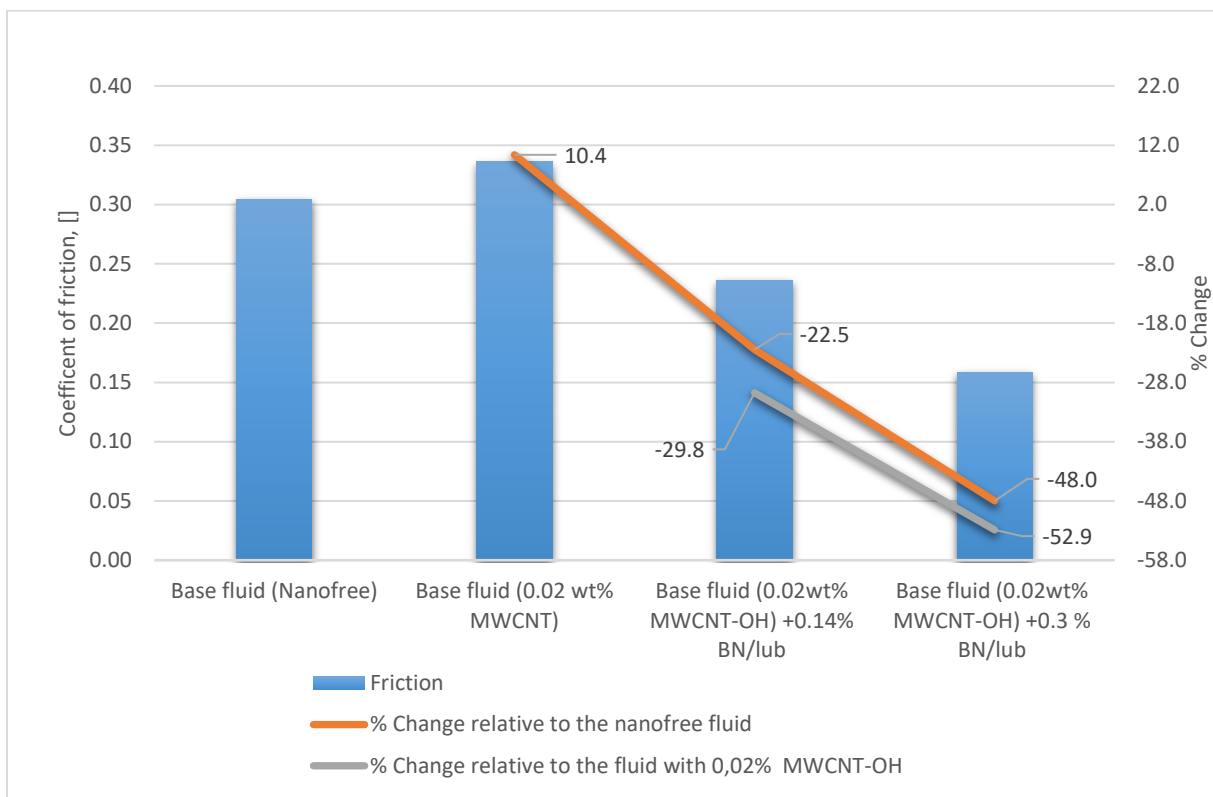


Figure 4-29: Effect of nanocomposite (in Duovis) on the coefficient of friction

4.8. Effect of mixing and pH on the lubricity.

This section evaluates the effect of different mixing techniques and pH on the friction coefficient. The fluids selected for these experiments contained dry Boron nitride nanoparticles, which were added in-situ. The weight ratio of nanoparticles in the mixtures was selected to see the effect of pH and mixing on the fluids with the highest and lowest concentrations.

4.8.1. Effect of mixing.

Strong intermolecular forces between nanoparticles facilitate agglomeration causing the stability problems in nanofluids [86]. Several publications have appeared in recent years documenting the effect of ultrasonic waves on the dispersion of solid dry nanoparticles. *W.U. Rehman et al. (2016)* carried out experimental work on Kapok Seeds oil (KSO) and Multi-Walled Carbon Nanotubes (MWCNTs) nanoparticles. They figured out that sonication has a significant effect on the dispersion of mentioned nanoparticles and reduce instability issues of the nano-containing mixtures. [87].

The purpose of these experiments was to determine the effect of sonication on the tribology of the fluids containing BN nanopowder. Three pairs of fluids were formulated and mixed mechanically, as was described in the previous sections. After mechanical blending, one fluid from each pair was subjected to a sonic bath for better agitation of particles. Sonication has been done for 1.5 hours at room temperature using the same sonicator as for the grafting (shown in **Figure 3-3 (a)**). One of the sets was tested with pH adjusting to evaluate the tribological response of sonicated fluids with high pH.

Figure 4-30 depicts the mean values of the lubricity coefficient for the fluids mixed mechanically and sonically. The friction values increased for all the samples subjected to the sonication, as compared to the fluids mixed in a traditional way. The rise in the coefficient of friction was marginal for the fluids with low concentrations of BN. The 7% increase was documented for the specimen with low pH and 5% increase in the fluid with adjusted pH. On the other hand, deterioration in tribological data was more noticeable for the sample with

high concentration of nanoparticles, where the friction for the sonicated fluid increased by 17% compared to the fluid mixed mechanically.

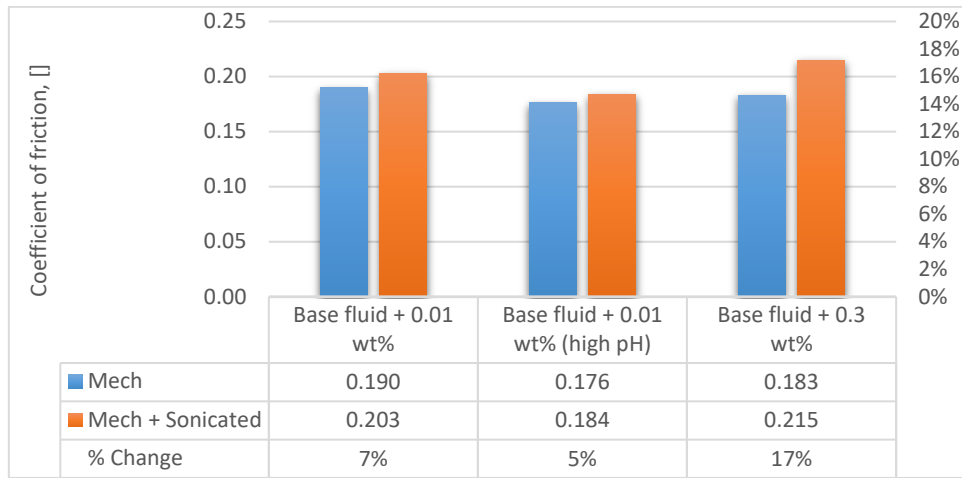


Figure 4-30: Effect of mixing on the coefficient of friction

4.8.2. Effect of pH.

Bar chart 4-31 shows how the pH of the mixture can influence the lubricating properties of the drilling mud. Two batches of the fluids, both having the low concentration of BN nanoparticles, were formulated for this experiment. The first fluid batch was mixed only with a mechanical mixer, whereas the second one was sonicated in addition. For both pairs, the fluids with high pH exhibited better lubricity values as compared to counterparts having low pH. 7% and 9% improvement was observed for the systems mixed in a mechanical and sonic way, respectively.

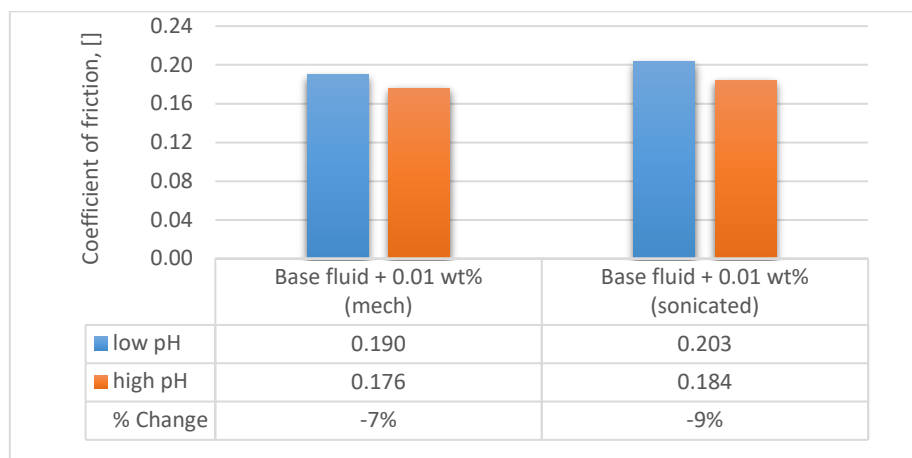


Figure 4-31: Effect of pH on the coefficient of friction

4.9. Effect of temperature on the rheology of BN nanoparticle treated fluids.

This section aims to study the rheological stability of the nano-enhanced drilling fluids against the elevated temperature. The base fluid along with the fluids containing various concentrations of dry BN nanoparticles was subjected to the analysis. The experimental samples were formulated in the presence of 0.04wt.% of Lignosulfonate, which serves as a thinner agent. The nanoparticles were added in-situ, and the Duovis polymer was used in the mixture. To investigate the temperature effect on the rheology, the viscometer data of the fluids were recorded at different temperatures. The samples were tested in the heating cup (**Figure 4.32**) where the temperature was gradually increased, and the readings were documented at 70 °F, 130 °F and 180 °F.



Figure 4-32: Viscometer along with the heating cup

Figure 4-33 shows the rheological response of the fluid with 0.01 wt.% dry Boron nitride nanoparticles at different temperatures. In general, the viscometer readings reduced with increasing temperature; however, the values for small RPM were almost identical. Further analysis was conducted by studying the Bingham and Power Law parameters.

The relationship between temperature and rheology of other experimental fluids is provided in **Appendix C**.

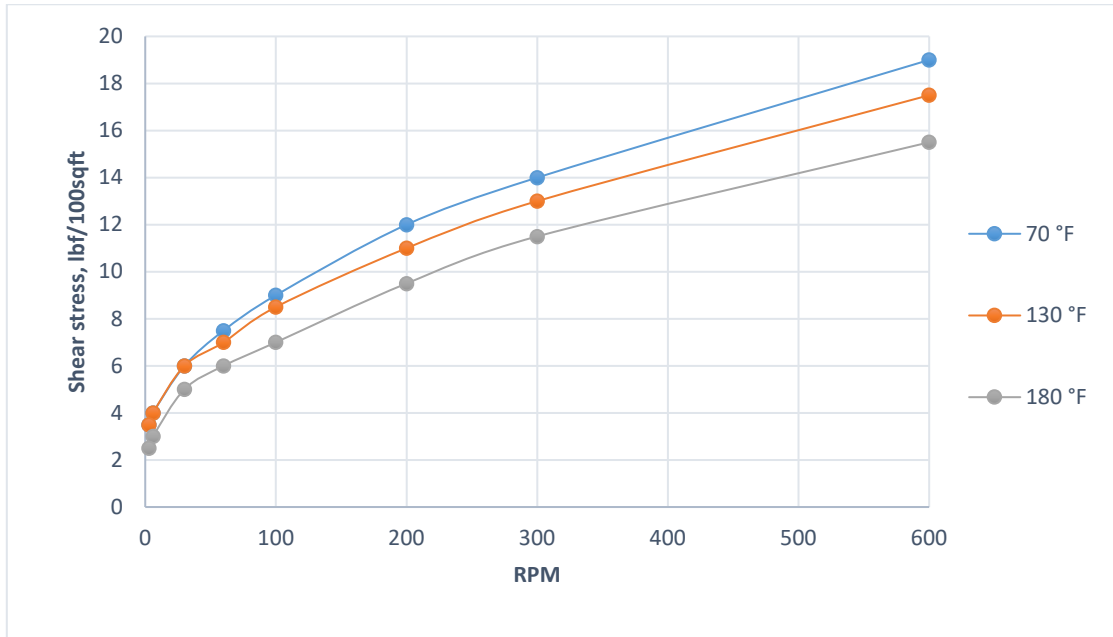


Figure 4-33: Effect of temperature on the viscometer readings of the nano-containing fluid

The Bingham parameters decreased when the temperature was raised (**Figure 4-34**). The reduction trend was fairly consistent for the plastic viscosity and yield stress; however, the values for the lower shear yield stress were constant at 70°F and 130°F. Further heating decreased the LSYS by 33%.

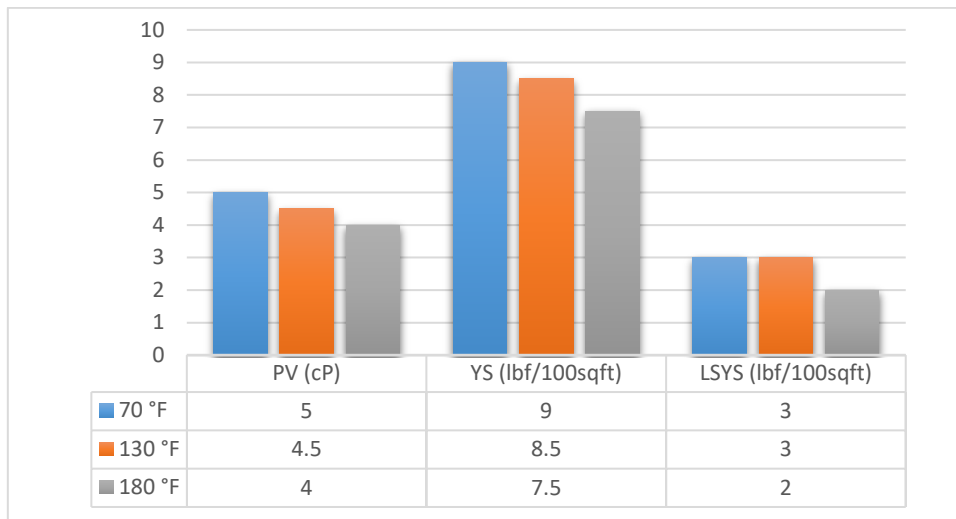


Figure 4-34: Effect of temperature on the Bingham parameters

The Power Law parameters are shown in **Graph 4-35**. The exponent law index (n) exhibited a constant behavior at all tested temperature ranges. On the other hand, the consistency index

slightly decreased when the fluid was heated to the maximum temperature. At lower temperature ranges the k -value remained unchanged.

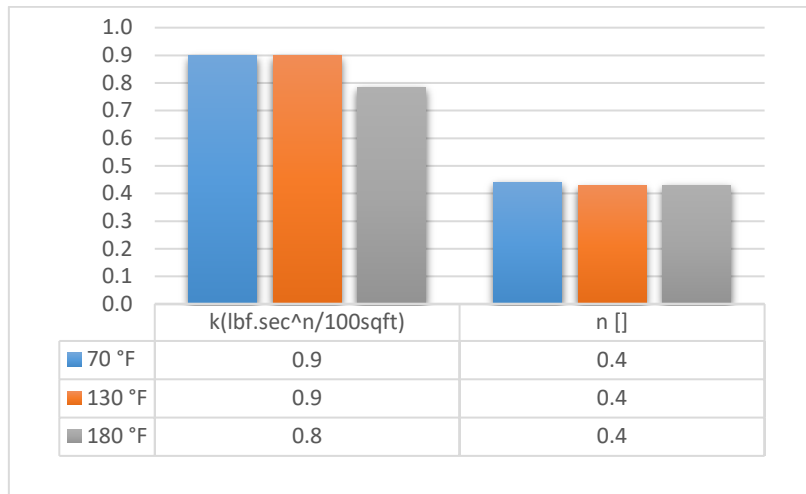


Figure 4-35: Effect of temperature on the Power Law parameters

4.10. Viscoelasticity.

This subchapter provides information about the effect of nano-additives on viscoelastic properties of the drilling fluids. The flow regime and pressure loss in circulation system are affected by the elastic properties of the mud. The gel strength, which defines the ability of the fluid to suspend the cuttings in a static condition, can be assessed by the viscoelastic test.

Based on the best tribological results, the nano-containing fluids with both Duovis and Xanthan Gum polymers were evaluated in this section and compared to the corresponding reference system (“Base fluid”). Only one fluid for each polymer was analyzed in details, whereas the remaining test results can be found in **Appendix B**. The selected drilling muds are presented in **Table 4.19**.

Polymer	Fluid System
Duovis	Base fluid
	Base fluid + 0.03 wt.% Dry BN
	Base fluid + 0.2 wt.% Grafted BN
	Base fluid + 0.16 wt.% BN/lubricant
	Base fluid + 0.3 BN/lubricant
Xanthan Gum	Base fluid
	Base fluid + 0.03 wt.% Dry BN
	Base fluid + 0.2 wt.% Grafted BN
	Base fluid + 0.12 wt.% BN/lubricant
	Base fluid + 0.3 BN/lubricant

Table 4.19: Drilling fluids used for viscoelasticity measurements

The An Anton Paar MCR 302 rheometer (**Figure 4.36**) was used to carry out the viscoelastic experiments. All the specimens were tested at room temperature with the invariable frequency of 10 rad/s. The shear stress, damping factor, storage modulus and loss modulus were plotted against the gradually increased strain from 0.000498% to 99.8%. For some samples, the curves representing storage and loss modulus were unstable. Thus, it was not possible to determine LVER. Instead, the information about the flow points for each fluid was retrieved and compared. As was mentioned in theory behind these experiments, the flow point corresponds to the point where the storage modulus and loss modulus intersect. The portion of the graph where storage modulus and loss modulus exhibits a constant behavior can be interpreted as a linear viscoelastic range (LVER).

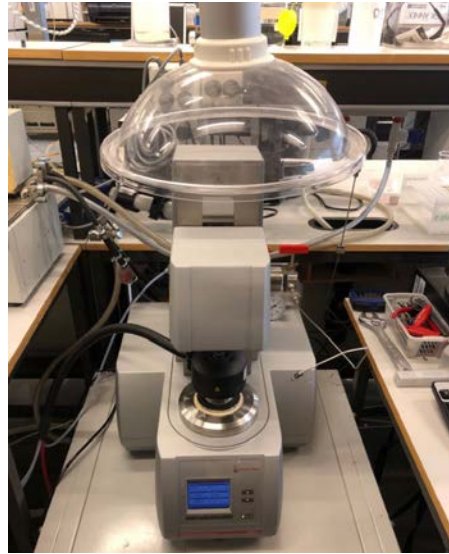


Figure 4-36: Rheometer

4.10.1. Oscillatory amplitude sweep test for Duovis-based fluids.

Figure 4-37 presents the oscillatory amplitude sweep measurements for the reference fluid formulated in Duovis polymer. The storage modulus (G') exceeds the loss modulus (G'') over the entire linear viscoelastic range indicating that the fluid was dominated by elastic properties and behaves like the viscoelastic gel. The shear stress at the strain, where the curves of storage modulus and loss modulus overlaps, corresponds to the flow point. At this point, the viscous and elastic portions are even, and the loss angle is equal to 45° . After the strain exceeds the flow point, the behavior is prevailed by viscous properties, and the fluid starts to flow.

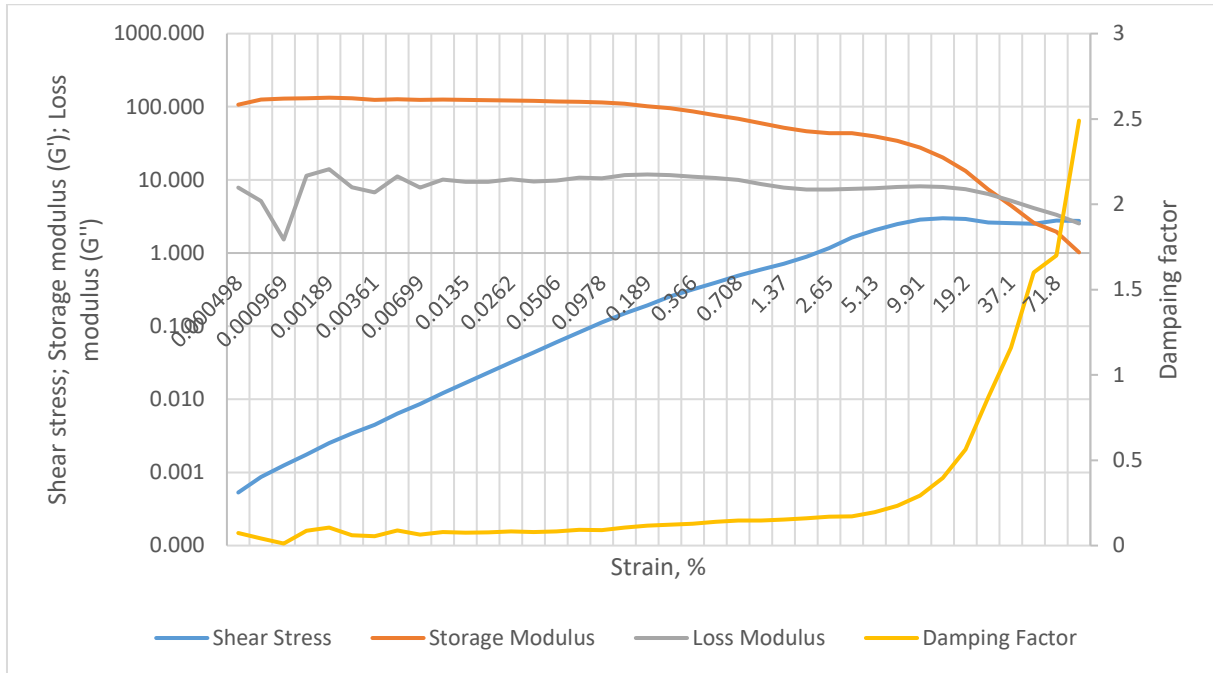


Figure 4-37: Plot of amplitude sweep measurements for the base fluid (Duovis)

The bar chart below depicts the flow point shear stress values for the Duovis-based samples. From the figure, it can be seen that presence of unmodified or modified particles increased the flow point, while the particles together with a lubricant at the concentration of 0.16 wt.% reduced the flow point. The most significant impact showed the addition of 0.2 wt.% grafted particles (rise with 48,26%). Presence of 0.16 wt.% BN/lubricant decreased the flow point by 19.31%. Whereas the highest concentration of additives (0.3 wt.%) barely affected the flow point, showing a minor increase of 1,54% as compared to the reference fluid.

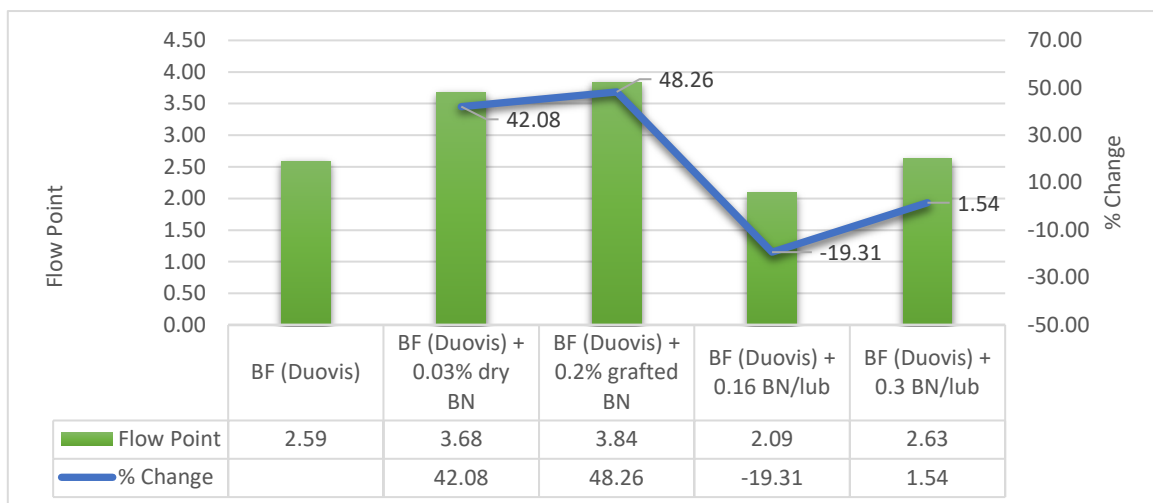


Figure 4-38: Effect of the nano-additives on the flow point (Duovis)

4.10.2. Oscillatory amplitude sweep test for XG-based fluid.

Figure 4-39 illustrates the oscillatory amplitude sweep measurements for the reference fluid formulated in the Xanthan Gum polymer. Similar to the Base fluid with Duovis polymer, the storage modulus curve was higher than the loss modulus on the entire strain range before the flow point, indicating that fluid verified gel-like behavior. However, the flow point was more than two times higher for this specimen, as compared to the previous case.

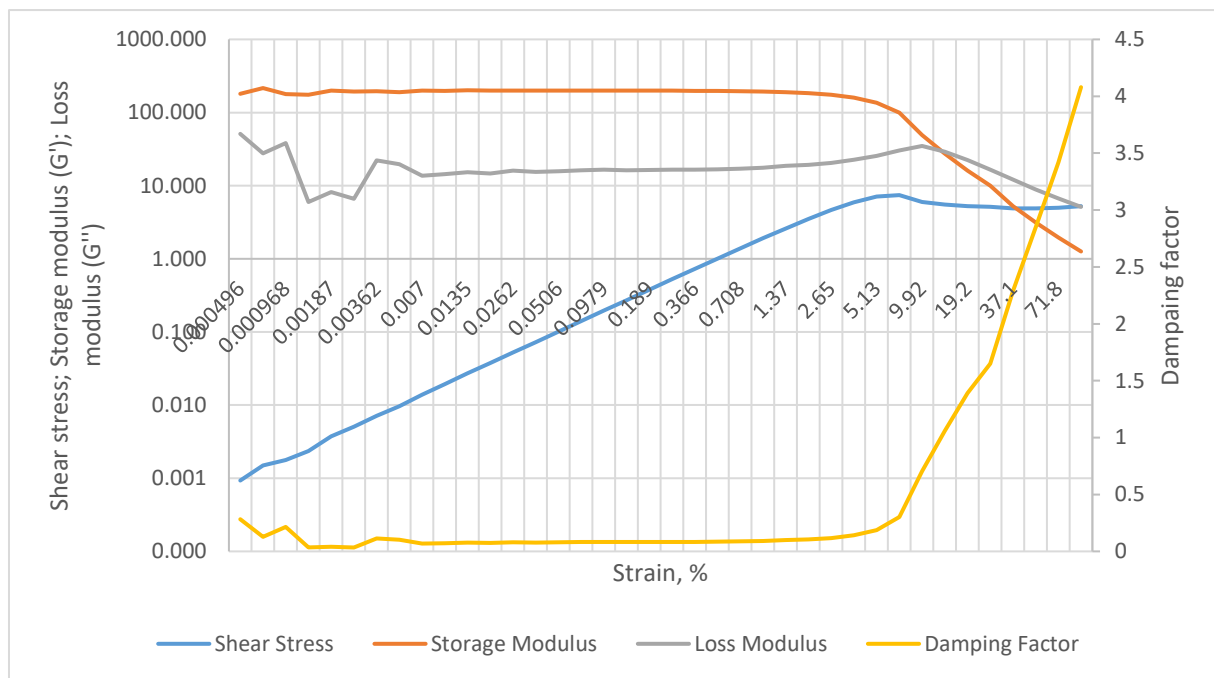


Figure 4-39: Plot of amplitude sweep measurements for the base fluid (XG)

The effect of nano-additives on the flow point of the fluids formulated in Xanthan gum system has been illustrated in **Chart 4-40**. All tested additives increased the flow point of the reference fluid. The presence of dry BN nanoparticles at the concentration of 0.03% by weight did not show any strong effect on the flow point of the reference fluid. On the other hand, the flow point surged by 139.25% when 0.2 wt.% of grafted BN particles were added to the base fluid. The addition of 0.12 wt.% of BN/lub almost doubled the flow point value. The most significant increment to the flow point was observed by addition of 0.3% BN/oil, which showed an increase of 215.19%.

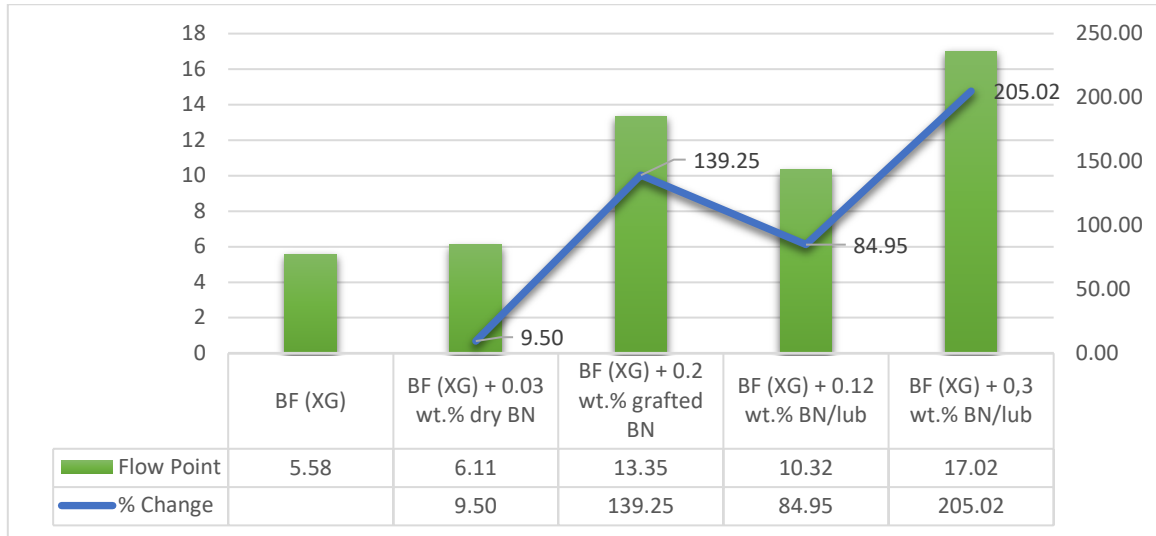


Figure 4-40: Effect of the nano-additives on the flow point (XG)

5. SIMULATION STUDY.

This chapter presents the application of experimental results in the simulation study to analyze decisive parameters for successful drilling operations. The chapter comprises the rheological modeling, torque and drag simulations, hydraulics and hole cleaning simulations. The procedure of the simulations was initiated with the selection of fluid systems in accordance with the best tribological results. First, the rheological modeling was conducted to evaluate the correlation of the drilling fluids with selected rheological models. The torque and drag simulations allowed to compare the maximum well length of the wells drilled with nano-enhanced and conventional fluids. Furthermore, the simulation of hole cleaning efficiency was performed to analyze the capability of selected fluids to transport cuttings; whereas the hydraulic modeling afforded to compare frictional pressure loss and ECD in circulation loop. Simulation results contributed to the selection of the additives and concentrations capable of operating in real well conditions.

5.1. Rheological modeling.

The primary objective of this section was finding a model that more accurately describes the rheological behavior of the formulated drilling fluids. The Fann Viscometer readings were used as input data in excel calculator to compute the parameters according to the following rheological models:

- Bingham Plastic model.
- Power Law model.
- Herschel-Bulkley model.
- Robertson-Stiff model.
- Unified model.

The drilling muds are mainly non-Newtonian fluids; therefore, the Newtonian model was not considered in this simulation study. Trend lines were plotted for each model, and percent deviation between the model and the original measurements was calculated. Additionally, the corresponding equations with relevant parameters were generated.

5.1.1. Rheological modeling of the Duovis-based fluids.

This section presents the rheological modeling of the fluids formulated in Duovis system. Based on the study of the friction, the fluids with dry Boron Nitride nanoparticles, grafted Boron Nitride nanoparticles and Boron Nitride nanoparticles mixed in a lubricant were analyzed along with the nano-free reference system. **Matrix 5.1** summarizes the systems selected for the study.

<i>Polymer</i>	<i>Nano-additives</i>	<i>Concentrations</i>
Duovis	Nano-free Base fluid	-
	Dry BN	0.03 wt.%
	Grafted BN	0.2 wt.%
	BN with lubricant	0.16 wt.%
	BN with lubricant	0.3 wt.%

Table 5.1: Duovis-based drilling fluids used for rheological modelling

5.1.1.1. Reference fluid (Duovis)

In this section, the rheological analysis of the Duovis-based reference fluid was carried out. **Figure 5-1** illustrates the trend-lines of different models along with the Fann viscometer measurements. The relevant equations for each model and parameters were presented in **Table 5.2**.

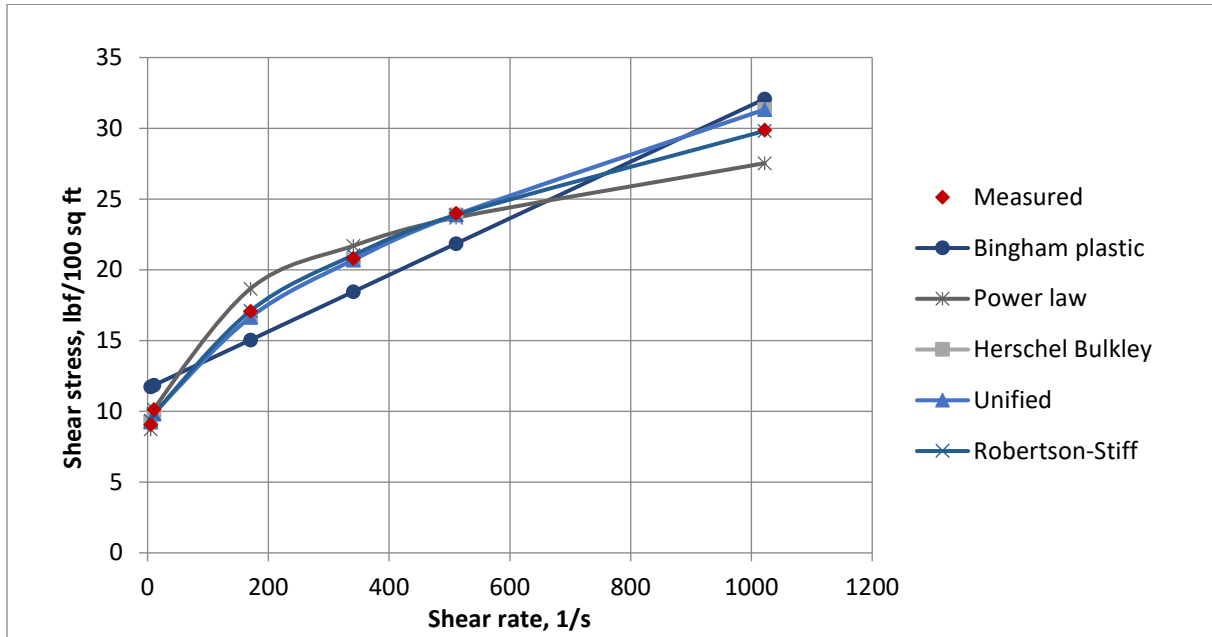


Figure 5-1: Modelled trend-lines along with measured data for the Base fluid (Duovis)

As seen from the graph, the Bingham plastic model failed to follow the pattern of measurements and showed a deviation about 14.3%. The Power Law model overestimated the values at low shear rates; however, when the shear rate exceeded 500 s^{-1} , the measured data exceeded the values predicted by this model. The error of this model was approximately 4.4%. The Herschel-Bulkley and Unified models showed approximately similar deviations from original data, about 2.2%. The most precise model among others was Robertson-Stiff model, which showed an error of 1.37%.

Model	Equation	Parameters				% Deviation	cP
		τ_0, τ_y, A	k, C	n, B	μ_p		
Bingham	$11.639 + 0.02 \cdot \gamma$	11.639			0.0200	14.3	9.576
Power Law	$6.1296 \cdot \gamma^{0.2168}$		6.1296	0.2168		4.44	
Herschel-Bulkley	$8.009 + 0.5015 \cdot \gamma^{0.5541}$	8.009	0.5015	0.55410		2.23	
Unified	$8.003 + 0.5049 \cdot \gamma^{0.5531}$	8.003	0.5049	0.5531		2.2	
Robertson-Stiff	$2.9497 \cdot (26.838 + \gamma)^{0.3326}$	2.9497	26.8380	0.3326		1.37	

Table 5.2: Modelled equations for the Base fluid (Duovis)

5.1.1.2. Reference fluid (Duovis) + 0.03 wt.% dry BN.

This section contains the review of the rheological models regarding the fluid with 0.03 wt.% of dry Boron nitride nanoparticles. The trend lines of different models and the table with the parameters and errors are shown below.

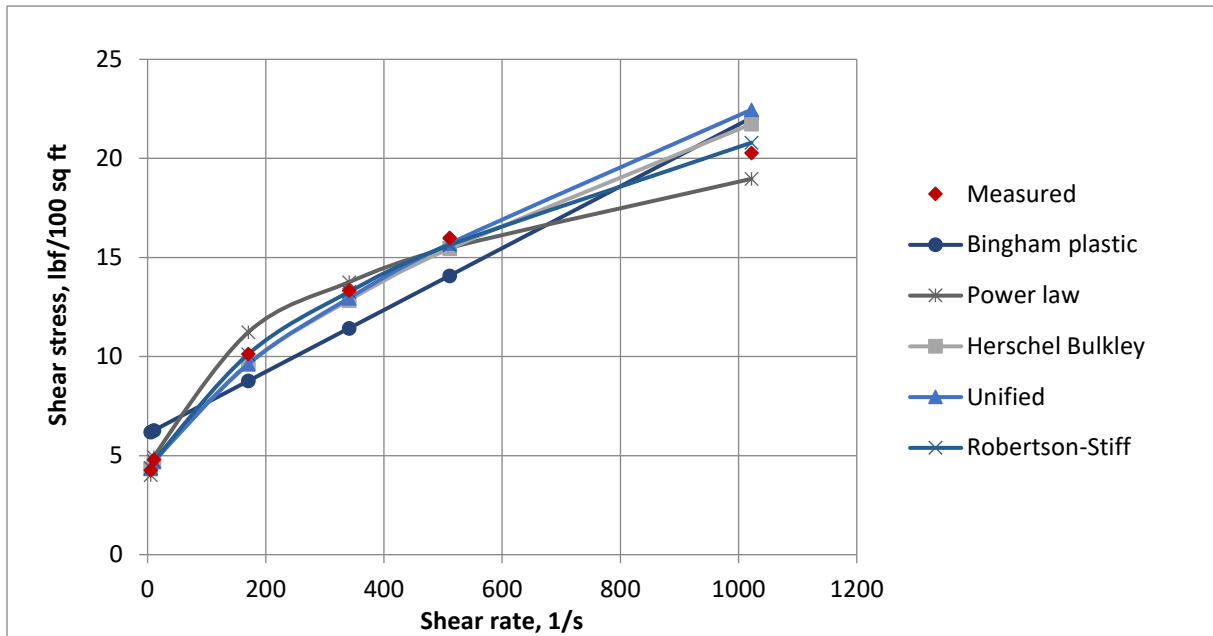


Figure 5-2: Modelled trend-lines along with measured data for the “Base fluid + 0.03 wt.% dry BN” (Duovis)

For the drilling fluid having 0.03 wt.% of dry BN nano-additives, the Robertson-Stiff model was the most suitable, which deviates only by 1.67 percent from the original data. The Bingham model had the highest deviation percentage of 20.71%. The rest of models described the fluid with the error range from 3.82% to 5.32%.

Model	Equation	Parameters				% Deviation	cP
		τ_0, τ_y, A	k, C	n, B	μ_p		
Bingham	$6.111 + 0.0156 * \gamma$	6.111			0.0156	20.71	7.46928
Power Law	$2.4959 * \gamma^{0.2927}$		2.4959	0.2927		5.32	
Herschel-Bulkley	$3.642 + 0.2532 * \gamma^{0.6161}$	3.642	0.2532	0.6161		3.82	
Unified	$3.735 + 0.213 * \gamma^{0.646}$	3.735	0.213	0.646		4.14	
Robertson-Stiff	$1.0827 * (21.5633 + \gamma)^{0.4252}$	1.0827	21.5633	0.4252		1.67	

Table 5.3: Modelled equations for the “Base fluid + 0.03 wt.% dry BN” (Duovis)

5.1.1.3. Reference fluid (Duovis) + 0.2 wt.% grafted BN.

From this section onwards, only the table with the rheological parameters for each model, accommodating equations and deviations from the original data will be presented. The chart below depicts the results of the rheological study conducted for the fluid with 0.2 wt.% modified BN nanoparticles. The Bingham model illustrated a significant deviation from the original data and was not considered as a proper model to describe the behavior of the given fluid. The remaining models were quite accurate showing a deviation of around 3%. Nevertheless, the performance of the Robertson-Stiff model seemed to be the most precise among others.

Model	Equation	Parameters				% Deviation	cP
		τ_0, τ_y, A	k, C	n, B	μ_p		
Bingham	$14.289 + 0.0247*\gamma$	14.289			0.0247	16.01	11.82636
Power Law	$7.2397*\gamma^{0.2247}$		7.2397	0.2247		3.22	
Herschel-Bulkley	$8.843 + 0.9389*\gamma^{0.4967}$	8.843	0.9389	0.4967		2.74	
Unified	$9.070 + 0.8152*\gamma^{0.5179}$	9.070	0.8152	0.5179		3.08	
Robertson-Stiff	$4.1884*(17.6043+\gamma)^{0.3117}$	4.1884	17.6043	0.3117		2.27	

Table 5.4: Modelled equations for the "Base fluid + 0.2 wt.% grafted BN" (Duovis)

5.1.1.4. Reference fluid (Duovis) + 0.16 wt.% BN/lubricant.

The following table outlines the results of the rheological modelling of the fluid with 0.16 wt.% of BN mixed in oil. As for the previous fluids, the Robertson-Stiff model fitted the viscometer data in the best way. Power Law, Herschel-Bulkley and Unified models exhibited the deviation from 2.61% to 3.05%. The Bingham model experienced a substantial error of 16.34%.

Model	Equation	Parameters				% Deviation	cP
		τ_0, τ_y, A	k, C	n, B	μ_p		
Bingham	$13.639 + 0.0217*\gamma$	13.639			0.0217	16.34	10.38996
Power Law	$7.0293*\gamma^{0.216}$		7.0293	0.216		2.75	
Herschel-Bulkley	$8.301 + 0.9838*\gamma^{0.4744}$	8.301	0.9838	0.4744		2.61	
Unified	$8.536 + 0.8503*\gamma^{0.4961}$	8.536	0.8503	0.4961		3.05	
Robertson-Stiff	$4.2585*(16.5839+\gamma)^{0.2957}$	4.2585	16.5839	0.2957		1.86	

Table 5.5: Modelled equations for the "Base fluid + 0.16 wt.% BN/lub" (Duovis)

5.1.1.5. Reference fluid (Duovis) + 0.3 wt.% BN/lubricant.

The error values presented in **Table 5.6** depicts the highest deviation of 14.93% for the Bingham model. Except for the Robertson-Stiff (0.97% deflection), the remaining models exhibited errors higher than 2.54%. Therefore, the model, which suits the data with less deflection, was selected to be the Robertson-Stiff model.

Model	Equation	Parameters				% Deviation	cP
		τ_0, τ_y, A	k, C	n, B	μ_p		
Bingham	$15.665 + 0.0246*\gamma$	15.665			0.0246	14.93	11.77848
Power Law	$8.3637*\gamma^{0.2085}$		8.3637	0.2085		3.88	
Herschel-Bulkley	$10.84 + 0.6426*\gamma^{0.5526}$	10.840	0.6426	0.5526		2.54	
Unified	$11.204 + 0.4677*\gamma^{0.6011}$	11.204	0.4677	0.6011		3.47	
Robertson-Stiff	$4.5223*(22.4858+\gamma)^{0.3061}$	4.5223	22.4858	0.3061		0.97	

Table 5.6: Modelled equations for the "Base fluid + 0.3 wt.% BN/lub" (Duovis)

5.1.1.6. Model matching and comparison.

The bar chart below depicts the deviation of the rheological models for all the simulated fluids with Duovis as a polymer. The analysis of the data can be summarized as follows: the Bingham model had the most significant deviation for all the selected fluids; on the other hand, the Robertson-Stiff model was most reliable and described the rheological parameters of the fluids with errors from 1% to 2.3%. The Power Law, Herschel-Bulkley and Unified models delineated the pattern of the measured rheological values with varied success exhibiting a deviation of 2.2% - 5.6%.

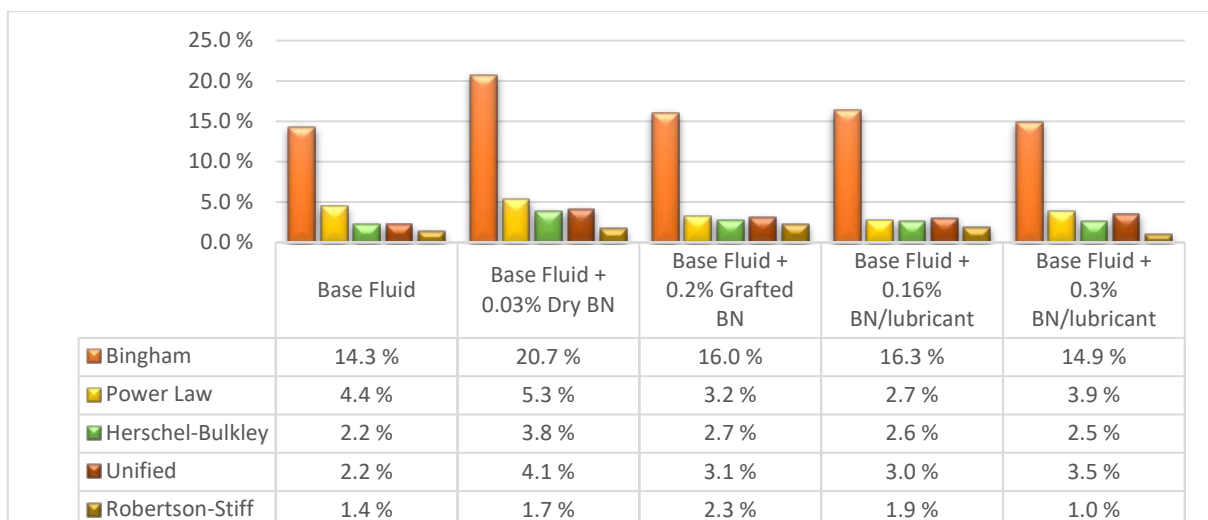


Figure 5-3: Deviation of the rheological models from the measured data (Duovis-based samples)

5.1.1.7. Effect of nano-additives in Duovis system on the rheological parameters.

Table 5.7 brings together the rheological parameters of the chosen fluids. The parameters of nano-enhanced fluids were compared to those of the nano-free base mud and the deviation in percentage was included in the table.

		Base fluid (Duovis)	Base fluid + 0.03 wt.% Dry BN	Base fluid + 0.2 wt.% Grafted BN	Base fluid + 0.16 wt.% BN/lub	Base fluid + 0.3 wt.% BN/lub
Bingham	τ_y	11.639	6.111	14.289	13.639	15.665
	% deviation		<u>-47.5%</u>	<u>22.77%</u>	<u>17.18%</u>	<u>34.59%</u>
	μ_p	0.02	0.0156	0.0247	0.0217	0.0246
	% deviation		<u>-22%</u>	<u>23.5%</u>	<u>8.5%</u>	<u>23%</u>
Power Law	k	6.1296	2.4959	7.2397	7.0293	8.3637
	% deviation		<u>-59.28%</u>	<u>18.11%</u>	<u>14.68%</u>	<u>36.45%</u>
	n	0.2168	0.2927	0.2247	0.216	0.2085
	% deviation		<u>35.01%</u>	<u>3.64%</u>	<u>-0.37%</u>	<u>-3.83%</u>
Herschel-Bulkley	τ_o	8.009	3.642	8.843	8.301	10.84
	% deviation		<u>-54.53%</u>	<u>10.41%</u>	<u>3.65%</u>	<u>35.35%</u>
	k	0.5015	0.2532	0.9389	0.9838	0.6426
	% deviation		<u>-49.51%</u>	<u>87.22%</u>	<u>96.17%</u>	<u>28.14%</u>
	n	0.5531	0.6161	0.4967	0.4744	0.5526
	% deviation		<u>11.39%</u>	<u>-10.2%</u>	<u>-14.23%</u>	<u>-0.09%</u>
Unified	τ_y	8.003	3.735	9.070	8.536	11.204
	% deviation		<u>-53.33%</u>	<u>13.33%</u>	<u>6.66%</u>	<u>40%</u>
	k	0.5049	0.213	0.8152	0.8503	0.4677
	% deviation		<u>-57.81%</u>	<u>64.46%</u>	<u>68.41%</u>	<u>-7.37%</u>
	n	0.5531	0.646	0.5179	0.4961	0.6011
	% deviation		<u>16.8%</u>	<u>-6.36%</u>	<u>-10.31%</u>	<u>8.68%</u>
Robertson-Stiff	A	2.9497	1.0827	4.1884	4.2585	4.5223
	% deviation		<u>-63.29%</u>	<u>41.99%</u>	<u>44.37%</u>	<u>53.31%</u>
	C	26.838	21.5633	17.6043	16.5839	22.4858
	% deviation		<u>-19.65%</u>	<u>-34.41%</u>	<u>-38.21%</u>	<u>-16.22%</u>
	B	0.3326	0.4252	0.3117	0.2957	0.3061
	% deviation		<u>27.84%</u>	<u>6.28%</u>	<u>-11.09%</u>	<u>-7.97%</u>

Table 5.7: Rheological modelling summary of the Duovis-based fluids

The summary of the table:

- **Biggam model:** The yield stress (τ_y) of the simulated sample with dry BN nanoparticles decreased by 47.5%; on the other hand, the fluids with grafted BN and BN/oil as an additive exhibited an opposite effect, which indicates that higher shear stress needs to be applied to launch the flow. Addition of grafted particles yielded an increased of 22.77%. BN/lubricant at the concentration of 0.16 wt.% and 0.3 wt.% showed a growth of 17.18% and 34.59%, respectively. The plastic viscosity of the fluids containing modified BN and BN/oil additives increased, as compared to the base system. The increment for the fluid containing 0.3% of BN mixed in oil and for the fluid with grafted BN was around 23%. The fluid with 0.16 percent weight of BN/oil increased the PV by 8.5%. On the other hand, the plastic viscosity of the specimen with 0.03% dry particles dropped by 22%.
- **Power Law:** The consistency index decreased for the “Base fluid + 0.03 wt.% Dry BN” by almost 60%, while the fluids either with BN/lubricant or modified BN exhibited an increase from 14.68% to 36.45% in accordance with increased concentration. Meanwhile, the flow behavior index rose by 35% for the fluid with dry BN and varied insignificantly for the remaining fluids.
- **Herschel-Bulkley:** The yield stress value (τ_0) dropped by more than half (54.53%) for the system with dry BN at 0.03% mass ratio, whilst the presence of grafted particles or BN/oil addition showed an increase of this value. The change of the τ_0 value for the fluids with 0.16% and 0.3% BN/oil was 3.65% and 35.35%, respectively. The introduction of modified nanoparticles increased the yield stress by 10.41%. The consistency index reduced by 49.51% for the fluid with dry particles, while the “Base fluid + 0.16% BN/lubricant” or the “Base fluid + 0.2% grafted BN” almost doubled the k -value. The system with the highest content of additives (0.3 wt.% BN/oil) showed an increase of consistency index by 28.14%. The flow behavior index rose by 11.39% when dry BN particles were added at 0.03%; in contrast to the other three fluids, which showed the reduction of n -value up to 14.23%
- **Unified model:** The lower shear yield point (τ_y) increased when the base fluid was diluted with BN/oil additives with the rise in percentage by 6.66% for the fluid with 0.16 wt.% concentration and by 40% for the fluid with 0.3 wt.% of additives. An increase of 13.33%

was also observed for the fluid with 0.2% grafted BN. On the other hand, dry BN particles at 0.03% percent ratio lowered the τ_y value sharply by 53.33%. The k -value dropped with 57.81% for the “Base fluid + 0.03 wt.% Dry BN” and 7.37% for the “Base fluid + 0.3 wt.% BN/lubricant”; whilst it surged by average 66% percent for the “Base fluid + 0.16 wt.% BN/lubricant” and the “Base fluid + 0.2 wt.% Grafted BN”. The n -value showed a rise of 16.8% and 8.68% for the fluids with 0.03 wt.% dry BN and 0.3% BN/oil, respectively. However, this parameter increased by average 8% for the remaining two fluids.

- **Robertson-Stiff:** The A-parameter, which is similar to the k -value of Power Law model, dropped significantly by 63.29% for the sample with dry nanoparticles, while the growth of around 50% was observed for the rest three samples. The B parameter (similar to the n -value) climbed by 27.84% for the “Base fluid + 0.03 wt.% Dry BN” and decreased by average 10% for the specimens containing BN/oil. The fluid having grafted BN showed a growth of 6.28%. The C value decreased for all samples. The most prominent drops of 38.21% and 34.41% were noted for the fluids with 0.16% BN/oil and 0.2% BN modified, respectively. The remaining fluids showed a fall of 18 percent on average.

5.1.2. Rheological modeling of the XG based fluids.

This section provides information about rheological modeling of the fluids formulated in the Xanthan gum system. The fluid selection is summarized in **Table 5.8**. Instead of giving a thorough review of each fluid system along with figures and tables, only the chart with model deviation and the table of models’ comparison have been presented.

<i>Polymer</i>	<i>Nano-additives</i>	<i>Concentrations</i>
Xanthan Gum	Nano-free Base fluid	-
	Dry BN	0.03 wt.%
	Grafted BN	0.2 wt.%
	BN with lubricant	0.12 wt.%
	BN with lubricant	0.3 wt.%

Table 5.8: XG-based drilling fluids used for rheological modelling

5.1.2.1. Model matching and comparison.

The given diagram demonstrates the deviation of the models from the measurements of each system. As in the case with Duovis polymer, the highest deviation was observed for the Bingham model. The Power Law model described the Base fluid and the fluid with 0.03 wt% of dry BN particles with sufficient accuracy (around 2% error); however, for other systems, the deviation almost doubled. The performance of Herschel-Bulkley, Robertson-Stiff and Unified models varied from system to system, but, in general, they all exhibited quite good cohesion to the original data having an average deviation of 2.4%. It should be noted that all the models exhibited the highest error value for the fluid containing grafted nanoparticles as compared to the other simulated fluids.

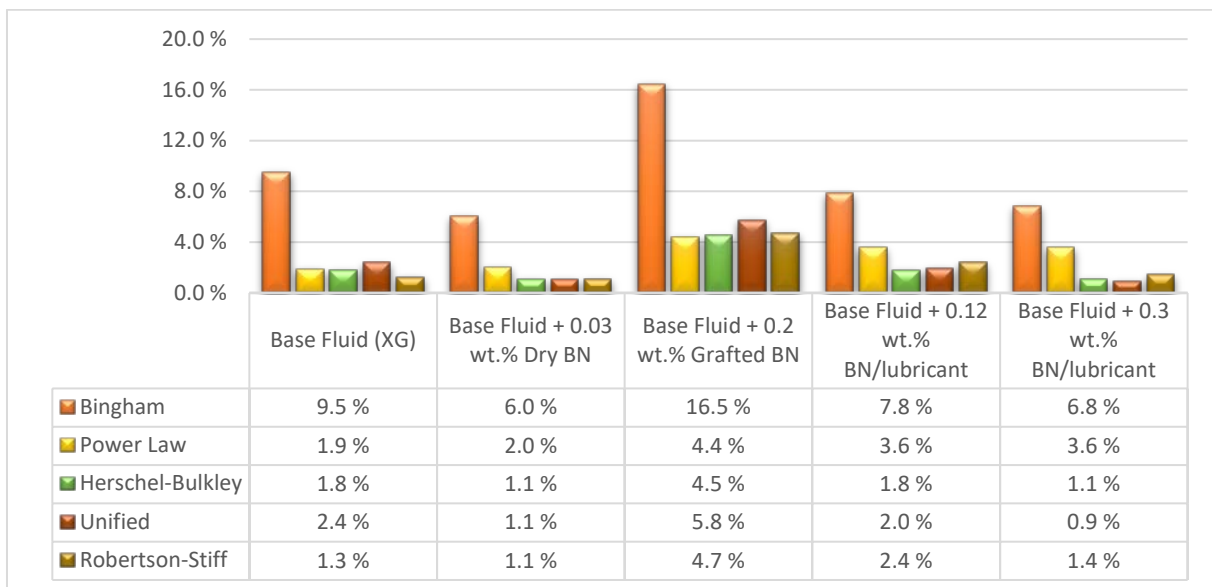


Figure 5-4: Deviation of the rheological models from the measured data (XG-based samples)

5.1.2.2. Effect of nano-additives on the rheological parameters (XG system).

Table data below presents the information about the parameters of different rheological models and compares the changes of those parameters with the reference fluid.

		Base fluid (XG)	Base fluid + 0,03 wt.% Dry BN	Base fluid + 0.2 wt.% Grafted BN	Base fluid + 0,16 wt.% BN/lub	Base fluid + 0,3 wt.% BN/lub
Bingham	τ_y	31.756	43.662	31.88	34.195	38.148
	% deviation		<u>37.49</u>	<u>0.39</u>	<u>7.68</u>	<u>20.13</u>
	μ_p	0.0243	0.0223	0.0348	0.0281	0.0298
	% deviation		<u>-8.23</u>	<u>43.21</u>	<u>15.64</u>	<u>22.63</u>
Power Law	k	22.036	34.236	17.804	24.073	27.667
	% deviation		<u>55.36</u>	<u>-19.2</u>	<u>9.24</u>	<u>25.55</u>
	n	0.1218	0.0834	0.1797	0.1217	0.1137
	% deviation		<u>-31.53</u>	<u>47.54</u>	<u>-0.08</u>	<u>-6.65</u>
Herschel-Bulkley	τ_o	24.320	36.811	5.248	26.04	32.245
	% deviation		<u>51.36</u>	<u>-78.42</u>	<u>7.07</u>	<u>32.59</u>
	k	1.6645	1.6706	13.244	2.145	0.9972
	% deviation		<u>0.37</u>	<u>695.67%</u>	<u>28.87</u>	<u>-40.09</u>
	n	0.42100	0.4053	0.2111	0.397	0.5109
	% deviation		<u>-3.73</u>	<u>-49.86</u>	<u>-5.70</u>	<u>21.35</u>
Unified	τ_y	25.075	36.812	13.871	25.608	32.01
	% deviation		<u>46.81</u>	<u>-44.86</u>	<u>2.13</u>	<u>27.66</u>
	k	1.2042	1.67	6.1683	2.4344	1.1269
	% deviation		<u>38.68</u>	<u>412.23</u>	<u>102.16</u>	<u>-6.42</u>
	n	0.4682	0.4054	0.3039	0.3792	0.4926
	% deviation		<u>-13.41</u>	<u>-35.09</u>	<u>-19.01</u>	<u>5.21</u>
Robertson-Stiff	A	15.903	24.547	16.893	15.101	15.818
	% deviation		<u>54.35</u>	<u>6.23</u>	<u>-5.04</u>	<u>-0.53</u>
	C	19.9407	33.6429	1.5455	31.8329	44.0331
	% deviation		<u>68.71</u>	<u>-92.25</u>	<u>59.64</u>	<u>120.82</u>
	B	0.1735	0.1258	0.1881	0.1953	0.2015
	% deviation		<u>-27.49</u>	<u>8.41</u>	<u>12.56</u>	<u>16.14</u>

Table 5.9: Rheological modelling summary of the XG-based fluids

- **Bingham model:** According to the table, the yield stress increased for all fluids meaning higher shear stress is needed to initiate the fluid motion. The most significant growth of 37.49% was noted for the fluid with 0.03 wt.% of dry BN, whereas the fluid with 0.12 wt.% and 0.3 wt.% BN/lubricant showed 7.68% and 20.13% change, respectively. The presence of grafted nanoparticles barely affected the yield stress. The plastic viscosity decreased by

8.23% for the sample with dry BN and increased for the fluids with BN/oil at 0.12 wt.% and 0.3 wt.% concentration by 15.64% and 22.63%, respectively. An increase of 43.21% was observed for the sample with BN grafted.

- **Power Law:** The consistency index went up for all nano-enhanced samples, except to the fluid with grafted BN, which showed a decrease of 19.2%. The growth was by 55.36% for the fluid with 0.03 wt.% dry BN; 9.24% for the fluid with 0.12 wt.% BN/oil and 25.55% for the fluid with 0.3 wt.% BN/oil. The n -value decreased by 31.53% for the specimen containing dry BN; however, for the fluids with BN mixed in oil, the drop was less than 7%. The reduction in flow behavior index shows that fluids behave more like pseudoplastic, as compared to the reference system. On the other hand, the specimen with modified nanoparticles increased the flow index by 47.54%.
- **Herschel-Bulkley:** The yield point (τ_0) value decreased by 78.42% when modified BN particles were introduced to the base fluid. For the remaining simulated fluids, the yield point uplifted. The fluid with 0.12 wt.% BN/oil increased the value only by 7.07%. Whereas, systems with 0.03 wt.% of dry BN and 0.3 wt.% of BN/oil exhibited a significant rise with 51.36% and 32.59%, respectively. The k -value remained virtually unchanged for the “Base fluid + 0.03 wt.% Dry BN”, although there was observed an increment of 28.87% for the “Base fluid + 0.12 wt.% BN/lub”, and a reduction of 40,09% for the “Base fluid + 0,3% BN/oil”. The addition of 0.2 wt.% grafted nanoparticles rocketed the consistency index exhibiting a rise by almost eight times. The flow behavior index reduced insignificantly by average 4% for the fluids with dry BN and BN/oil at 0.12 wt.% concentration, whilst the sample containing 0.2 wt.% grafted nanoparticles dropped by 49.86%. The addition of BN/oil in mixture at 0.3 wt.% increased the n -value by 21.35% representing less pseudoplastic behavior.
- **Unified model:** The lower shear yield stress (τ_y) rose by 46.81% and 27.66% for the Base fluid with 0.03 wt.% of dry BN and 0.3 wt.% of BN/oil, respectively. The minor growth of 2.13% was documented for the case with 0.12 wt.% of BN/oil. In contrast, the addition of modified BN declined the τ_y by 44.86%. The consistency index of the “Base fluid + 0.12 wt.% BN/lub” more than doubled as compared to the reference system, and increased by

38,68% for the specimen with 0.03 wt.% of dry BN particles. The dramatic rise of k -parameter by 412.23% was observed grafted BN particles were introduced to the system. The slight decline of 6.42% was documented for the “Base fluid + 0.3 wt.% BN/lub”. The flow behavior index dropped by average 16% when the reference system was diluted with dry particles or 0.12 wt.% BN particles mixed in lubricant. The modest rise of 5.21% contributed to the n -value when BN/oil was added at 0.3% by weight. The grafted BN lowered the flow index of the reference fluid by 35.09%

- **Robertson-Stiff:** The A parameter exhibited growth of 54.35% for the “Base fluid + 0.03% dry BN”, while other samples showed slight variations up to 6.23%. The B parameter declined by 27.49% when the fluid with dry BN was simulated. The addition of modified BN had a minor increasing effect on B parameter (8.41%). The samples with BN/lubricant showed an average increase of 14%. On the other hand, the C value of all the fluids was seriously affected. The “Base fluid + 0.03 wt.% Dry BN” and “Base fluid + 0.12 wt.% BN/lub” had a rise of 68.71% and 59,64%. The C parameter more than doubled (120.82%) when the fluid was mixed with BN/lub at the concentration of 0.3% by weight, while the presence of modified BN decreased the C parameter by 92.25%.

5.2. Torque and drag simulation.

Torque and drag simulation is of major importance in well planning to predict and prevent pipe-related problems. Drill string mechanics must be designed appropriately using computer models to ensure that the desired well trajectory can be drilled and completed safely. A modern software used for well planning can adequately predict the limits for the rotary and hoisting equipment and help to design a drill string in a most efficient way.

As was mentioned in the theory about torque and models, one of the reasons for the excessive torque and drag is high friction between contacting surfaces in the well. The experimental study showed that addition of nanoparticles alone, or together with a lubricant to the water-based mud could improve lubricating properties of the fluid. This, in turn, leads to the reduction of expenses and risks related to high torque and drag and solves environmental issues associated with using OBM.

This section is devoted to torque and drag simulation that illustrates how the trajectory of a well can be altered by implementing the drilling fluids containing nanoparticles.

5.2.1. Simulation setup.

The torque and drag simulations were executed through WellPlan™ software developed by Halliburton. A well consisted of a vertical section up to 4012.5 ft. cased with intermediate (13 3/8") casing and a deviated 12.615" open hole section, which was extended in accordance with the frictional and rheological properties of the selected fluid. As was observed from the simulations, the tripping out tension was the limiting parameter for the length of the well in the most cases. For simplicity, the coefficient of friction in the open hole and cased hole sections was assumed to be equal. The drill pipe had the outer and inner diameter of 5" and 4.86" respectively. The RPM was 30, and the tripping speed was set to 60 ft/min for both running in and out of the hole. The flow rate was suggested to be 500 gpm with a fluid having the density of 8.5 ppg. The figure below depicts the trajectory of the modelled well, while other well and drill string configurations are outlined in **Appendix E**.

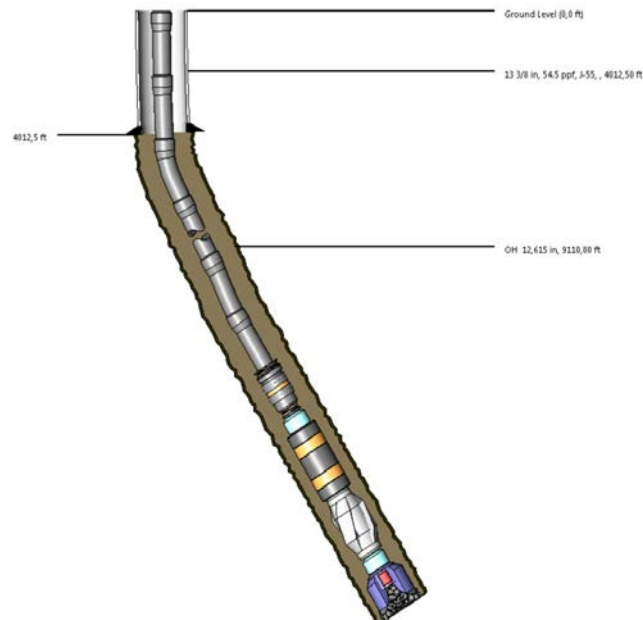


Figure 5-5: Well setup for the Torque&Drag simulations

5.2.2. Simulation example.

This section aims to show an example of the torque and drag analysis and data interpretation. Two samples formulated in the Duovis system will be reviewed, namely nano-free reference fluid and the fluid with 0.3 wt.% of BN/lubricant.

First, the reference fluid was used as drilling mud, and the string was analyzed in terms of stresses, tension and torque. The length of the well was gradually increased until all the above-mentioned parameters are in the safe window. The maximum possible length, which was possible to achieve using the base fluid was 12300 ft. If the well length were extended beyond this value, it would lead to the pipe failure. The length was limited by tripping out tension.

Afterwards, the fluid input was altered to the frictional and rheological parameters of the fluid with BN/lubricant at the concentration of 0.3 wt.%. The initial MD was set to 12300 ft (the limit for the previous scenario) and was increased according to the limits. Similar to the case above, the well trajectory was confined by the tension limit; however, due to improved characteristics of the fluid, it was possible to extend the well up to 13500 ft.

The graphs below illustrate the loads on the string when the base fluid is used. In addition, the critical loads (tripping out tension, tripping out torque and Von-Misses stress) were plotted for the case with the nano-enhanced fluid. This visually demonstrates the shift in the load distribution along the string when the fluid properties were improved, and the well was extended.

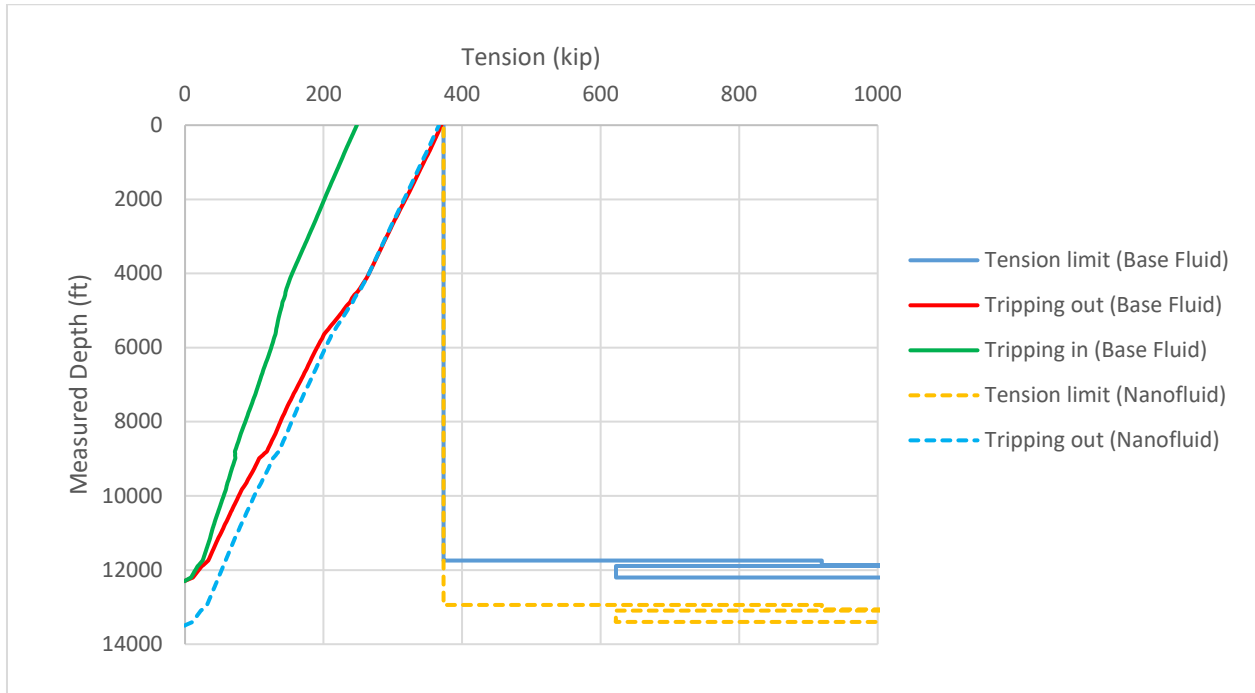


Figure 5-6: Drag loads and limits for the "Base fluid" and the "Base fluid + 0.3 wt.% BN/lub"

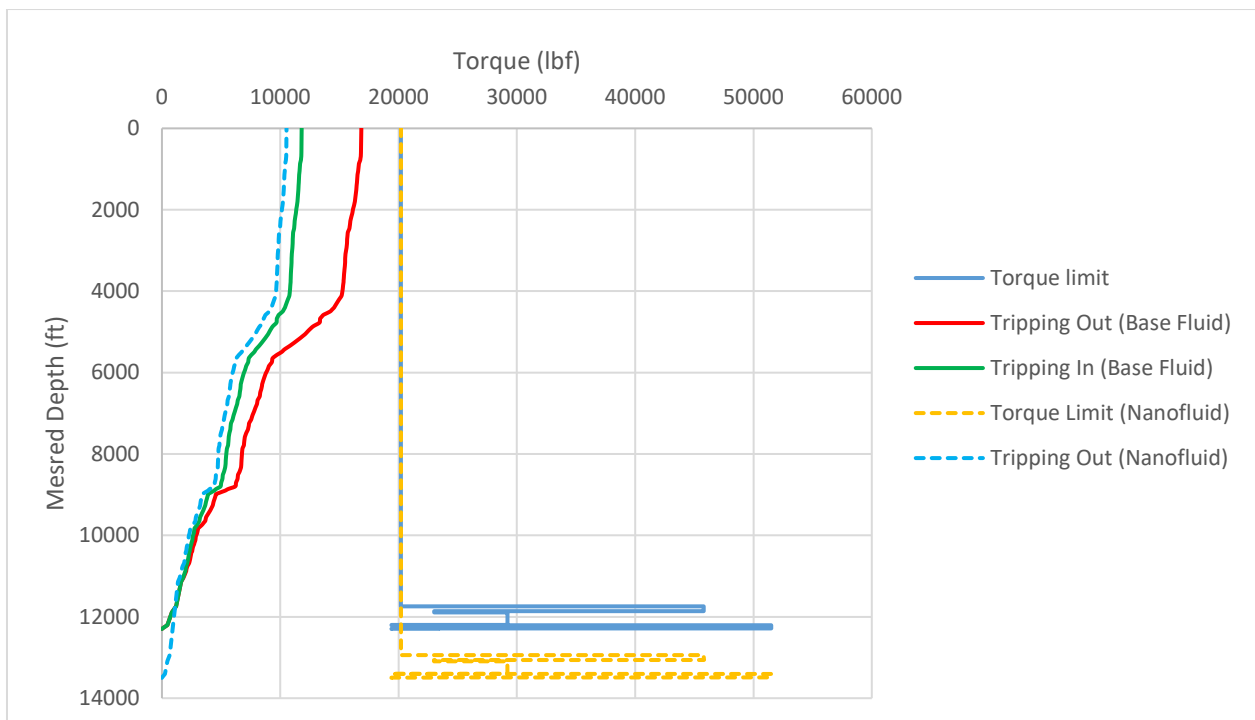


Figure 5-7: Torque loads and limits for the "Base fluid" and the "Base fluid + 0.3 wt.% BN/lub"

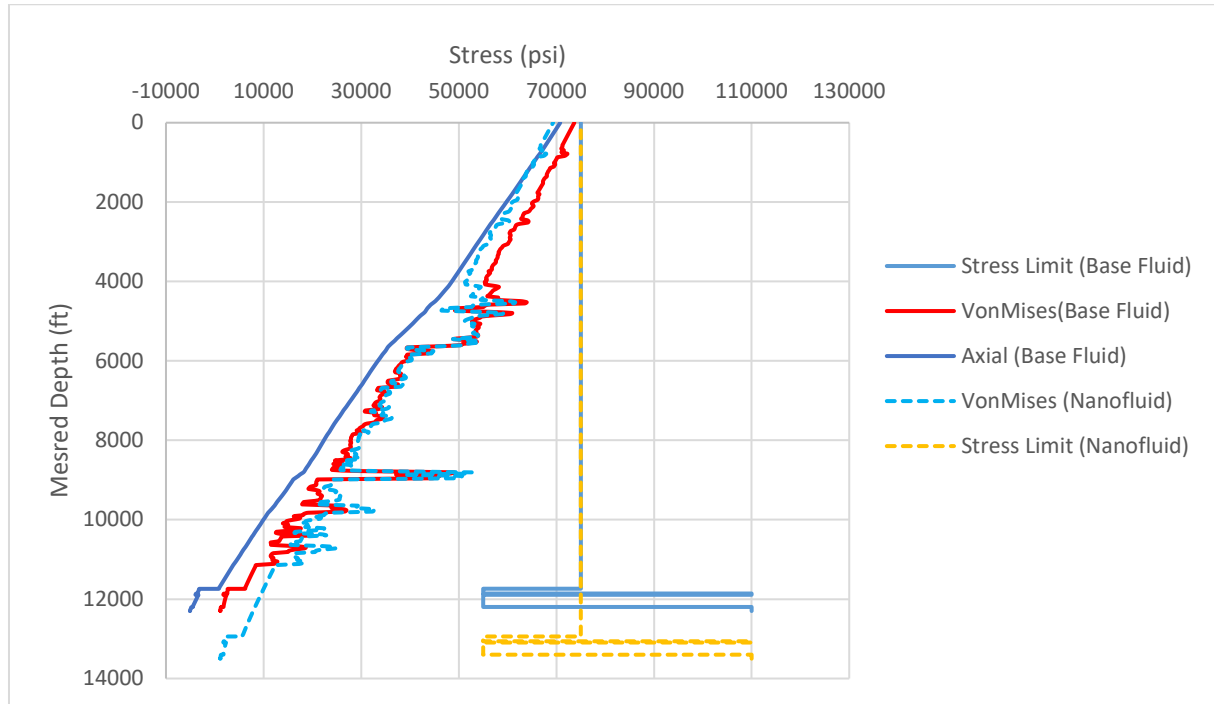


Figure 5-8: Stresses and limits for the "Base fluid" and the "Base fluid + 0.3 wt.% BN/lub"

5.2.3. Simulation result.

This section outlines the results from the modeling of the drill string loads when the well is assumed to be drilled with selected fluids. As previously discussed, the tribology of the samples from different batches was measured with different contacting surfaces. Thus, there might be uncertainties when compare the lubricity of the fluids containing various additives. Since the friction factor is the decisive input parameter for this study, the selected fluids were prepared again, and the tribology was measured under the same conditions. This allows to compare the well length alteration for the fluids formulated with various nano-additives.

The extension of the wells drilled with the Duovis-based fluids is presented in **Figure 5-9**. From the graph, it can be seen that commercial Boron nitride NPs allowed prolonging the well only by 3.3%. The maximum extension of 13500 ft. was achieved when 0.3 wt.% of BN/lubricant was added to the Base Fluid. This counts for 9.8% increment to the well length as compared to the case with the reference fluid. The utilization of the grafted BN nanoparticles allowed to drill up to 13450 ft., prolonging the well drilled with the conventional mud by 9.3%.

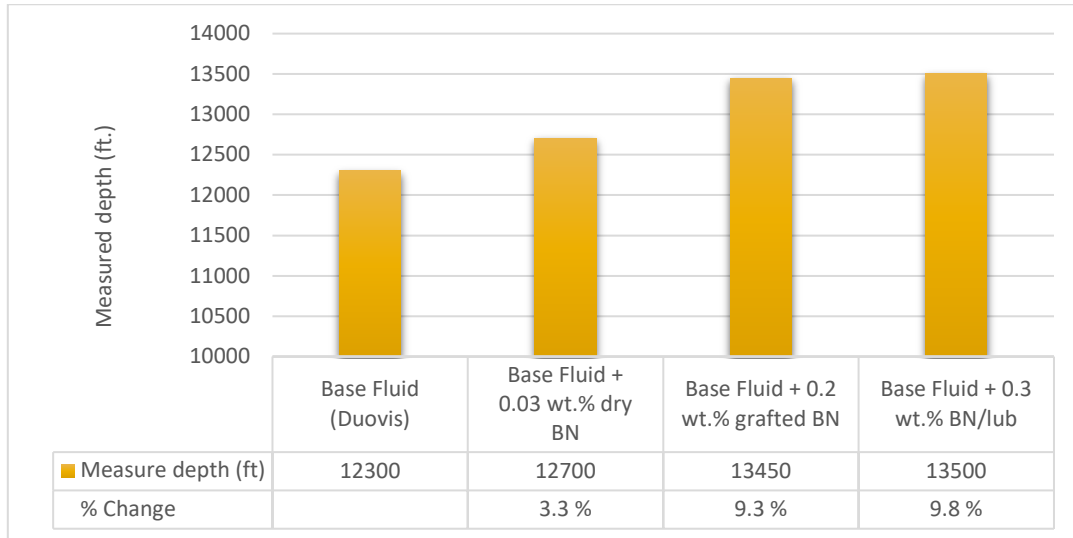


Figure 5-9: Effect of nano-additives on the simulated well length (Duovis)

Chart 5-10 represents the length alteration when the XG-based drilling fluids are used in the simulations. Similar to the previous case, the maximum well length was achieved with the fluid containing 0.3 wt.% of BN/lubricant. It was possible to extend the well by 18.3% compared to the case with the nano-free fluid. The addition of grafted nanoparticles at 0.2 wt.% made possible to prolong the well by almost 13%. Dry BN nanoparticles showed the possibility to extend the length only by 5%.

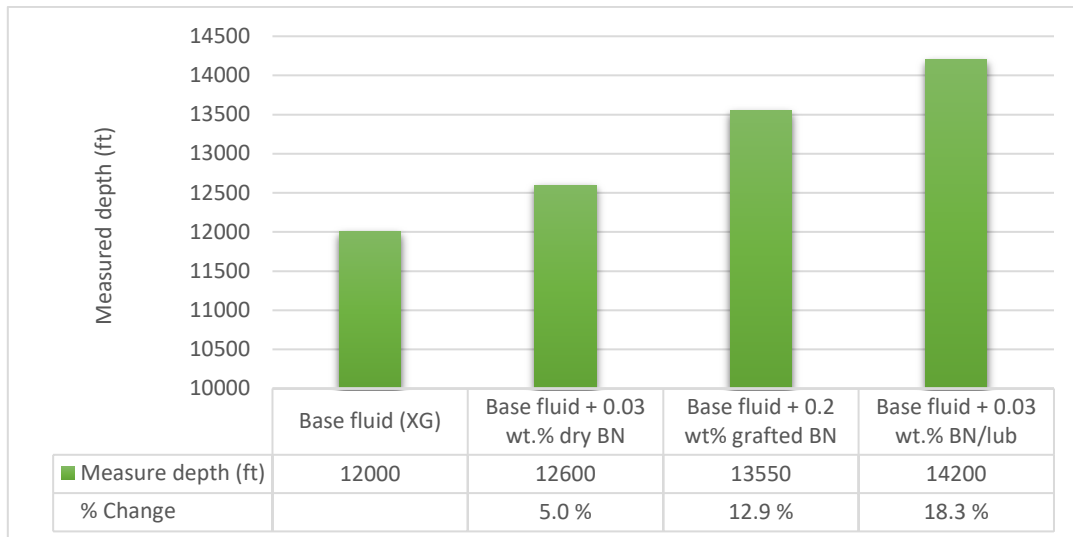


Figure 5-10: Effect of nano-additives on the simulated well length (XG)

5.3. Hydraulics simulation.

The ECD management is of great importance in drilling operations, since it is a critical parameter in avoiding kicks, lost circulation, formation damage, stuck pipe, as well as excessive stress induced to a drill pipe. This simulation analyzed the dynamic pressure losses in the circulating system when different nano-treated drilling fluids are used. The output of the simulation is total pressure loss and ECD in the well, which was used later to compare the hydraulic performance of nano-enhanced fluid with conventional drilling mud. The theoretical background of hydraulic simulations and the summary of equations used in the chosen model was presented in **Section §2.4**.

5.3.1. Simulation setup.

The hydraulic simulations were conducted in Excel calculator assuming a vertical well with TVD of 10000 ft. The inside diameter of the last casing string was 8.5", and the drill string OD and ID were 5" and 4.8", respectively. The drill bit was assumed to have three nozzles with a diameter of $28/32$ inch. For simplicity, we ignore the pressure loss in the surface equipment and assume it to be zero. The flow rate was altered from 50 to 600 gpm. The density of all the fluid systems has been accepted to be 1.025 sg (8.539 ppg).

5.3.2. Hydraulic simulation of the Duovis based fluids.

This subchapter presents information about the hydraulic modeling of the fluids formulated in Duovis system. There were five simulated drilling fluids, namely "Base fluid", "Base fluid + 0.03 wt.% dry BN", "Base fluid + 0.2 wt.% grafted BN" and "Base fluid + 0.3 wt.% BN/lub".

Graph 5-11 compares the total pressure loss for the simulated samples. Overall, the pressure loss increased linearly with increasing flow rate for all the samples. All fluids showed a similar pattern of growth. The highest pressure loss was observed for the system containing BN particles mixed in the lubricant. On the other hand, the fluid with 0.03 wt.% of dry BN particles decreased the pressure loss by average 32% for the whole spectrum of flow rates, as compared to the base fluid. The simulated fluid containing grafted BN particles showed a rise in pump pressure by approximately 16%.

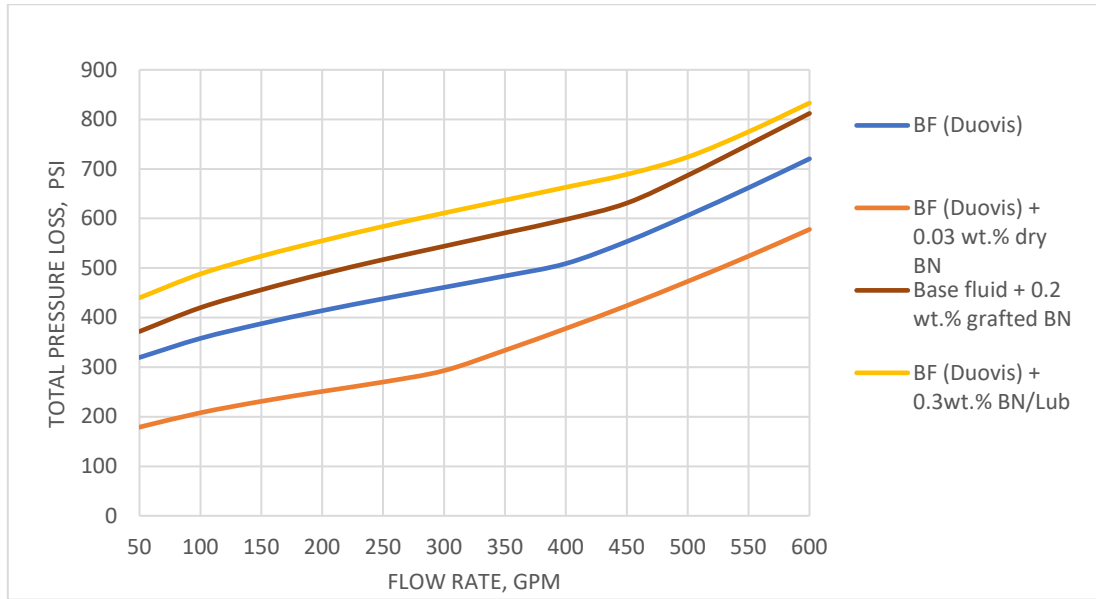


Figure 5-11: Effect of nano-additives (in Duovis) on the pressure loss

The figure below depicts the ECD results of the modeling. The ECD values demonstrate annular pressure loss, which is one of constituent elements of the total pressure loss. Hence, the total pressure loss and ECD exhibited the similar tendency. The largest ECD values for all range of flow rates were observed for the case with 0.3 wt.% BN/lub, while the fluid with 0.03 wt.% of dry BN particles showed the lowest ECD. Based on the results of the Duovis-based samples, it can be concluded that the fluid with dry BN nanoparticles is the most practical in terms of hydraulics.

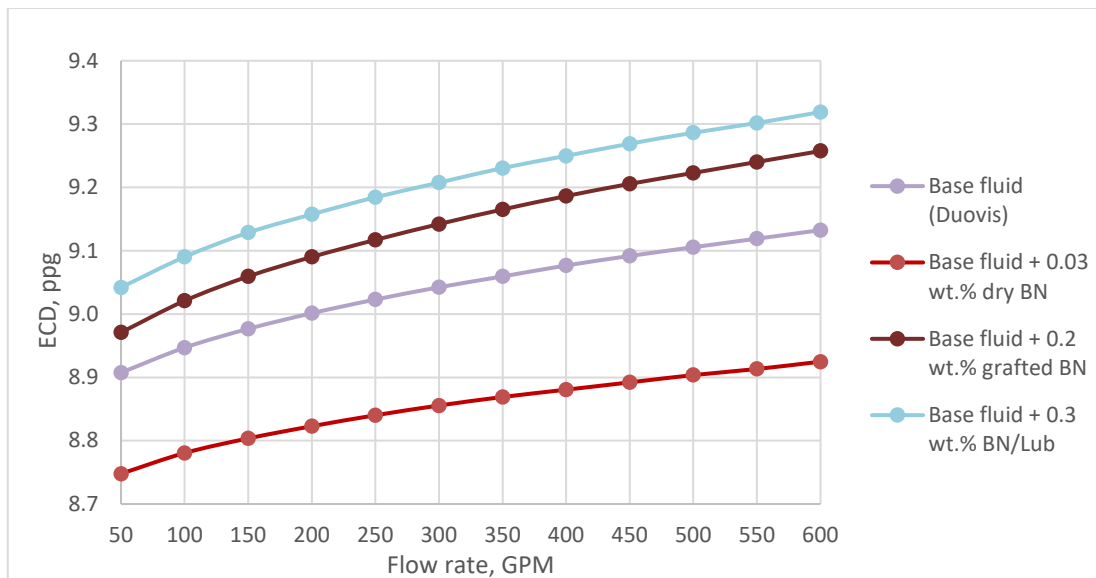


Figure 5-12: Effect of nano-additives (in Duovis) on the ECD

5.3.3. Hydraulic simulation of the XG based fluids.

The simulation output of XG-based drilling fluids is summarized in this subchapter. The fluid selection was based on the best frictional results. The rheological data of the reference fluid (“Base fluid”), fluid with 0.03 wt.% dry BN, fluid with 0.2 wt.% grafted BN and fluid with 0.3 wt.% BN/lub was used as input data to analyze the hydraulic performance.

The following graph illustrates the total pressure loss in the circulation system for each fluid when different flow rates were assumed. The same line profile for all the systems indicates the similar hydraulic response on the flow rate variations. The minimum pressure loss at low flow rates was observed for the fluid with grafted nanoparticles. However, at flow rates higher than 450 gpm, the base fluid showed the least pressure loss. In contrast to the case with Duovis polymer, the fluid with 0.03% dry BN required the highest pump pressure among the whole tested samples. The fluid containing BN nanoparticles together with a lubricant also showed a rise in pressure required to overcome the friction in the circulating system.

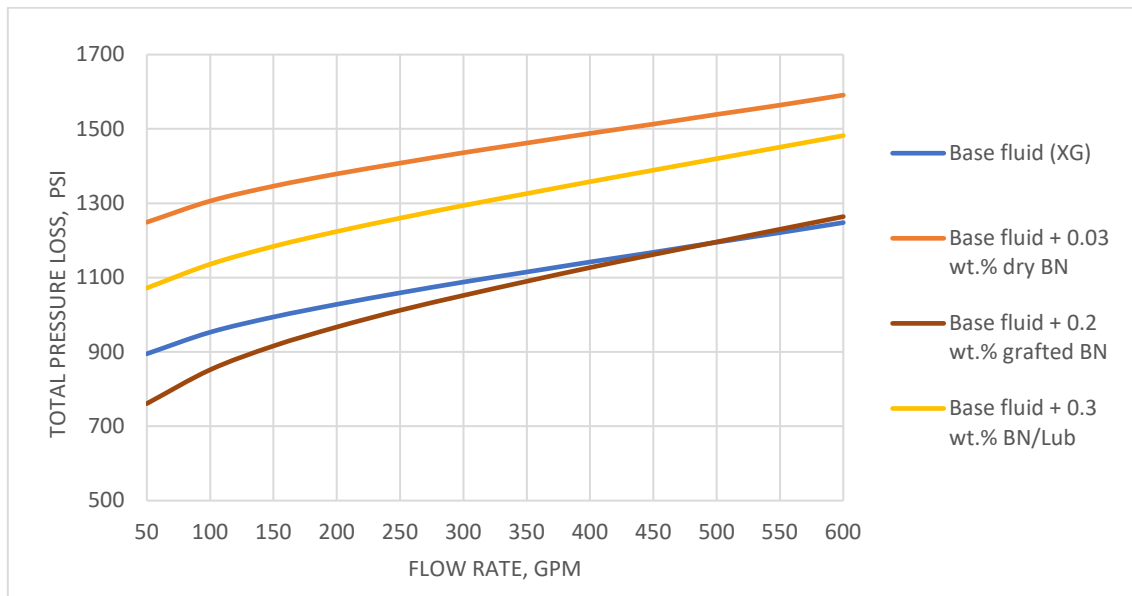


Figure 5-13: Effect of nano-additives (in XG) on the pressure loss

As was discussed earlier, the ECD value is dependent on the total pressure loss, and the pattern of the total pressure loss lines is repeated for the ECD graph. The distribution between the fluids was also similar: the mud with grafted BN nanoparticles had the least ECD value at low flow rates, while, the curve exceeded the Base fluid at flow rates higher than 170 gpm.

Addition of known nanoparticles together with a lubricant increased the ECD as compared to the base sample. The fluid with dry BN nanoparticles claimed the maximum ECD in the whole spectrum.

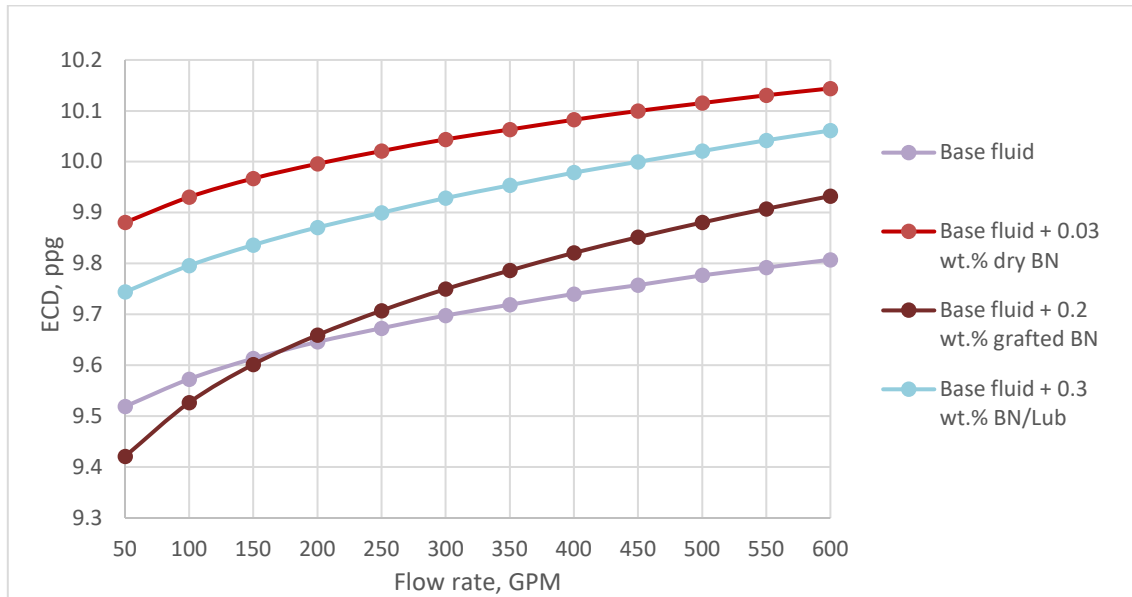


Figure 5-14: Effect of nano-additives (in XG) on the ECD

5.4. Hole cleaning simulation.

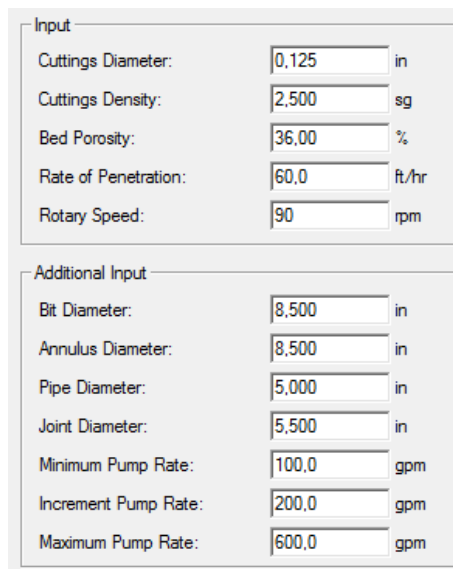
One of the fundamental functions of the drilling mud is cuttings transport, the efficiency of which is governed by fluid density and rheology. However, the minimum flow rate required to transport drilled cuttings is not only a function of the fluid but also a function of a wellbore trajectory, the cuttings characteristics and operational conditions. In general, the minimum is defined by settling velocity and governed by [19]:

- Operational conditions (Rate of penetration and RPM)
- Well configuration (inclination, depth, hole size, pipe size and eccentricity)
- Drilling mud properties
- Cuttings specification (size, shape, density)

The hole cleaning simulation evaluates the ability of nano-treated drilling fluid to carry cuttings by assessing minimum flow rate for different inclinations.

5.4.1. Simulation setup.

The simulations were performed in the WellPlan™ software. The efficiency of the hole cleaning was analyzed regarding the minimum flow rate required to transport cuttings at different inclinations. The angles varied from 0° (vertical well) to 90° (horizontal well). **Figure 5-15** summarizes the input configurations for the given well. It was assumed that all the cuttings have the same size and density.



Input	
Cuttings Diameter:	0.125 in
Cuttings Density:	2.500 sg
Bed Porosity:	36.00 %
Rate of Penetration:	60.0 ft/hr
Rotary Speed:	90 rpm

Additional Input	
Bit Diameter:	8.500 in
Annulus Diameter:	8.500 in
Pipe Diameter:	5.000 in
Joint Diameter:	5.500 in
Minimum Pump Rate:	100.0 gpm
Increment Pump Rate:	200.0 gpm
Maximum Pump Rate:	600.0 gpm

Figure 5-15: Simulation setup for the hole cleaning simulations

5.4.2. Simulation result.

In this section, the fluids formulated in the Duovis polymer were analyzed. **Graph 5-16** shows the difference between minimum flow rates of the reference fluid and the fluids with nano-additives. From the graph, one can observe same flow rates in vertical section; however, increasing angle induces a rise of the flow rate for all the fluids. The presence of grafted BN and BN/lub enhanced the hole cleaning performance of the drilling fluid. The improvement was more significant as the trajectory approached horizontal. The average decrease of 25.4% relative to the base fluid was noted for the fluid with 0.2 wt.% grafted BN; and 28.2% for the fluid with 0.3 wt.% of BN/oil. On the other hand, the addition of dry BN at the concentration of 0.03 wt.% showed vague effect. The flow rate required for the fluid with dry BN additives

was higher than the flow rate for the reference fluid at the angles less than 60°. However, at larger angles, the Base fluid claimed higher flow rates to clean the hole.

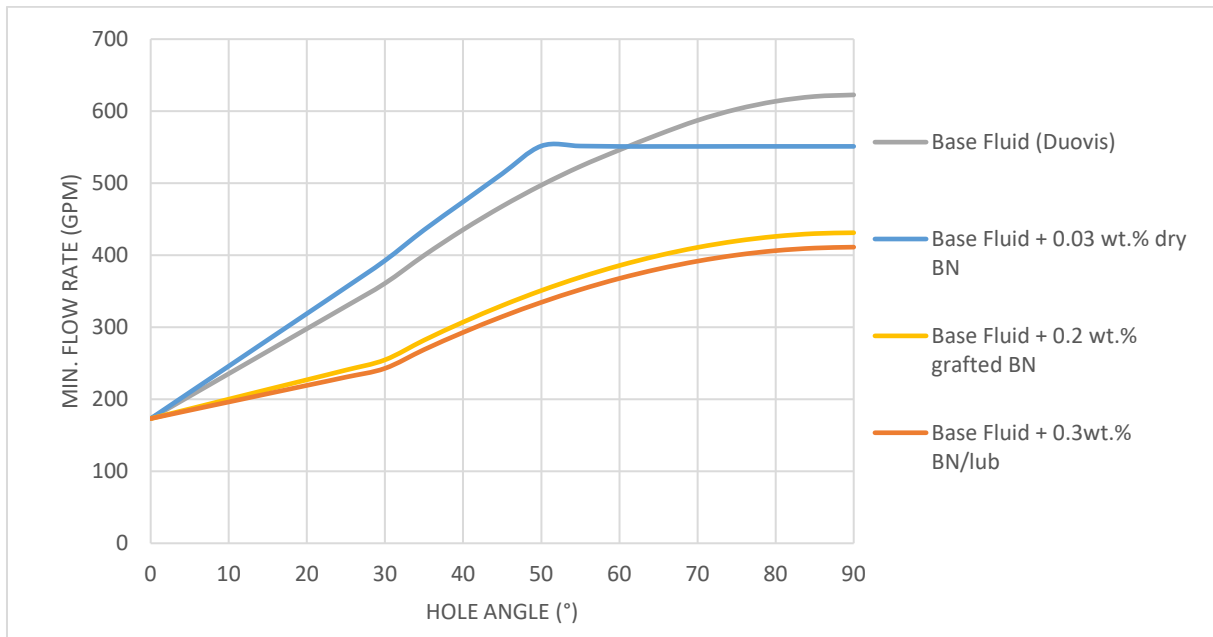


Figure 5-16: Effect of nano-additives (in Duovis) on the minimum flow rate for cuttings transport

6. RESULTS SUMMARY AND DISCUSSION.

This chapter aims to provide a comprehensive summary and discussion of the results of this thesis work obtained from the experimental and simulation study. In the experimental part, the focus of attention was to investigate the effect of Boron nitride nanoparticles on the tribology of laboratory formulated water-based drilling fluid. On the basis of the highest lubricity results, the fluids were further characterized concerning rheology, filtrate loss, pH and viscoelasticity.

6.1. Effect of dry BN particles.

The effect of dry BN powder was tested both in Duovis and Xanthan gum biopolymers. First, the performance of nanoparticles will be discussed in each polymer separately. Afterwards, the comparative review between two systems will be presented.

6.1.1. Dry BN in Duovis biopolymer system.

As it was mentioned, the experiments started with the screening test to determine the most feasible concentrations in terms of tribology. The selection of the fluids for the further tests and simulation was based on the friction results.

Effect on the Tribology.

The friction tests were carried out using a CMI Tribometer at room temperature. The experimental procedure and results were discussed in **Chapter 4**. The friction results of the fluids containing nanoparticles at various concentrations were compared to the conventional nano-free fluid formulated in the same polymer.

In general, the addition of dry BN at all concentrations improved the lubricating properties of the mud. However, it has been found that the friction reduction was not linear with the increased concentration. The most significant decrease of 23.6% was observed when the fluid was mixed with dry BN nanoparticles at the concentration of 0.03% by weight.

Effect on the Rheology.

The data obtained from the viscometer measurements indicated a slight increase in shear stress readings of nano-enhanced samples, as compared to the reference fluid. The change in

concentration showed a consistent effect on Bingham parameters. The yield stress and lower shear yield stress decreased when the percentage of nanoparticles raised; in contrast to plastic viscosity, which showed the most prominent increase of 70% for the fluid with 0.3 wt.% of nano-additives.

The consistency index of Power Law model exhibited a linear drop, while the flow behavior index increased with raised concentration. The results showed that both k -value and n -value had the maximum change of 64% for the fluid containing 0.3 wt.% of dry BN nanopowder.

Effect on the Filtrate loss and pH.

The experiments demonstrated that nanoparticles, at both high and low concentrations, had an adverse effect on filtrate loss. However, the fluid with 0.03 wt.% of dry additives did not provide any change and had the same filtrate loss value as the reference system. The most prominent deterioration was observed when the fluid with the highest concentration of known nanoparticles was tested, which showed a rise of filtrate volume by 33.3%.

The pH of the mixtures was solely affected by the presence of BN additives. The variation of all systems were less than 1%, which may be neglected.

Effect on the Viscoelasticity.

Among the whole batch, only the reference fluid and the fluid with the best friction result (0.03 wt.% of dry nanoparticles) were used for viscoelastic measurements. The value of shear stress obtained at the intersection of Storage modulus and Loss modulus curves showed that addition of nano at stated concentration increased the flow point by 42% as compared to the base system.

Drilling fluid performance simulation.

Simulation is an effective way to verify the efficiency of formulated fluids in the actual drilling conditions. The study covers the fluid having the most attractive concentration of dry BN in terms of lubricity, which proved to be 0.03% by weight.

To illustrate the compliance of the rheological data with the measured data, modeling was performed. The Robertson-Stiff was found out to be the best model, which describes the rheology of the nanofluid with 1.4% deviation.

As mentioned in the theory review, the lubricity of the drilling fluid has a significant impact on the torque and drag loads, which in turn is a limiting factor for the drilling depth. The highest lubricity impact obtained by addition of dry BN particles in Duovis-based mud was the reduction by 23.6%. Torque and drag simulation study has shown that this mud allows extending a well length by 3.1% as compared to the nanoparticle free conventional drilling fluid.

The hydraulic simulation analyzed dynamic pressure loss and ECD in the circulating system. The output showed that the drilling mud with dry BN nanoparticles at 0.03% by weight in Duovis system reduced the pressure loss by 32%, and ECD by relatively small degree (2%).

Hole cleaning performance of the fluid was analyzed with regard to the minimum flow rate required to transport the cuttings. It has been found that in the vertical section and the sections with the inclination less than 60° the nanofluid required higher flow rate; however, when the trajectory was close to the horizontal, the minimum flow rate of BN-enhanced fluid was lower than those of nano-free system.

6.1.1.1. Dry BN in XG system.

The choice of nanoparticles ratio was similar to the case with the Duovis polymer. As in the previous case, the attention has been paid to the systems with low concentrations. The viscoelasticity experiment and simulation study were performed on the fluid having the best lubricating properties.

Effect on the Tribology.

The addition of BN particles in XG system showed a positive effect on lubricity at all concentrations. The presence of nano-additives at low mass ratio barely affected the friction; however, the fluid with BN at 0.03% by weight decreased the friction value noticeably, showing an improvement of lubricity by around 17%, which was the best result in the whole batch. The high presence of nanoparticles provided only 10% reduction in friction factor.

Effect on the Rheology.

Generally speaking, the dry Boron nitride nanoparticles added to the XG system increased the viscometer response compared to the conventional fluid. However, there was not observed an evident relationship between the viscometer data and amount of nanoparticles. The plastic viscosity of Bingham model was barely affected by the presence of nano-additives, while the yield stress increased for all samples. The LSYS went up for the small concentration; however, the high amount of BN reduced the value considerably. The consistency index gradually increased when more particles were added to the suspension, while flow behavior index went down.

Effect on the Filtrate loss and pH.

Unlike the Duovis system where the addition of BN nanoparticles at all concentrations increased the filtrate volume, the presence of BN particles at the concentration up to 0.02% reduced the filtrate loss. Further increased amount of particles had an adverse effect on filtration, exhibiting the largest volume of filtrate loss for the sample with the presence of nano-additives at 0.3%.

Similarly to the first case, the addition of BN nanoparticles did not have any significant effect on the alkalinity of the drilling fluid.

Effect on the Viscoelasticity.

The viscoelastic experiments of the XG-based fluids covered the analysis of the fluid with 0.03 wt.% of dry BN. The comparison between the systems indicated that additives at mentioned concentration raised the flow point by 9.5% as compared to the reference fluid.

Drilling fluid performance simulation.

The most attractive concentration of dry BN particles in XG system seems to be 0.03% by weight. Thus, all the simulations have been performed assuming the fluid with the mentioned ratio.

The rheological modeling illustrated that all the models, except for Bingham, cover the measurements quite accurately. The Robertson-Stiff, Herschel-Bulkley and Unified models

were opted to be the most precise and described the rheological behavior with the same accuracy of 1.1%.

The maximum improvement of lubricity compared to the base fluid was documented as 16.9%. The properties of the reference fluid and the fluid with the best tribology results were used as input parameter for torque and drag simulations. The analysis of the maximum well length based on critical loads indicated the possibility to extend the length by 5% if nanofluid is used.

From the hydraulics viewpoint, the properties were deteriorated by the addition of dry BN nanoparticles to the XG-system at the concentration of 0.03 wt.%. The pump pressure required to overcome the friction in the circulating system increased by average 32.2% as compared to the reference system. The ECD was not affected that considerably and rose in average by 3.6% for the chosen range of flow rates.

Hole cleaning efficiency of the fluid with XG biopolymer was not affected by the presence of Boron nitride nanoparticles.

6.1.2. Comparative study of the systems.

The results obtained from both experiments and simulations indicated that performance of the nanoparticles is dependent on the polymer. This section compares the effect of dry Boron Nitride nanoparticles on properties of water-based mud formulated in Duovis and Xanthan Gum polymers.

In respect of rheology, the addition of nanoparticles shifted the viscometer data upwards in either of systems. However, the nanoparticles had a reverse effect on the Bingham parameters when comparing two systems. For instance, the increased concentration of nanoparticles resulted in decreasing trend of the yield stress of Duovis-based fluids, whereas this parameter went up when the particles were added to the XG system. The same reverse behavior was observed for the k and n parameters of Power Law model.

As was mentioned earlier, it is not feasible to compare the friction values of the two systems utilizing different contact surfaces in the tribometer. Instead, the reduction in friction

coefficient relative to the reference fluid has been compared for the corresponding concentrations. Overall, the best lubricity properties in both systems has been obtained when the BN particles were added at a low concentration of 0.03% by weight. However, it should be mentioned that for the whole range of nanoparticle concentrations, the friction reduction was more prominent in the Duovis system.

The filtrate measurements showed deterioration at high concentration of NPs for both systems. However, the filtrate volume increased more significantly for the fluid formulated in Duovis polymer. In addition, the low concentration of BN nanoparticles mixed in XG system exhibited a slight improvement of filtrate loss.

The pH value was not affected strongly by the presence of nanoparticles in both Duovis and Xanthan gum polymers.

The relative increase of the flow point, caused by addition of BN, was more significant in the Duovis biopolymer rather than in XG biopolymer.

The rheological modeling illustrated the adequate compatibility of the Robertson-Stiff model with the viscometer data for the fluids formulated in Duovis polymer as well as for the fluids formulated in XG polymer. This statement is valid for both BN-treated fluid and base fluid. However, the remaining models predicted the rheological behavior of the XG-based fluids more accurately than those of the Duovis-based fluids.

For both systems, the torque and drag simulation was performed assuming a drilling mud with 0.03 wt.% of BN particles. The possible well length was compared to the base fluid with the corresponding polymer. As stated above, the friction reduced more noticeably when particles were used in combination with Duovis polymer. However, it has been found from the simulations that the well can be prolonged more with the XG-based fluid.

With regard to hydraulics, the dry particles added to the Duovis polymer decreased the total pump pressure and ECD as compared to the base fluid, in contrast to the case with XG polymer. This output is a reflection of the different impact of nanoparticles on the rheological parameters of the fluid having various polymers.

Concerning the hole cleaning, the presence of dry additives in the XG-based fluid did not affect the flow rates for cuttings transport. However, the addition of the same type and amount of NPs to the Duovis-based fluid decreased the minimum flow rate value at inclinations more than 60° comparing to the base fluid. At lower angles, the reference fluid needed less flow rate to clean the hole.

6.2. Effect of grafted BN particles.

The previous sections discussed the performance of the commercially available nanoparticles. Whereas, this section analyzes the results of a pilot study aimed to enhance the functionality of known nanoparticles. The procedure of surface modification was covered in the literature review of Boron nitride nanoparticles. The effect of the additives was investigated both in Duovis and XG, and comparison between the systems was conducted.

6.2.1. Grafted BN in Duovis system.

This subchapter discusses the results obtained from the experimental and simulation studies of the Duovis-based drilling fluids containing modified BN nanoparticles.

Effect on the Tribology

The grafted BN nanoparticles mainly exhibited a linear dependency of friction on a concentration. Superior lubricating properties were achieved when known additives were added at relatively high concentrations. However, at low concentrations, the commercial BN nanoparticles showed a better lubricating effect on the drilling fluid than modified ones.

Effect on the Rheology.

The viscometer readings did not reveal any particular rheological dependence on the concentration of the grafted BN particles. However, the high concentration had an increasing effect on the viscometer response. The *YS* of the Bingham model and *k*-index of the Power Law model fluctuated and did not show any particular pattern. The *PV* and flow behavior index increased relative to those values of the reference fluid when the BN-grafted were added at high concentrations. The *LSYS* disclosed a drop for all the concentration as compared to the base system.

Effect on the filtrate loss and pH.

The filtration properties were mainly deteriorated by the presence of the grafted BN nanoparticles; besides the case with the lowest concentration, which showed a minor improvement. One should draw attention to the fact that the grafted nanoparticles did not degrade the filtration that significantly, as the commercial nanoparticles did. The maximum increment to filtrate volume was counted around 8%.

The pH measurements illustrated a minor effect of grafted BN, which can be disregarded.

Effect on the Viscoelasticity.

The viscoelastic test was conducted on the sample, which showed the best friction reduction, namely "Base fluid + 0.2 wt.% grafted BN". The results show that additives increased the flow point by 48% as compared to the base fluid.

Drilling fluid performance simulation.

The simulations were conducted on the fluid, which showed the best lubricity properties, namely the base fluid with 0.2 percentage concentration of grafted BN nanoparticles. The rheological modeling revealed that the Robertson-Stiff model comply with the measured data in the most accurate way.

The analysis of the drill string loads revealed that improved rheological and tribological properties by the addition of grafted BN allowed to prolong the well length by 9%.

It was not possible to improve the hydraulic performance of the drilling fluid by using modified Boron nitride nanoparticles.

Hole cleaning modeling showed that the addition of grafted BN decreased the flow rate required for the reference fluid to carry the cuttings by average 25%.

6.2.2. Grafted BN in XG system.

The performance of the oil grafted BN nanoparticles was studied in XG polymer as well. The percentage of additives in the fluid was chosen to be similar to the fluids formulated in the Duovis polymer.

Effect on the Tribology

The dependency of friction reduction on the concentration of additives was identical to the Duovis based fluids. The best friction reduction was obtained when the particles were added at 0.2 percent by weight. Mentioned concentration corresponded to the 44% decrease in friction as compared to the base fluid. Higher percent weight did not yield the better result.

Effect on the Rheology.

The viscometer readings increased when the grafted nanoparticles were introduced to the system. The increase was more prominent for the fluid with 0.01 wt.% of additives. The LSYS and consistency index exhibited a decreasing tendency when the concentration was increased. On the other hand, the increase of concentration caused a rise in flow index and plastic viscosity values. The yield stress sharply increased when the nanoparticles were introduced to the system at the lowest concentration. This was followed by the gradual decrease of the YS when more nanoparticles were added. However, the nanofluids at all range of concentrations had higher YS value than the reference sample.

Effect on the filtrate loss and pH.

The filtrate measurements revealed a slight improvement up to 2.9% when the fluid was diluted with 0.01 wt.% of grafted particles. Higher concentrations had an adverse effect on the filtrate loss. The worst filtration properties were exhibited by a fluids having the high amount of modified BN. These samples showed a growth of filtrate volume by 8.6%.

The maximum change of pH was documented as 2% decrease, which was noted for the sample at the lowest concentration of additives.

Effect on the Viscoelasticity.

The viscoelastic response on the grafted particles was evaluated in terms of flow rates. The data interpretation showed that addition of grafted BN powder at 0.2 wt.% more than doubled the flow point of the reference system.

Drilling fluid performance simulation.

The simulation study covered only the fluid with 0.2 wt.% of nanoparticles. It was the system with the best lubricating properties and therefore was subjected to the simulation analysis.

The rheological modeling defined the Power Law model as the most accurate to follow the viscometer data of the mentioned fluid. It should be mentioned that the Herschel-Bulkley and the Robertson-Stiff models described the rheology with approximately the same percent deviation. The Bingham model had the most substantial deviation from the original data.

The torque and drag analysis showed that the fluid enhanced with grafted BN nanoparticles made possible to drill a section longer by 13% as compared to the nano-free fluid.

The hydraulics of the base fluid was improved at low flow rates by the presence of 0.2 wt.% grafted BN. However, the ECD and the pump pressure of the nano-sample exceeded those parameters of the reference system at the relatively high flow rates.

The given additives did show any effect on the hole cleaning performance of the XG-based drilling fluid.

6.2.3. Comparative study of the systems.

This section deals with the comparison of the fluids formulated in the different polymers and containing grafted BN nanoparticles. The major differences obtained both from experimental and simulation analysis was mentioned below.

In general, the shear stress readings were increased by the presence of grafted BN in both systems. The plastic viscosity and flow behavior index also showed the similar trend in two systems. However, the response of the consistency index and LSYS value varied from system to system. There was possible to determine some relation between the concentration and mentioned parameters for the fluids with XG polymer. However, these parameters fluctuated in the Duovis polymer without any particular tendency.

The variations of particles' concentration showed the similar trend in the XG and Duovis systems, concerning the lubricity. The best results were obtained when the presence of grafted particles was limited to 0.2%. The nanoparticles exhibited better effect in the XG biopolymer where mentioned concentration reduced friction of nano-free system by 43.9%. In the case of Duovis polymer, the maximum friction reduction was documented as 35.4%.

In terms of filtration, the fluids with different polymers behaved similarly. The lowest concentration slightly decreased the filtrate volume of the reference fluid. Further increment of the additives ratio deteriorated the filtration properties. However, the increase of the filtrate was within 9%, which is not considered as a colossal effect.

The pH of the mixtures was insignificantly affected by the presence of modified particles. The analysis does not enable to define any relationship between the presence of nanoparticles and pH value.

The addition of grafted BN nanoparticles increased the flow point of the reference fluid formulated in either polymer. The viscoelasticity of the XG-based fluid though was more sensitive and showed greater rise of the flow point.

The best fluids in terms of tribology were chosen for the simulation study. The rheological modelling established the best correlation between the Power Law model and the viscometer data of the sample formulated in the XG polymer. On the other hand, the Robertson-Stiff model described the rheology of the Duovis-based fluid with the mentioned amount of nanoparticles better. Overall, the models were more precise to follow the pattern of the viscometer readings of the nanofluid with Duovis polymer.

The simulation of drill string loads showed that addition of grafted BN nanoparticles allowed for deeper penetration as compared to the conventional drilling fluid. It was possible to extend the well more noticeable when the XG was used in the mixture as a polymer.

The hydraulic behavior of the fluids with grafted BN was dependent upon the polymer. The addition of modified BN at the concentration of 0.2% to the fluid with Duovis polymer increased the pressure loss and ECD, compared to the base fluid. Whereas, the improvement of hydraulic parameters was observed when the nanoparticles were added to the XG system.

The hole cleaning performance of the fluid with XG polymer remained unaltered when the given NPs were introduced to the system. In contrast, it was possible to decrease the flow rate required for the cuttings carriage when the particles were added to the Duovis-based fluid.

6.3. Effect of BN particles in the presence of a lubricant.

This section analyzes the effect of BN nanoparticles along with oil on the properties of water-based mud. Similar to the case with dry nanoparticles, the performance of BN/lubricant was studied separately in both Duovis and XG polymers, and then the two systems were compared to each other.

6.3.1. BN/lubricant in Duovis system.

Effect on the Tribology

During the friction test, it was found that BN/lubricant additives improve the lubricity of the fluid proportionally with the increased concentration. One possible explanation is that the lubricity was improved not only due to the presence of nanoparticles but oil lubricant as well. The maximum friction reduction of 45% was observed when the fluid was diluted with BN/lubricant at the concentration of 0.3% by weight.

Effect on the Rheology.

The rheological measurements were carried out on the fluids with highest, lowest and moderate amount of BN/lubricant additives. The shear stress readings showed a sequential increase with increased concentration of additives. There was also observed a growing trend in Bingham and Power Law parameters; however, n -value of Power Law model slightly decreased, indicating an increase in shear thinning tendency.

Effect on the filtrate loss and pH.

The small and intermediate concentrations did not show any effect on filtrate volume, while the high concentration of 0.3% of BN/lubricant improved the filtrate loss by 11.8%.

The pH value illustrated the declining trend; however, the percentage change was minor.

Effect on the Viscoelasticity.

Along with the reference system, the fluids with relatively high (0.3 wt.%) and moderate (0.16 wt.%) concentrations were subjected to the viscoelastic tests. The results depicted that the flow point was barely affected for the sample with the high amount of additives; while, the fluid with the intermediate concentration of BN/lubricant lowered the flow point value.

Drilling fluid performance simulation.

The simulation study comprised the analysis of the fluids with the highest and moderate amount of BN/lubricant. The rheology modeling illustrated that for both concentrations, the Robertson-Stiff model covered the viscometer measurements with approximately the same deviation and seemed to be the most precise among other suggested models.

The torque and drag simulation illustrated that the most favorable fluid in terms of lubricity afforded to extend the well length by 10%.

The pump pressure required to overcome the friction in the system raised when the conventional fluids were diluted with BN/oil mixture. Higher concentration of additives yielded higher percentage increase. On the other hand, the ECD increased insignificantly, meaning that the friction loss in the annulus was not strongly affected by the presence of nano-additives.

The property of the Duovis-based drilling fluid to carry the cuttings was improved by the presence of BN/lubricant additives. This statement was based on the flow rates comparison, showing an average 28% reduction for the nano-containing fluid compared to the base system.

6.3.2. BN/lubricant in XG system.

The previous section showed that the BN/lubricant additives exhibited better lubricity properties at high concentrations. Thus, the effect of BN/lubricant in Xanthan gum polymer were mainly focused on the high concentrations.

Effect on the Tribology

The coefficient of friction decreased linearly with increasing concentration. The most prominent improvement was observed for the fluid with 0.3 wt.% BN/lubricant, when the value more than halved, as compared to the corresponding base system.

Effect on the Rheology.

The viscometer response increased quite consistently when the ratio of BN/lubricant in suspension was raised. The plastic viscosity, yield stress, lower shear yield stress and flow

index exhibited a gradual growth when the concentration was raised up; in contrast, the value of consistency index went down.

Effect on the filtrate loss and pH.

The filtrate loss was negatively affected by the presence of BN/lubricant in the XG-based fluid. The effect was most significant at the concentration of 0.25% by weight when the filtrate volume increased by 24.3% relative to the reference fluid.

The pH of the drilling fluids did not show any noticeable changes by the presence of BN/lub.

Effect on the Viscoelasticity.

The viscoelastic properties of the tested fluids were strongly affected by the addition of BN/lubricant. The flow point of nanofluids soared as compared to the base system. The increased concentration led to the more significant rise of flow point.

Drilling fluid performance simulation.

The rheological simulation revealed that the Unified model is the most suitable to describe the behavior of the BN/lubricant-enhanced fluid formulated in XG polymer. On the other hand, the rheology of the base fluid was delineated better by the Robertson-Stiff model.

The drill string analysis determined a remarkable decline of the loads exerted on the string when the XG-based fluid, which properties were enhanced with BN/lubricant, was used in the assumed well. This allowed to extend the well by more than 18%.

Simulation of hydraulics identified a linearly growing trend of pump pressure and ECD with increased concentration of BN/lubricant additives. As in the case with Duovis polymer, the increment of pressure loss occurred mainly inside the drill string rather than in the annulus. This was concluded by the difference in percentage rise between pump pressure and ECD.

Similar to the case with dry BN particles, the addition of BN/lub to the XG-based samples did not affect the hole cleaning performance of the fluid.

6.3.3. Comparative study of the systems.

The purpose of this subchapter is to discuss and differentiate the effect of BN nanoparticles mixed in a lubricant on properties and performance of the fluids formulated in different polymers.

The viscometer response on the presence of BN/lubricant additives was consistent and linearly related to the concentration of additives, i.e., the increased amount of BN/lubricant led to higher shear stress readings. This statement is relevant for both systems. For the two polymers, the Bingham parameters did not show precisely the same trend; however, there were observed similarities in the behavior when the concentration increased. On the other hand, the Power Law parameters responded differently for each system. As an example, the increase of the concentration reduced the flow behavior index in Duovis polymer; however, for the XG system, the increasing trend was noted.

The screening test for both Duovis-based and XG-based fluids proved that the best tribology improvement is obtained when BN/lubricant is added at high concentrations. In contrast to the case with dry BN particles, the XG system in combination with BN/lubricant depicted better friction improvement as compared to the Duovis system.

The experiments illustrated that high concentration of BN/lubricant could improve the filtrate loss of the Duovis-based system, whereas the filtrate properties of the XG-based system were deteriorated by the presence of these additives.

The pH value decreased slightly for the samples, which have Duovis as a polymer, while the XG-based system was barely affected by the presence of BN/lubricant.

It was challenging to determine LVER and YS from the viscoelasticity experiments; thus only the flow point values were compared for two systems with different polymers. The results from the viscoelasticity test showed that the flow point of the systems having the XG as a polymer were affected much stronger by the presence of BN/lubricant, and depicted an increase up to 215% as compared to the associated reference fluid. On the other hand, the addition of BN/lubricant did not influence the flow point of the Duovis-based fluids to the same extent.

Simulation has been performed on the fluids with high concentration of BN/lubricant as well as intermediate concentration. The Unified model fitted the rheological data of the XG-based fluid in a more precise way. On the other hand, the rheology of the fluids with Duovis polymer was covered better by the Robertson-Stiff model. Generally speaking, the models followed the pattern of the viscometer readings more accurately when the XG was used as a polymer.

The torque and drag simulations allowed to assume the maximum well length based on the critical loads on the drill string. The percentage change of the length relative to the reference system was calculated for the best lubricating fluid in each polymer. As mentioned earlier, the addition of 0.3 wt.% BN/lubricant led to higher friction reduction in the XG polymer. Therefore, it was possible to extend the well more significantly, when the nano-additives were used in the XG-based fluid. It is obvious that the friction coefficient was not the only parameter governing the well loads reduction. As seen from the experiments with dry BN nanoparticles, the system with improved rheology enabled to increase the well length more noticeably as compared to the system with higher friction reduction.

The hydraulic simulation depicted that addition of BN/lubricant negatively affected the pressure loss and hence ECD for the fluids with both polymers. However, the increase in pump pressure and ECD was more prominent when the mentioned additives were used in Duovis polymer.

The hole cleaning efficiency of the Duovis-based reference fluid was noticeably improved by the addition of BN nanoparticles mixed in a lubricant. At the same time, said nano-additives did not affect the minimum flow rate required for cuttings transport of the XG-based drilling fluid.

6.4. Effect of a nanocomposite.

As was mentioned in the experimental study, the MWCNT-OH added alone did not exhibit any significant improvement of lubricity. However, the tribological performance of the fluid containing MWCNT-OH and BN/lubricant nanocomposite was highly efficient, showing a sharp decrease in the coefficient of friction.

At the constant concentration of MWCNT-OH, the friction improvement was linearly related to the addition of BN/lubricant. The same dependency was observed for the samples having BN/lubricant as a single nano-additive. However, the analysis indicated that the nanocomposite yielded higher friction reduction than a nanofluid with only BN/lubricant additives.

6.5. Effect of mixing and pH on lubricity.

As stated in the literature, an ultrasonic bath is a very effective method for the better dispersion of nanoparticles, which tend to agglomerate due to strong van der Waals forces. The sonic waves disperse the nanoparticles evenly and prevent agglomeration and sedimentation [88]. Thus, it was expected to have a better lubricity performance of the fluids subjected to the sonication. Nevertheless, the experiments showed that the nanofluids mixed only mechanically yielded lower friction coefficient than sonicated samples. Higher concentration exhibited stronger deterioration of lubricity properties of the sonicated fluids as compared to the counterparts mixed in a conventional way.

On the other hand, the pH adjustment showed a positive effect on the lubricity of the samples containing the small amount of the BN nanoparticles. This statement is applicable both to the fluid mixed mechanically and ultrasonically.

6.6. Effect of temperature on rheology.

The rheological stability at high temperatures is one of the main concerns pertaining to the drilling fluids. The study was conducted to evaluate the behavior of the fluids containing dry BN nanoparticles at elevated temperatures and compare to the behavior of the nano-free system.

In general, all the samples regardless of the concentration of nanoparticles exhibited the similar response to the increased temperature. The shear stress values reduced linearly when the fluid was heated. The Bingham parameters also decreased for all the fluids, other than the sample with 0.03 wt.% of dry BN, where the increased temperature raised the plastic viscosity. The consistency index of the Power Law model showed a declining tendency when the fluid was heated up. This effect was more prominent for the fluid with the highest concentration

(0.03 wt.%). The flow behavior index remained unaltered and did not react on the temperature variations. Again, the sample with 0.03 wt.% of dry BN had a growth in n -parameter when was subjected to the high temperatures.

7. CONCLUSION.

The primary objective of the thesis was to investigate the impact of nano-sized BN on the properties of water-based drilling fluid having either Duovis or XG as a polymer. The author's attention was focused not only on the implementation of the commercial BN nanoparticles but also on the surface modification of them. From the experimental and simulation research that has been undertaken, the following presents the summary of main observations and the drawn conclusions:

General observations:

- The performance of the nanoparticles (NPs) varies from polymer to polymer.
- Sonication degraded the lubricity of the nanofluids.
- Increasing pH can reduce the friction coefficient up to 9%.
- Regardless the concentration, the plastic viscosity, yield stress and consistency index of the nanofluids decreases at elevated temperatures.
- The reduction in friction is not linearly proportional to the concentration of BN NPs.
- Dry BN nanoparticles improve tribological properties at their best at low concentrations, whereas grafted particles and particles mixed in oil perform better at high concentrations.
- Drill string loads are not only the function of the drilling fluid's lubricity properties but also rheology.
- Nanoparticles do not have any significant effect on the pH of the mixtures.
- The Robertson-Stiff model predicts the rheological behavior of the drilling fluids with lower percent deviation rate.

Dry Boron nitride nanoparticles:

- Dry BN nanoparticles improve lubricity better in Duovis polymer rather than in XG.
- The maximum friction reduction of 28.4% was observed when given nano-additives were introduced to the Duovis-based fluid at the concentration of 0.03 wt.%.
- The addition of BN at low concentrations in XG-based fluid slightly improve filtration, whereas in Duovis polymer, the filtrate volume increased up to 33% as compared to the nano-free system.

- Hydraulic simulation results showed that the presence of BN nanoparticles in Duovis system at 0.03 wt.% decreases the friction loss by average 32% at the given range of flow rates.

Grafted Boron nitride nanoparticles:

- Oil grafted BN nanoparticles have more pronounced potential to reduce the coefficient of friction as compared to the commercial dry BN nanoparticles. The effect is stronger in XG biopolymer rather than in Duovis biopolymer.
- Coefficient of friction reduced by 44% when the XG-base fluid was mixed with grafted BN at the concentration of 0.2 wt.%.
- The rheological parameters exhibited more consistent behavior with increasing concentration of said additives in XG polymer rather than in Duovis.

Boron nitride nanoparticles associated with a lubricant:

- BN nanoparticles along with a lubricant have a superior potential to decrease the friction, which is more pronounced in XG polymer.
- Adding of 0.3 wt.% of BN/lubricant improved the lubricity of the XG-base fluid by 54%.
- The rheological effect of the BN nanoparticles mixed in oil was similar to the effect of grafted ones.
- The addition of 0.3 wt.% of BN/lubricant mixture decreased the friction coefficient of the fluid having a small amount of MWCNT-OH nanoparticles by 52.9%.

This paper has clearly shown that lubricating effect of BN nanoparticles is reinforced when grafted/mixed with an environmental friendly lubricant. The results obtained in this thesis are valid in the considered polymer types. One may get different results by changing the base system.

Summing up the results, the modification techniques proposed hold a promise for enhancing the properties of commercial nanoparticles. The tribological performance of Boron nitride nanoparticles is the most effective when mixed with a lubricant. However, one should ensure the environmentally friendly lubricant to comply with the regulations of some countries such as Norway.

REFERENCES.

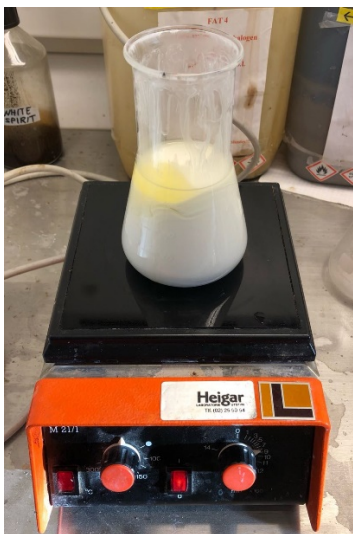
1. Growcock, F. and T. Harvey, *Chapter 2 - Drilling Fluids*, in *Drilling Fluids Processing Handbook*. 2005, Gulf Professional Publishing: Burlington. p. 15-68.
2. Fink, J.K., *Chapter 1 - Drilling Muds*, in *Petroleum Engineer's Guide to Oil Field Chemicals and Fluids*. 2012, Gulf Professional Publishing: Boston. p. 1-59.
3. Robert F. Mitchell, *Petroleum Engineering Handbook, Volume II ed., Editor-in-Chief Larry W. Lake, Ed. TX 75080-2040, USA: Society of Petroleum Engineers, 2006*.
4. Melbouci, M., Sau, A.C., 2008. *Water-based drilling fluids*. US Patent 7 384 892, assigned to Hercules Incorporated (Wilmington, DE), June 10, 2008.
5. *Oilfield Market Report*. 2004; Available from: www.spearsresearch.com.
6. Amani, M., M. Al-Jubouri, and A. Shadravan, *Comparative Study of Using Oil-Based Mud Versus Water-Based Mud in HPHT Fields*. 2012.
7. Abduo, M.I., et al., *Comparative study of using Water-Based mud containing Multiwall Carbon Nanotubes versus Oil-Based mud in HPHT fields*. Egyptian Journal of Petroleum, 2016. **25**(4): p. 459-464.
8. Falope, F.D., et al., *Improved Drilling Efficiency via Enhanced Water Based Mud in the Niger Delta*, in *SPE Nigeria Annual International Conference and Exhibition*. 2014, Society of Petroleum Engineers: Lagos, Nigeria.
9. Wang, X.-B. and W.-M. Liu, *Nanoparticle-Based Lubricant Additives*, in *Encyclopedia of Tribology*, Q.J. Wang and Y.-W. Chung, Editors. 2013, Springer US: Boston, MA. p. 2369-2376.
10. Kong, X. and M. Ohadi. *Applications of micro and nano technologies in the oil and gas industry-overview of the recent progress*. in *Abu Dhabi international petroleum exhibition and conference*. 2010. Society of Petroleum Engineers.
11. Hareland, G., et al., *Innovative Nanoparticle Drilling Fluid and Its Benefits to Horizontal or Extended Reach Drilling*, in *SPE Canadian Unconventional Resources Conference*. 2012, Society of Petroleum Engineers: Calgary, Alberta, Canada.
12. Wilson, A., *Wellbore Strengthening in Shales With Nanoparticle-Based Drilling Fluids*. 2015.
13. Wilson, A., *Novel Nanoparticle-Based Drilling Fluid Reveals Improved Characteristics*. 2012.
14. Hoxha, B.B., E.v. Oort, and H. Daigle, *How Do Nanoparticles Stabilize Shale?*, in *SPE International Conference on Oilfield Chemistry*. 2017, Society of Petroleum Engineers: Montgomery, Texas, USA.
15. Mahmoud, O., et al., *Nanoparticle-Based Drilling Fluids for Minimizing Formation Damage in HP/HT Applications*, in *SPE International Conference and Exhibition on Formation Damage Control*. 2016, Society of Petroleum Engineers: Lafayette, Louisiana, USA.
16. Mezger, T.G., *The rheology handbook : for users of rotational and oscillatory rheometers*. 2006, Hannover: Vincentz.
17. Gucuyener, I.H., *A Rheological Model for Drilling Fluids and Cement Slurries*, in *Middle East Oil Technical Conference and Exhibition*. 1983, Society of Petroleum Engineers: Manama, Bahrain.
18. Institute, A.P., *Recommended Practice on the Rheology and Hydraulics of Oil-well Drilling Fluids*. 2003: API.
19. Azar, J.J. and G.R. Samuel, *Drilling engineering*. 2007: PennWell Books.
20. Skjeggstad O., *Boreslamteknologi: Teori og praksis*. Alma Mater Forlag. 1989 (ISBN: 82-419-0010-4).
21. Bui, B., et al., *Viscoelastic properties of oil-based drilling fluids*. Annual Transactions of the Nordic Rheology Society, 2012. **20**: p. 33-47.

22. Chhabra, R.P., *Non-Newtonian Fluids: An Introduction*, in *Rheology of Complex Fluids*, J.M. Krishnan, A.P. Deshpande, and P.B.S. Kumar, Editors. 2010, Springer New York: New York, NY. p. 3-34.
23. Mewis, J. and N.J. Wagner, *Thixotropy*. *Advances in Colloid and Interface Science*, 2009. **147-148**: p. 214-227.
24. Barnes, H.A., *Thixotropy—a review*. *Journal of Non-Newtonian Fluid Mechanics*, 1997. **70**(1): p. 1-33.
25. Folayan, J.A., et al., *Selecting the Most Appropriate Model for Rheological Characterization of Synthetic Based Drilling Mud*. *International Journal of Applied Engineering Research*, 2017. **12**(18): p. 7614-7649.
26. Macosko, C., *Rheology: Principles, Measurements, and Applications* (VCH, New York, 1994). Google Scholar: p. 425-474.
27. Rashaida, A.A., *Flow of a non-Newtonian Bingham plastic fluid over a rotating disk*. 2005.
28. Vilorio Ochoa, M., *Analysis of drilling fluid rheology and tool joint effect to reduce errors in hydraulics calculations*. 2006, Texas A&M University.
29. KOK, M.V. and T. Alikaya, *Effect of polymers on the rheological properties of KCl/polymer type drilling fluids*. *Energy Sources*, 2005. **27**(5): p. 405-415.
30. Robertson, R. and H. Stiff Jr, *An improved mathematical model for relating shear stress to shear rate in drilling fluids and cement slurries*. *Society of Petroleum Engineers Journal*, 1976. **16**(01): p. 31-36.
31. Aarrestad, T.V., *Torque and drag-two factors in extended-reach drilling*. *Journal of Petroleum Technology*, 1994. **46**(09): p. 800-803.
32. Johancsik, C.A., D.B. Friesen, and R. Dawson, *Torque and drag in directional wells-prediction and measurement*. *Journal of Petroleum Technology*, 1984. **36**(06): p. 987-992.
33. Belayneh, M., *Lecture notes from the Advanced drilling class, PET 525*. 2017: University of Stavanger, Stavanger, Rogaland.
34. Aadnoy, B.S., *Mechanics of drilling*. 2006: Shaker.
35. *IADC Drilling Manual*. 2014 [cited 2018. March 15th]; Available from: <http://www.iadc.org/wp-content/uploads/2015/08/preview-hydr.pdf>.
36. Lapeyrouse, N.J., *Formulas and calculations for drilling, production, and workover*. 2002: Gulf professional publishing.
37. Sadigov, J., *Comparisons of Rheology and Hydraulics Prediction of Mud Systems in Concentric and Eccentric Well Geometry*. June 2013, University of Stavanger: Stavanger, Rogaland.
38. Kapusta, S., L. Balzano, and P.M. Te Riele. *Nanotechnology applications in oil and gas exploration and production*. in *International Petroleum Technology Conference*. 2011. International Petroleum Technology Conference.
39. Kasiralvalad, E., *The great potential of nanomaterials in drilling & drilling fluid applications*. *International Journal of Nano Dimension*, 2014. **5**(Issue 5): p. 463-471.
40. Salata, O.V., *Applications of nanoparticles in biology and medicine*. *Journal of nanobiotechnology*, 2004. **2**(1): p. 3.
41. Khan, I., K. Saeed, and I. Khan, *Nanoparticles: Properties, applications and toxicities*. *Arabian Journal of Chemistry*, 2017.
42. Nabhani, N., M. Emami, and A.T. Moghadam. *Application of nanotechnology and nanomaterials in oil and gas industry*. in *AIP Conference Proceedings*. 2011. AIP.
43. *Nanoscience and nanotechnologies : opportunities and uncertainties*. 2004: p. 155 p.
44. Ponmani, S., R. Nagarajan, and J. Sangwai. *Applications of nanotechnology for upstream oil and gas industry*. in *Journal of Nano Research*. 2013. Trans Tech Publ.
45. Krishnamoorti, R., *Extracting the benefits of nanotechnology for the oil industry*. *Journal of petroleum technology*, 2006. **58**(11): p. 24-26.

46. El-Diasty, A.I. and A.M.S. Ragab. *Applications of nanotechnology in the oil & gas industry: Latest trends worldwide & future challenges in Egypt*. in *North Africa Technical Conference and Exhibition*. 2013. Society of Petroleum Engineers.
47. Song, Y.Q. and C. Marcus, *Hyperpolarized Silicon Nanoparticles: Reinventing Oil Exploration?* Presentation, Schlumberger, 2007.
48. Bhatia, K.H. and L.P. Chacko. *Ni-Fe nanoparticle: An innovative approach for recovery of hydrates*. in *Brasil Offshore*. 2011. Society of Petroleum Engineers.
49. Huang, T. and J.B. Crews, *Nanotechnology applications in viscoelastic surfactant stimulation fluids*. *SPE production & operations*, 2008. **23**(04): p. 512-517.
50. Kumar, D., et al., *Scale Inhibition Using nano-silica Particles*, in *SPE Middle East Health, Safety, Security, and Environment Conference and Exhibition*. 2012, Society of Petroleum Engineers: Abu Dhabi, UAE.
51. Ogolo, N., O. Olafuyi, and M. Onyekonwu. *Enhanced oil recovery using nanoparticles*. in *SPE Saudi Arabia section technical symposium and exhibition*. 2012. Society of Petroleum Engineers.
52. Moradi, B., et al. *Application of SiO₂ nano particles to improve the performance of water alternating gas EOR process*. in *SPE Oil & Gas India Conference and Exhibition*. 2015. Society of Petroleum Engineers.
53. Vryzas, Z., et al. *A Comprehensive Approach for the Development of New Magnetite Nanoparticles Giving Smart Drilling Fluids with Superior Properties for HP/HT Applications*. in *International Petroleum Technology Conference*. 2016. International Petroleum Technology Conference.
54. Caldarola, V., et al. *Potential Directional Drilling Benefits of Barite Nanoparticles in Weighted Water Based Drilling Fluids*. in *50th US Rock Mechanics/Geomechanics Symposium*. 2016. American Rock Mechanics Association.
55. Cedola, A., et al., *Nanoparticles in weighted water based drilling fluids increase loss gradient*. 2016.
56. Vryzas, Z., et al. *Development and testing of novel drilling fluids using Fe₂O₃ and SiO₂ nanoparticles for enhanced drilling operations*. in *International Petroleum Technology Conference*. 2015. International Petroleum Technology Conference.
57. Kang, Y., et al., *Strengthening shale wellbore with silica nanoparticles drilling fluid*. *Petroleum*, 2016. **2**(2): p. 189-195.
58. Ying, J.Y. and T. Sun, *Research needs assessment on nanostructured catalysts*. *Journal of Electroceramics*, 1997. **1**(3): p. 219-238.
59. Esmaeili, A. *Applications of nanotechnology in oil and gas industry*. in *AIP Conference Proceedings*. 2011. AIP.
60. Wang, Y., et al. *Progress in preparation, properties and application of boron nitride nanomaterials*. in *AIP Conference Proceedings*. 2017. AIP Publishing.
61. Oku, T., *Synthesis, Structures and Properties of Boron Nitride Nanoparticles*. *Handbook of Nanoparticles*, 2016: p. 1-40.
62. Arenal, R. and A. Lopez-Bezanilla, *Boron nitride materials: an overview from 0D to 3D (nano) structures*. *Wiley Interdisciplinary Reviews: Computational Molecular Science*, 2015. **5**(4): p. 299-309.
63. Alvi, M.A.A., et al., *The Effect of Micro-Sized Boron Nitride BN and Iron Trioxide Fe₂O₃ Nanoparticles on the Properties of Laboratory Bentonite Drilling Fluid*, in *SPE Norway One Day Seminar*. 2018, Society of Petroleum Engineers: Bergen, Norway.
64. Christian, S. and F. Laszlo, *Multiwall carbon nanotubes*. *Physics World*, 2000. **13**(6): p. 37.
65. Dresselhaus, M.S., G. Dresselhaus, and P.C. Eklund, *Chapter 2 - Carbon Materials*, in *Science of Fullerenes and Carbon Nanotubes*. 1996, Academic Press: San Diego. p. 15-59.

66. Premalatha, M. and A.K.S. Jeevaraj, *Preparation and characterization of hydroxyl (-OH) functionalized multi-walled carbon nanotube (MWCNT)–Dowtherm A nanofluids*. Particulate Science and Technology, 2017: p. 1-6.
67. Khan, W.A., et al., *MWCNT for Enhancing Mechanical Properties of Oil Well Cement for HPHT Applications*, in *SPE/IADC Middle East Drilling Technology Conference and Exhibition*. 2016, Society of Petroleum Engineers: Abu Dhabi, UAE.
68. Mehrali, M., et al., *Investigation of thermal conductivity and rheological properties of nanofluids containing graphene nanoplatelets*. Nanoscale research letters, 2014. **9**(1): p. 15.
69. Caenn, R., H. Darley, and G. Gray, *Clay Mineralogy and the Colloid Chemistry of Drilling Fluids*. Composition and Properties of Drilling and Completion Fluids, 2011: p. 137-177.
70. Kutlić, A., G. Bedeković, and I. Sobota, *Bentonite processing*. Rudarsko-geološko-naftni zbornik, 2012. **24**(1): p. 61-65.
71. Al-Homadhi, E.S. *Improving Local Bentonite Performance for Drilling Fluids Applications*. in *SPE Saudi Arabia Section Technical Symposium*. 2007. Society of Petroleum Engineers.
72. Fink, J., *Petroleum engineer's guide to oil field chemicals and fluids*. 2015: Gulf Professional Publishing.
73. A., K., B. G., and S. I., *Bentonite Processing Oplemenjivanje Bentonita*. University of Zagreb, Faculty of Mining, Geology and Petroleum Engineering, 2012.
74. Strand, S., *Øvinger i Bore og Brønnvæsker*. Compendium in the BIP 200 class, University of Stavanger, Stavanger, Rogaland, 2014.
75. Mercier, J.P., G. Zambelli, and W. Kurz, *Introduction to materials science*. 2012: Elsevier.
76. Hughes, B., *Drilling Fluids Reference Manual*. Houston, Texas, 2006.
77. Benchabane, A. and K. Bekkour, *Rheological properties of carboxymethyl cellulose (CMC) solutions*. Colloid and Polymer Science, 2008. **286**(10): p. 1173.
78. Palaniraj, A. and V. Jayaraman, *Production, recovery and applications of xanthan gum by Xanthomonas campestris*. Journal of Food Engineering, 2011. **106**(1): p. 1-12.
79. Luvielmo, M.d.M., et al., *Structure of xanthan gum and cell ultrastructure at different times of alkali stress*. brazilian journal of microbiology, 2016. **47**(1): p. 102-109.
80. Garcia-Ochoa, F., et al., *Xanthan gum: production, recovery, and properties*. Biotechnology advances, 2000. **18**(7): p. 549-579.
81. Clark, R., et al., *Polyacrylamide/potassium-chloride mud for drilling water-sensitive shales*. Journal of Petroleum technology, 1976. **28**(06): p. 719-727.
82. Brien, D.E. and M.E. Chenevert, *Stabilizing Sensitive Shales With Inhibited, Potassium-Based Drilling Fluids*. 1973.
83. Caenn, R., H.C. Darley, and G.R. Gray, *Composition and properties of drilling and completion fluids*. 2011: Gulf professional publishing.
84. Forthun, S.C., *Effect of Nano Additives on Friction in a Bentonite Water Based System*, in *Faculty of Science and Technology*. 2016, University of Stavanger: Stavanger, Rogaland.
85. Mijić, P., N. Gaurina-Međimurec, and B. Pašić, *The Influence of SiO₂ and TiO₂ Nanoparticles on the Properties of Water-Based Mud*. 2017(57762): p. V008T11A002.
86. Yu, W. and H. Xie, *A Review on Nanofluids: Preparation, Stability Mechanisms, and Applications*. Journal of Nanomaterials, 2012. **2012**: p. 17.
87. Ur Rehman, W., et al., *Effect of Sonication on the Stability of Nanofluids Based on the Mixture of Kapok Seeds Oil and Multi Walled Carbon Nanotubes*. Vol. 694. 2016. 213-217.
88. Pradhan, S., et al., *Effect of sonication on particle dispersion, administered dose and metal release of non-functionalized, non-inert metal nanoparticles*. Journal of Nanoparticle Research, 2016. **18**(9): p. 285.

APPENDIX A: Photographs from grafting procedure.



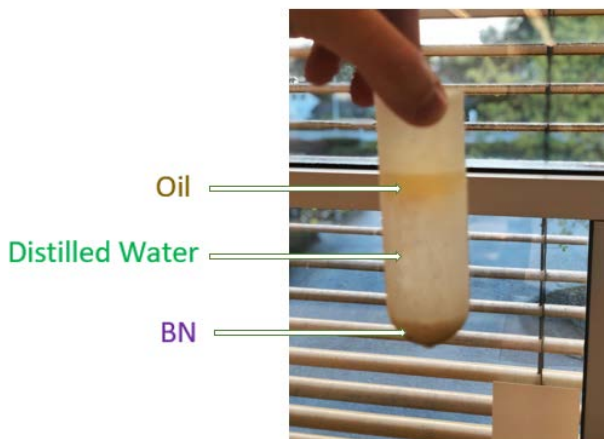
Magnetic stirring of BN + Lubricant



Sonication of BN + Lubricant



Centrifugation



Separated phases after Centrifugation

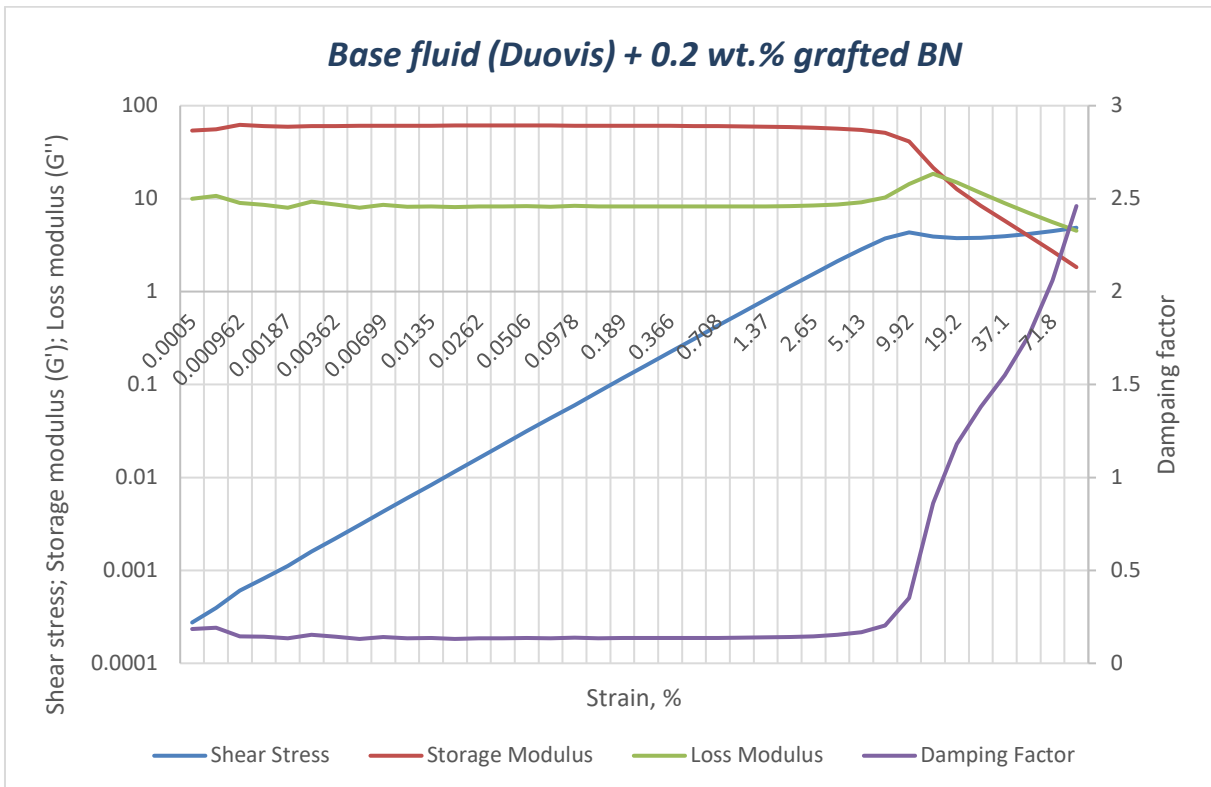
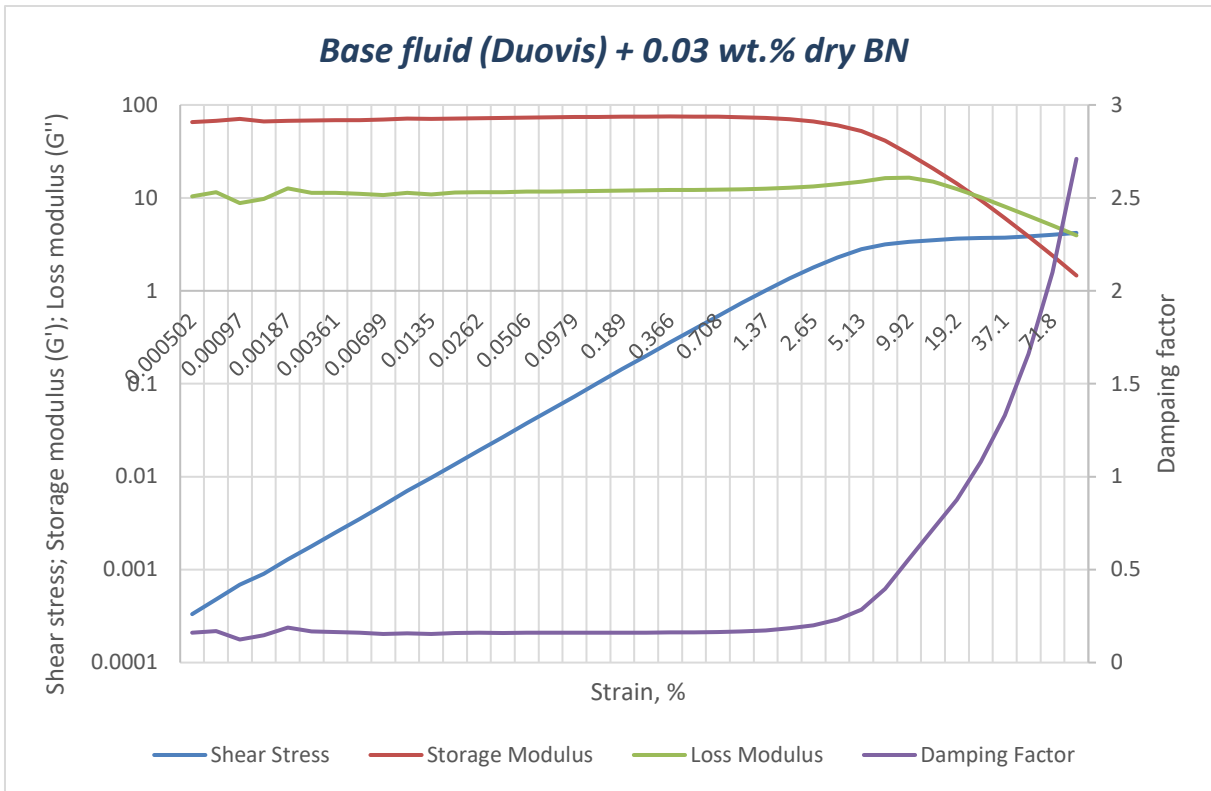


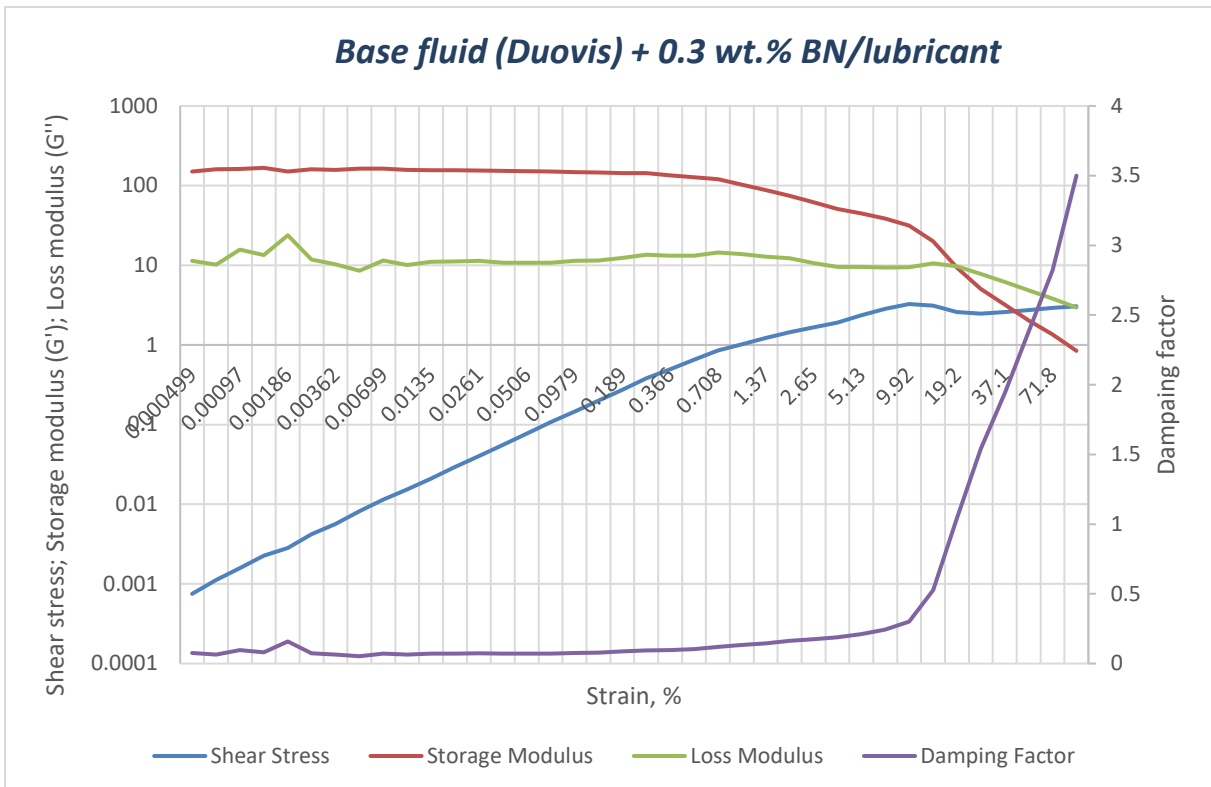
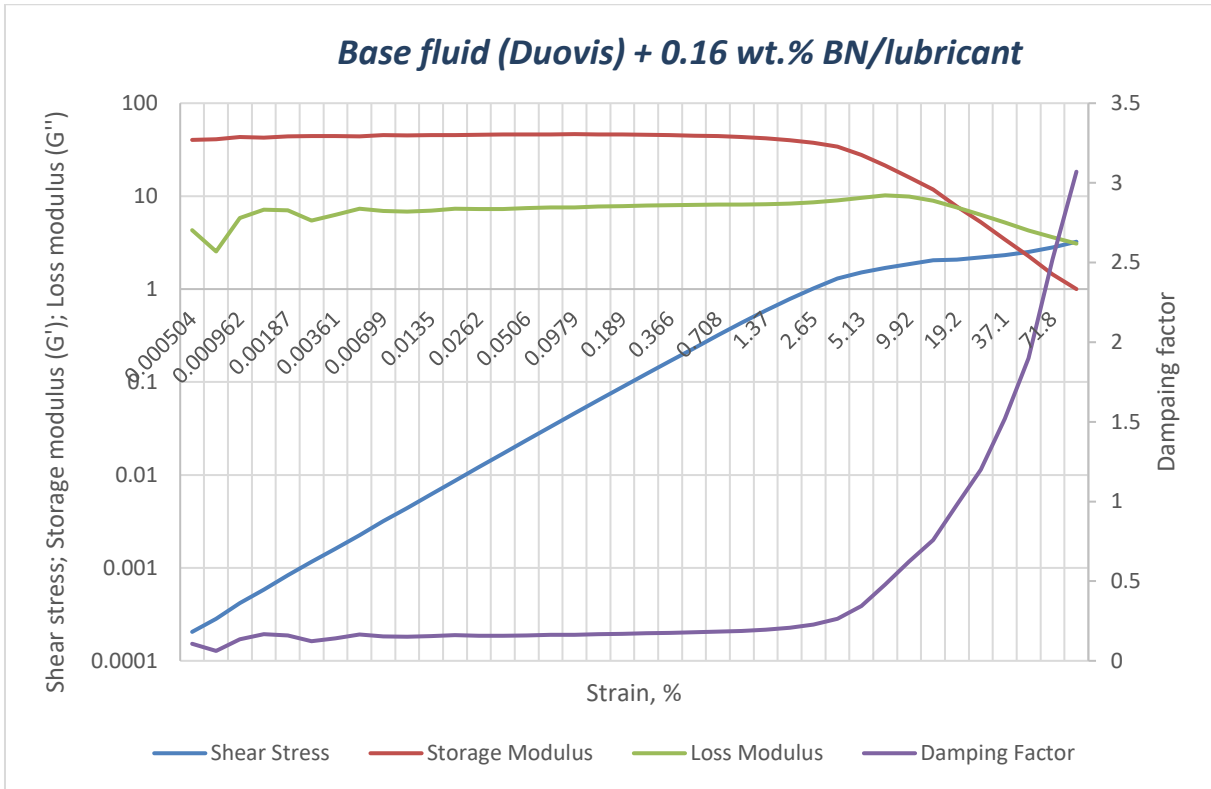
Drying of the grafted BN

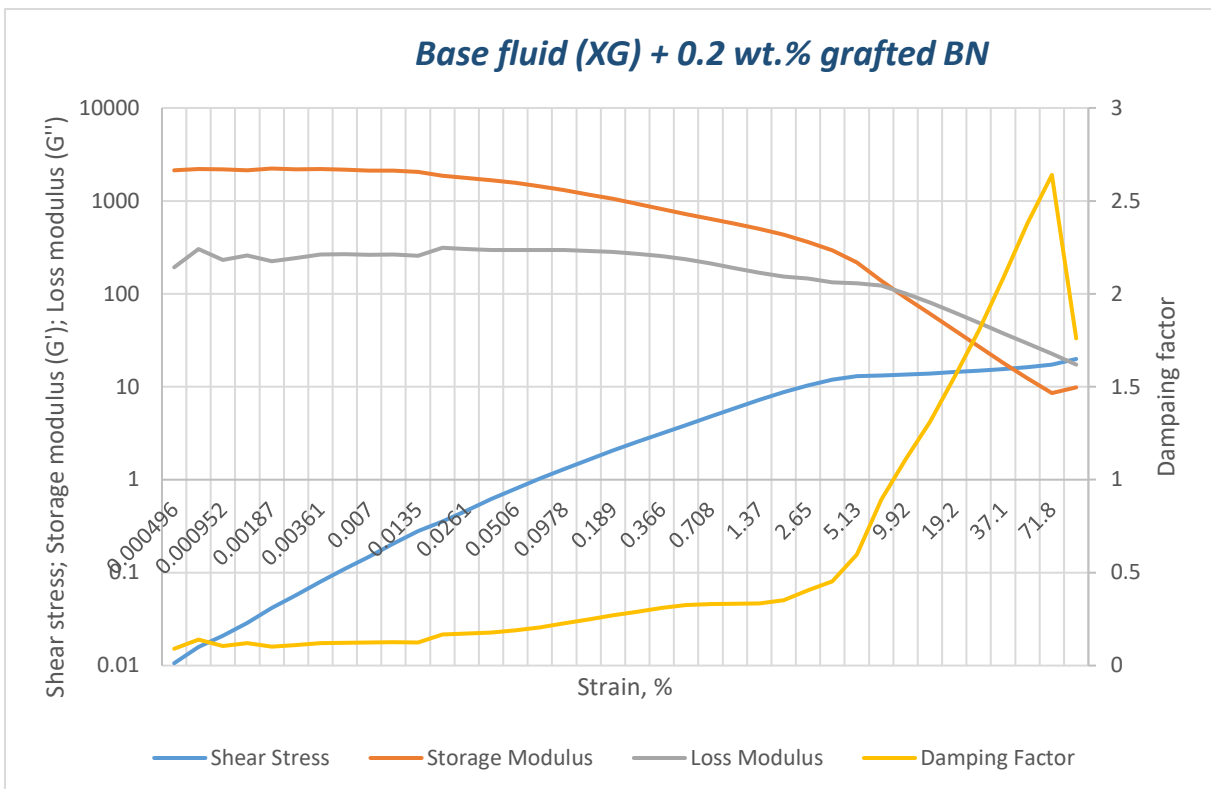
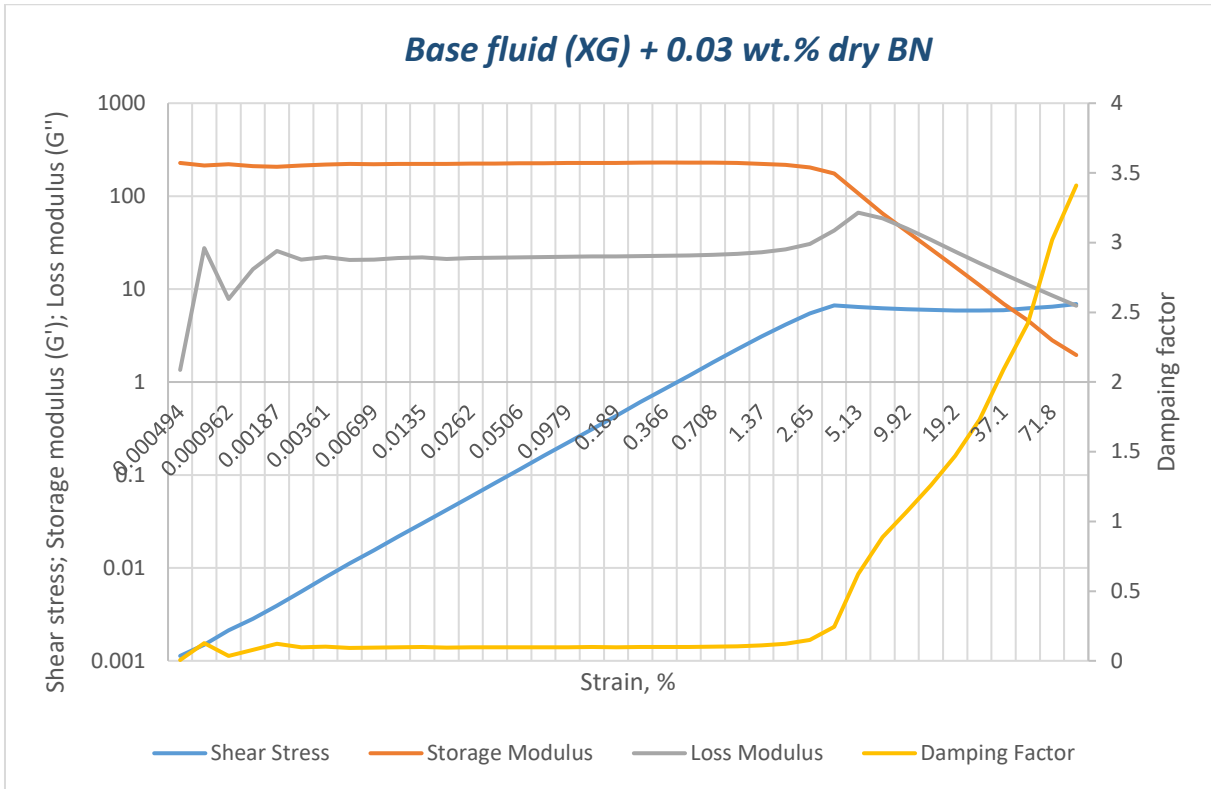


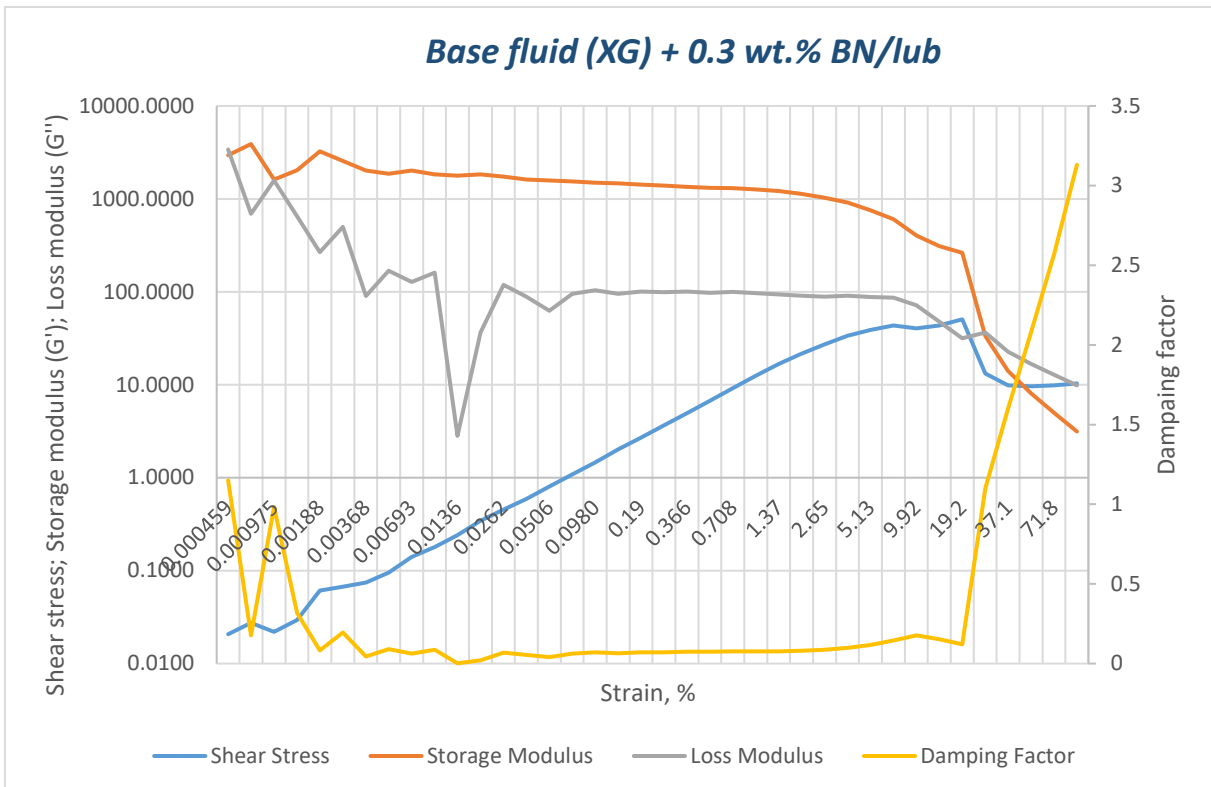
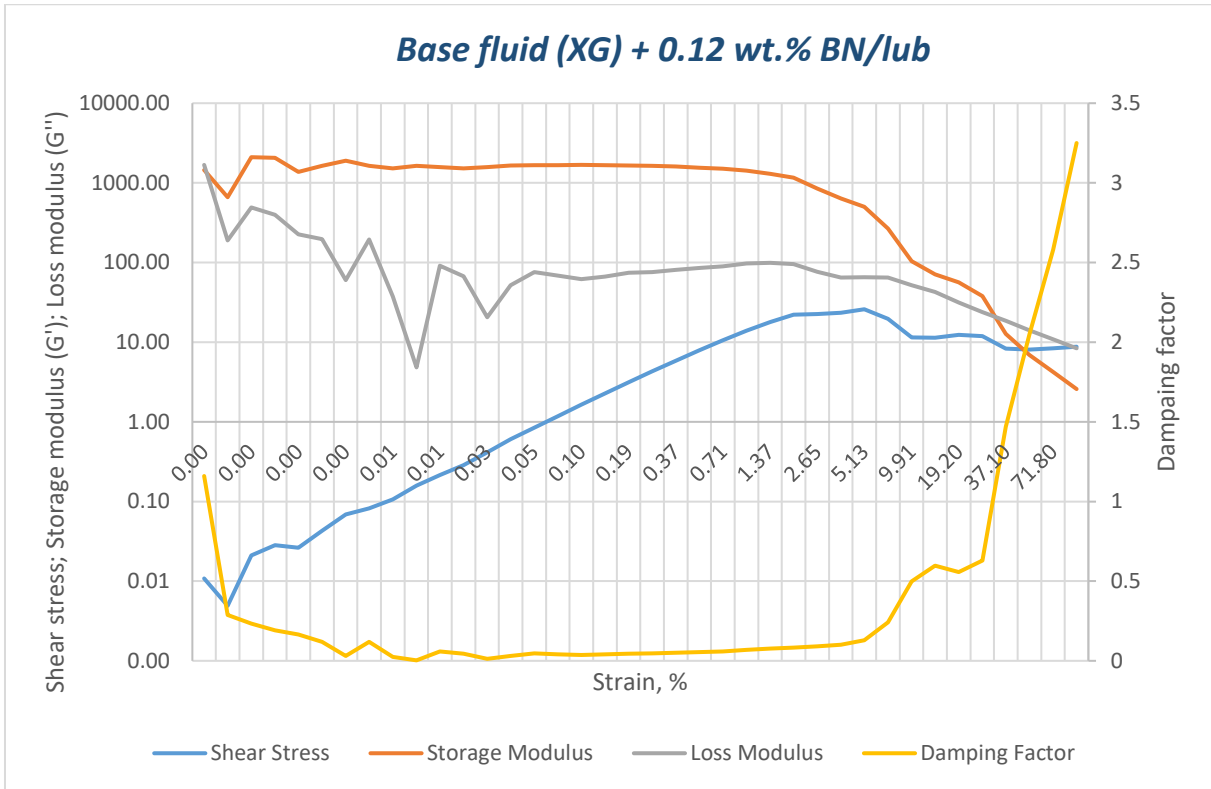
Grafted BN

APPENDIX B: Amplitude Sweep Measurements of drilling fluids.



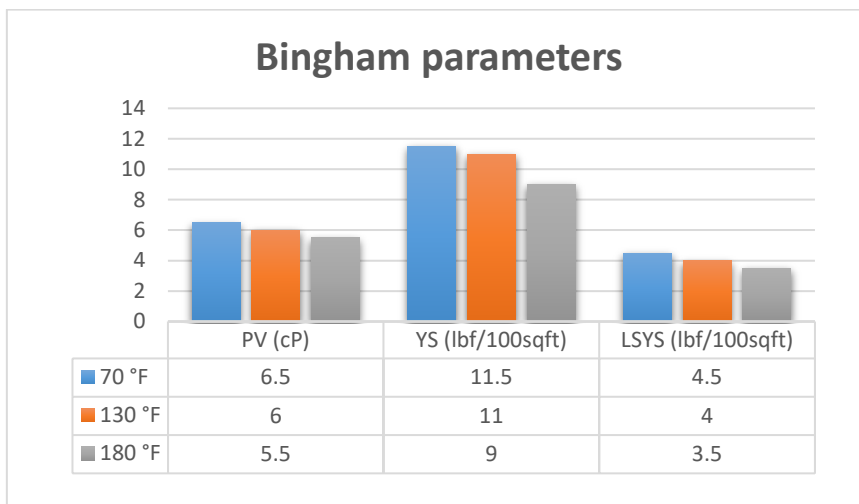
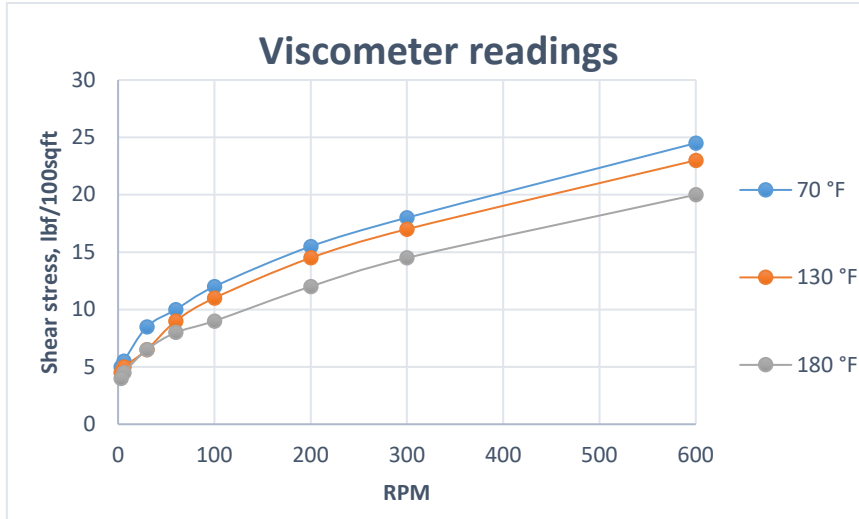




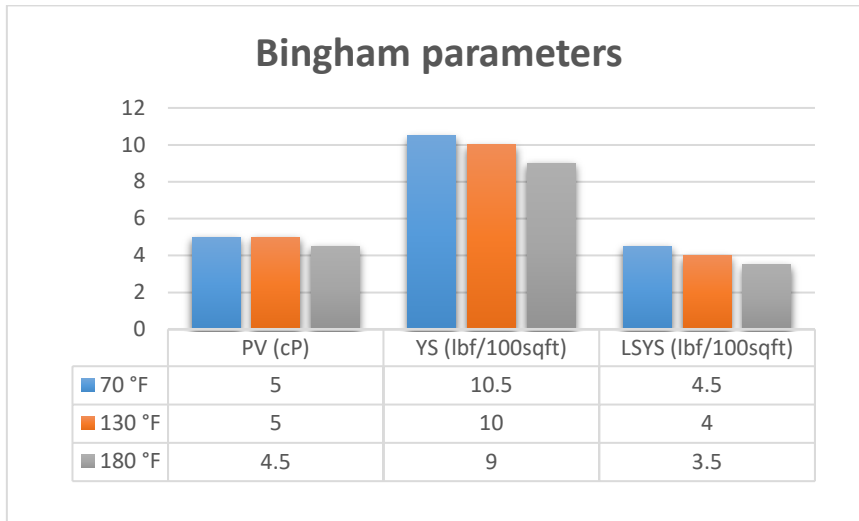
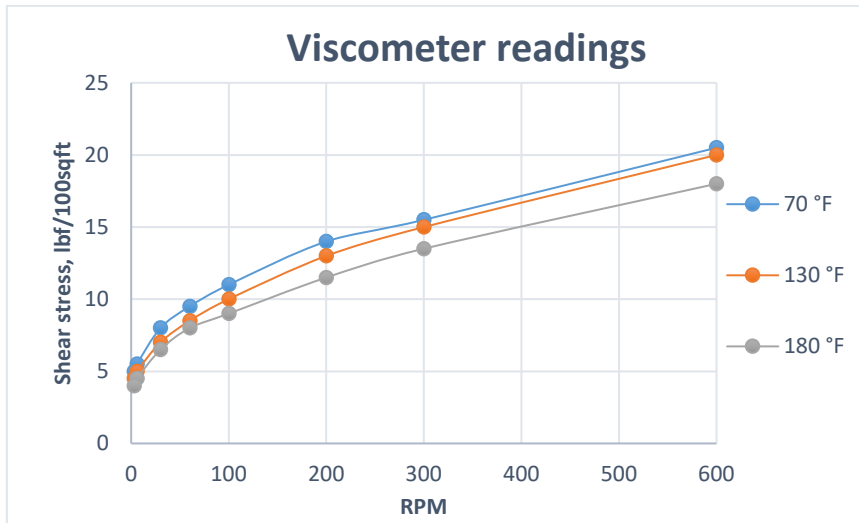


APPENDIX C: Effect of temperature on the rheology of drilling fluids.

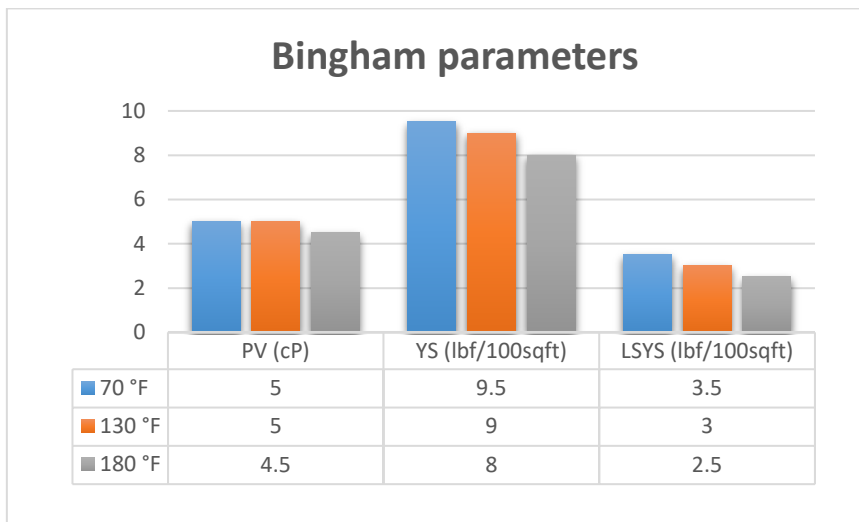
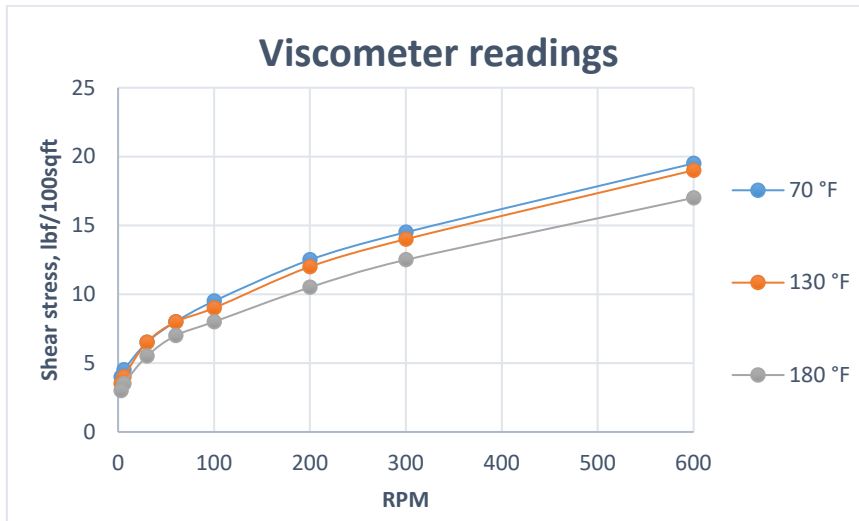
Base fluid (Duovis)



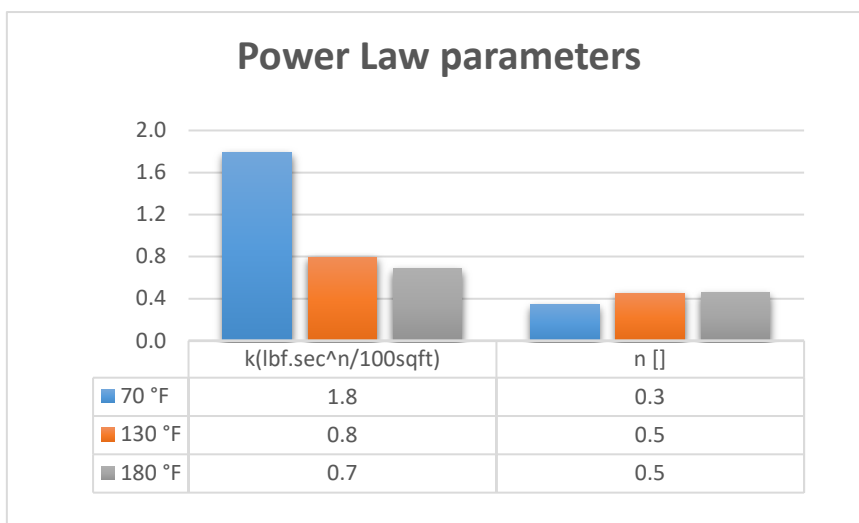
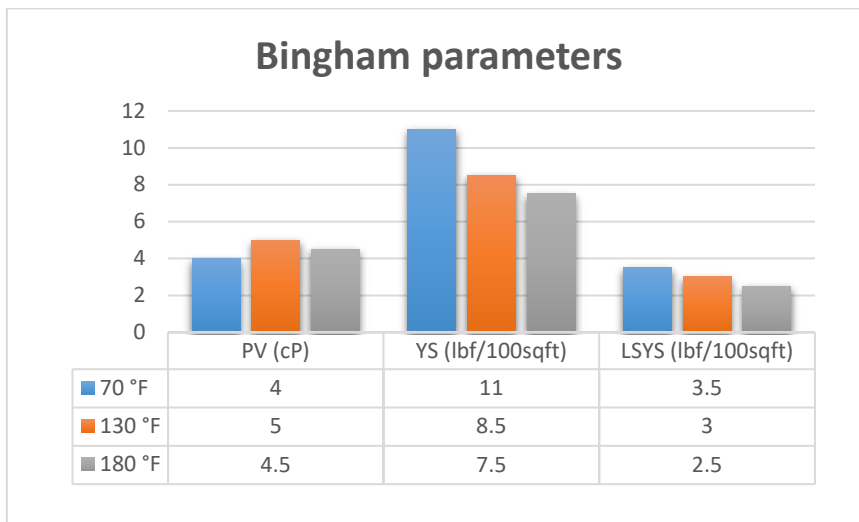
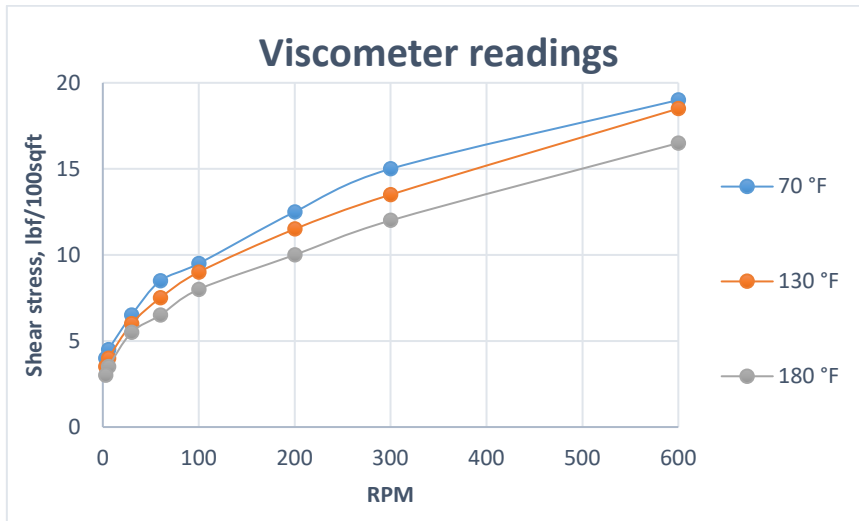
Base fluid (Duovis) + 0.04 wt.% Lignosulfonate



Base fluid (Duovis) + 0.02 wt.% dry BN + 0.04 wt.% Lignosulfonate

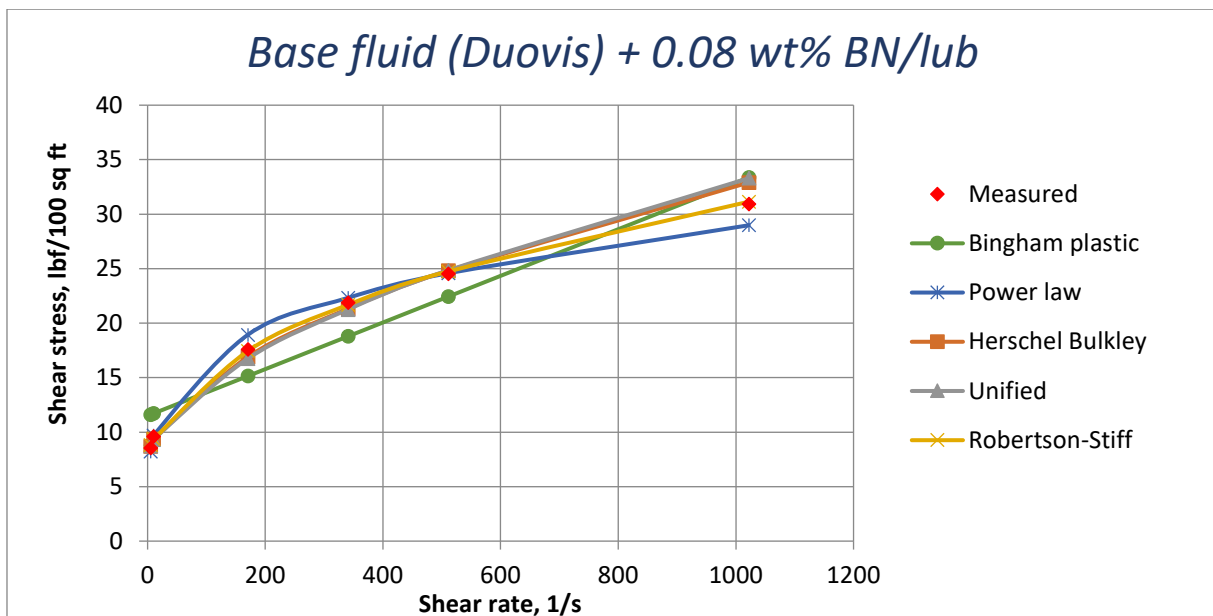
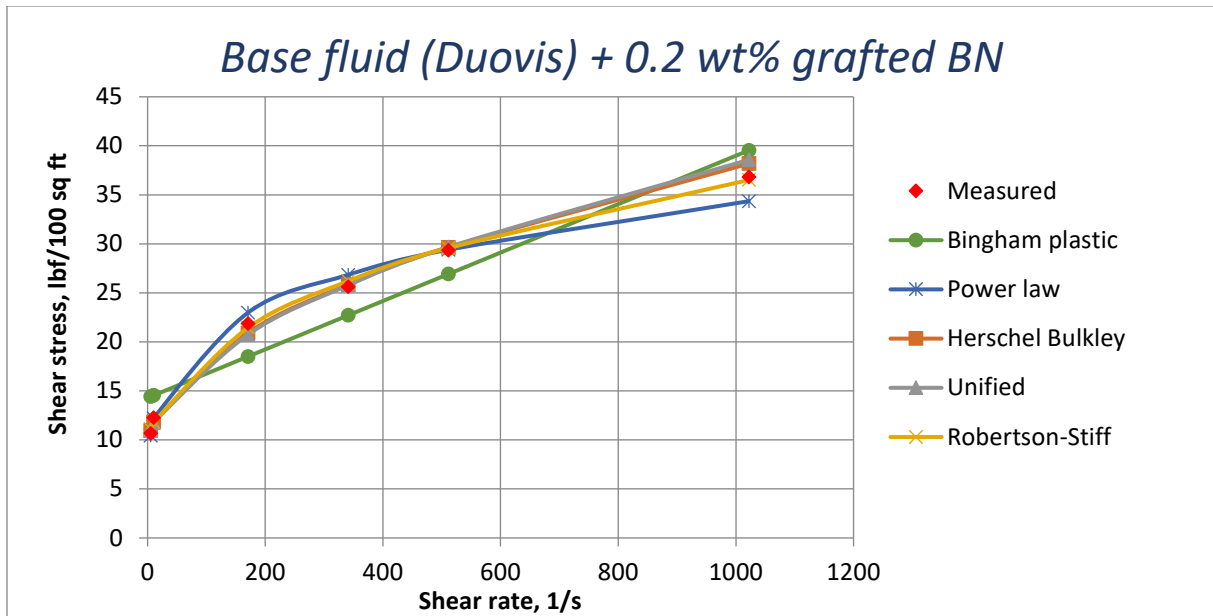


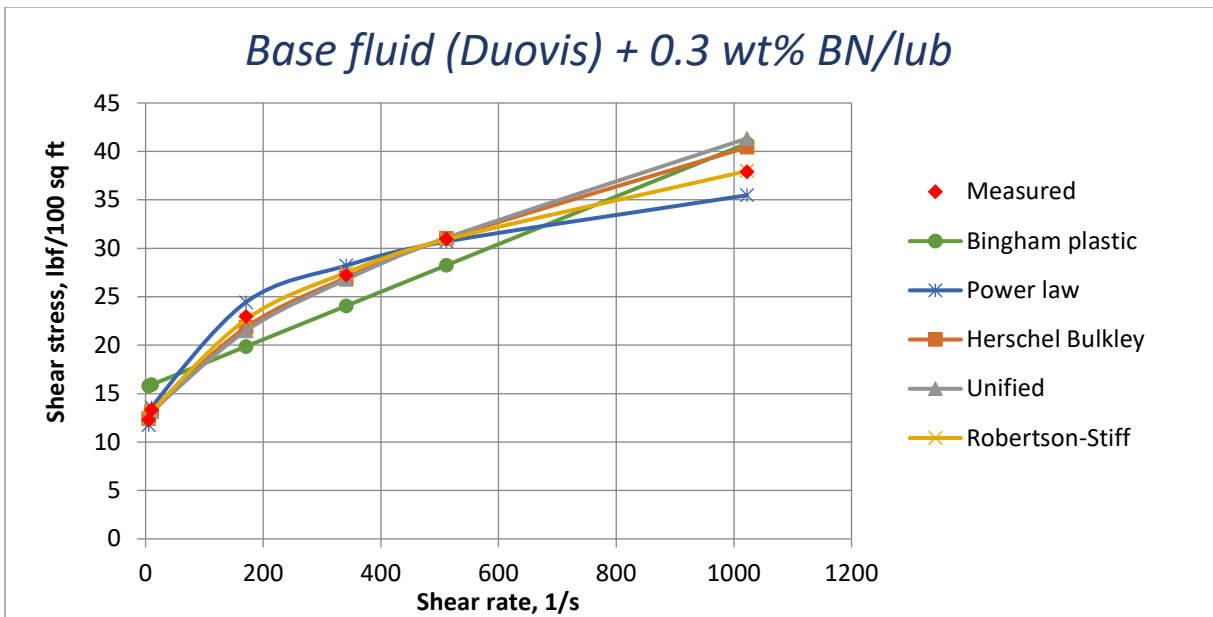
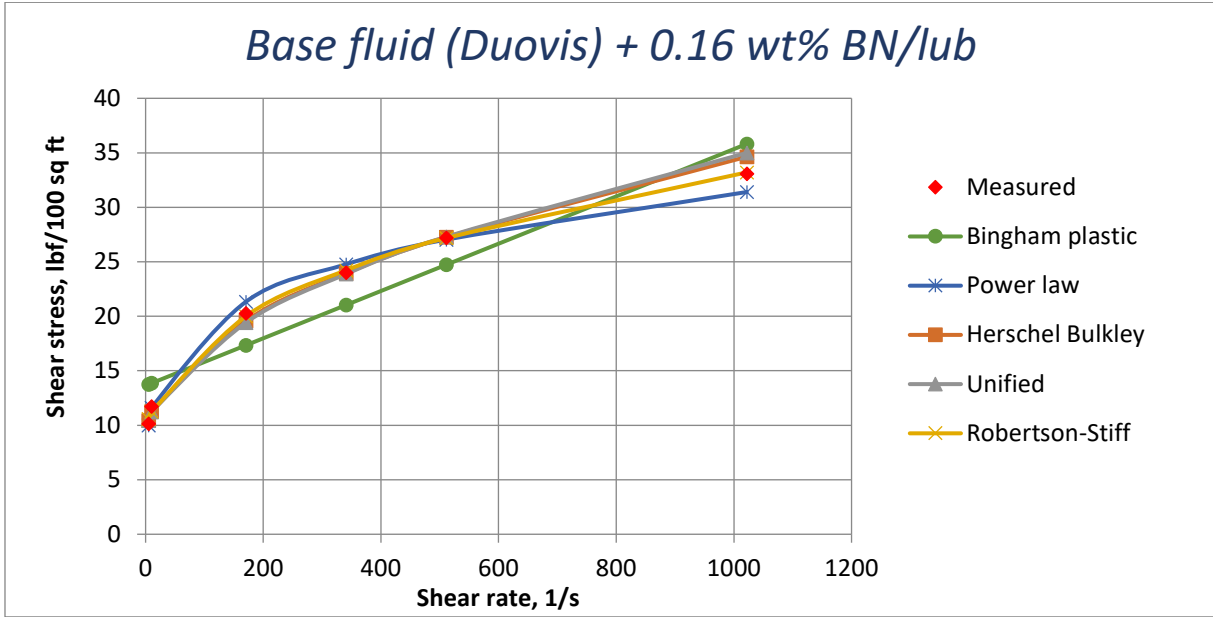
Base fluid (Duovis) + 0.03 wt.% dry BN + 0.04 wt.% Lignosulfonate

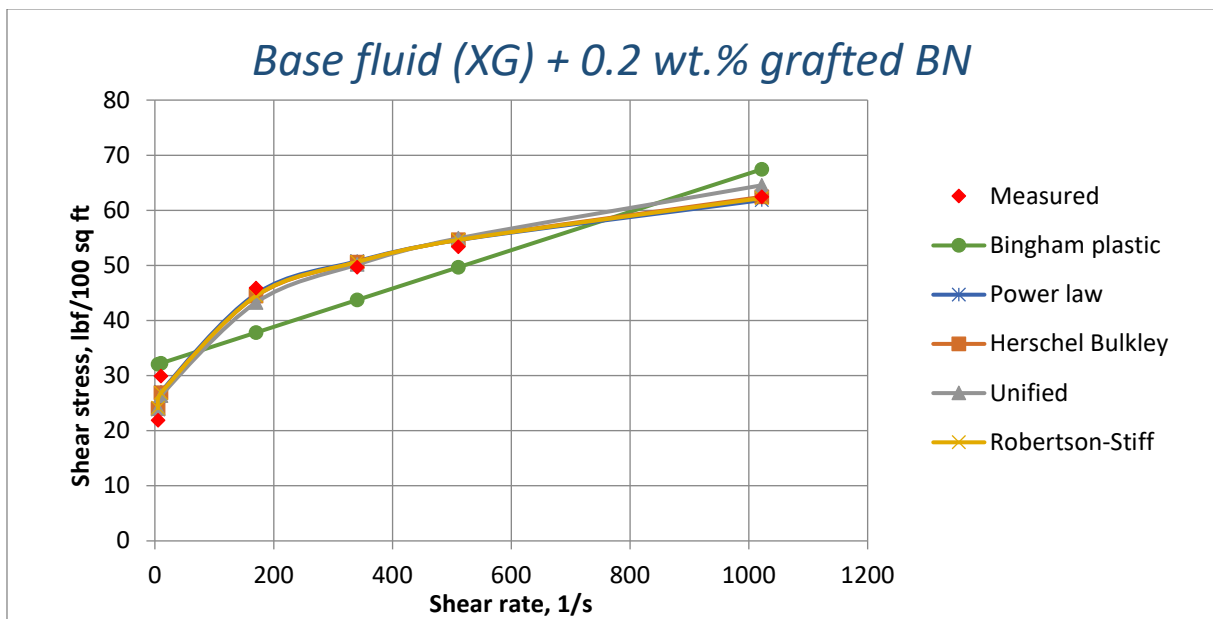
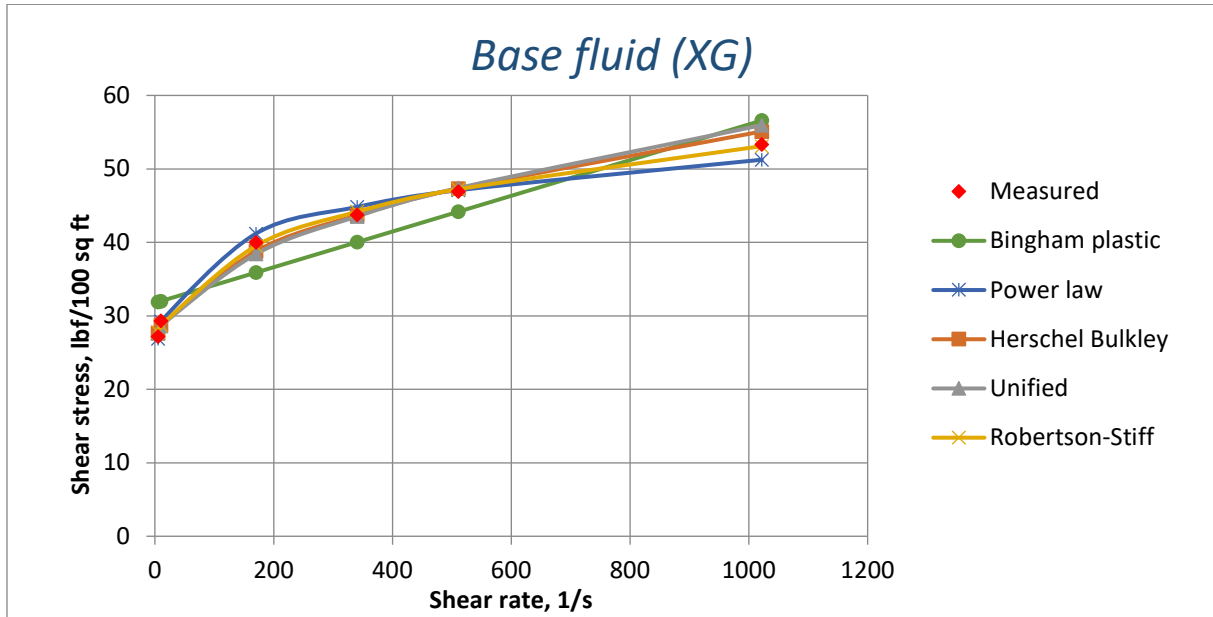


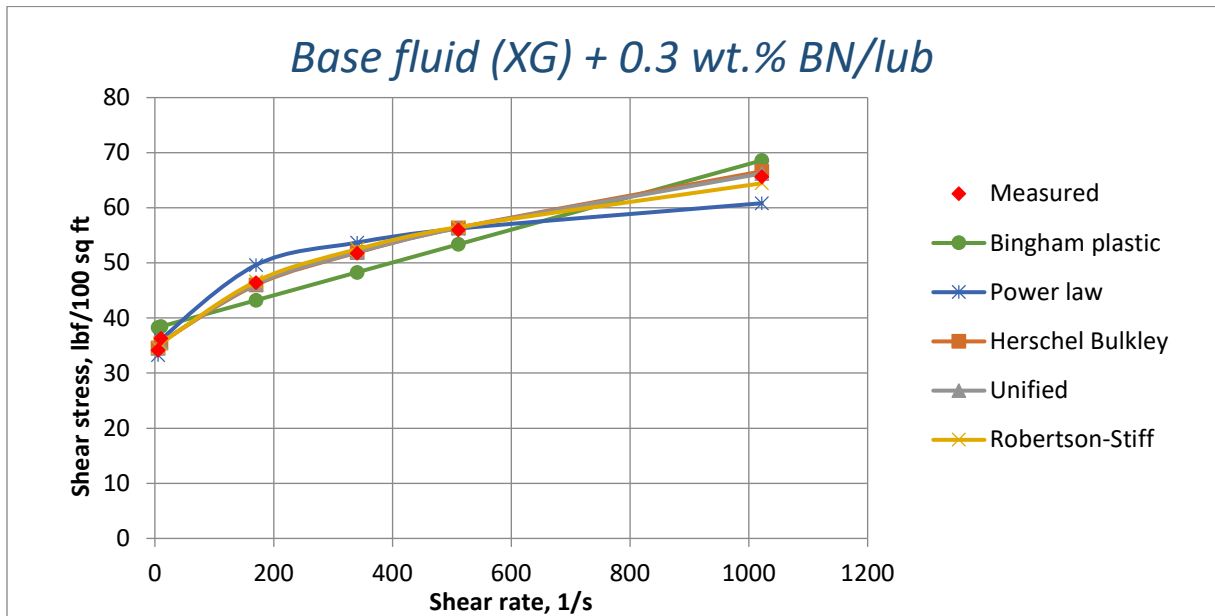
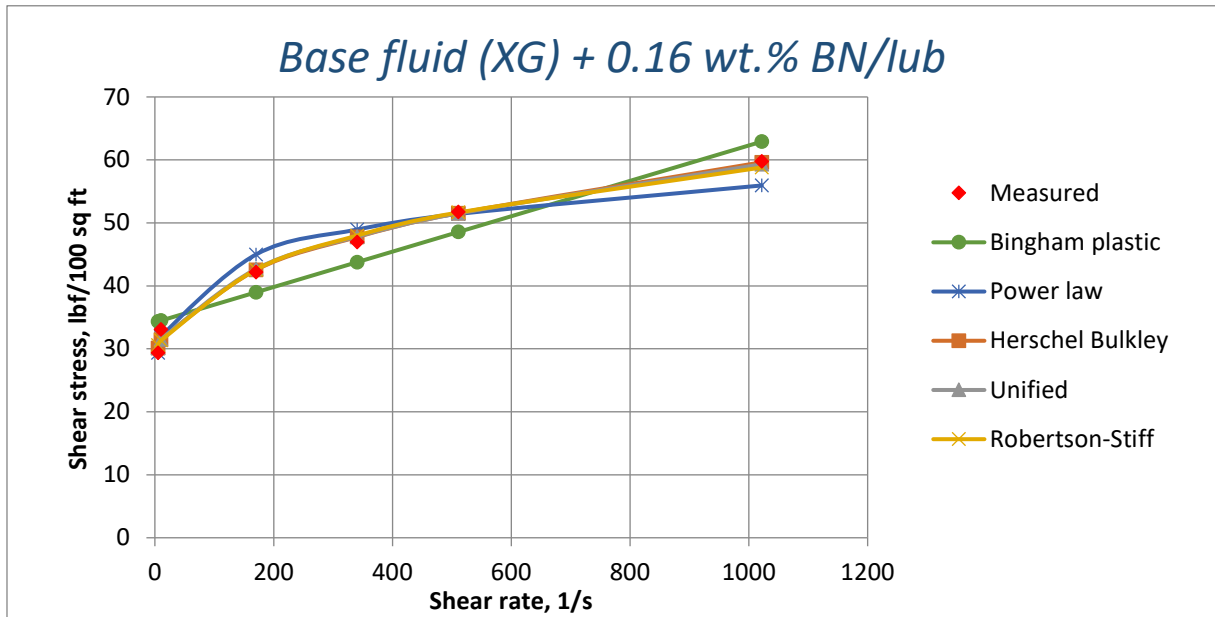
APPENDIX D: Rheological modelling.

Viscometer data along with modelled trend-lines.









APPENDIX E: Setup for Torque and Drag simulations.

Hole Data

Hole Section Editor									
Hole Name:		Hole Section		Import Hole Section					
Hole Section Depth (MD):		11000.0 ft		Additional Columns					
	Section Type	Measured Depth (ft)	Length (ft)	ID (in)	Drift (in)	Effective Hole Diameter (in)	Friction Factor	Linear Capacity (bbl/ft)	Item Description
1	Casing	4012.5	4012.50	12.615	12.459	12.615		0,1547	13 3/8 in, 54.5 ppf, J-55,
2	Open Hole		6987.50	12.615		12.615		0,1546	
3									

Friction factor is according to the fluid. Length of the open hole is adjusted according to the critical loads.

Drill String Data

String Initialization							Library	
String Name:		Assembly					Export	
String (MD):				Specify: Top to Bottom		Import String		
Import								
	Section Type	Length (ft)	Measured Depth (ft)	OD (in)	ID (in)	Weight (ppf)	Item Description	
1	Drill Pipe			5.000	4.000	28.26	Drill Pipe 5 in, 25.60 ppf, E, 5 1/2 FH, P	
2	Heavy Weight	120.00	10561.0	6.625	4.500	70.50	Heavy Weight Drill Pipe Grant Prideco, 6 5/8 in, 70.50 ppf	
3	Jar	33.00	10594.0	6.500	2.750	91.79	Hydraulic Jar Dailey Hyd., 6 1/2 in	
4	Heavy Weight	305.00	10899.0	5.000	3.000	49.70	Heavy Weight Drill Pipe Grant Prideco, 5 in, 49.70 ppf	
5	Sub	5.00	10904.0	6.000	2.400	79.51	Bit Sub 6, 6 x2 1/2 in	
6	MWD	85.00	10989.0	8.000	2.500	154.36	MWD Tool 8, 8 x2 1/2 in	
7	Stabilizer	5.00	10994.0	6.250	2.000	93.72	Integral Blade Stabilizer 8 1/2" FG, 6 1/4 x2 in	
8	Sub	5.00	10999.0	6.000	2.400	79.51	Bit Sub 6, 6 x2 1/2 in	
9	Bit	1.00	11000.0	10.625		166.00	Tin-Cone Bit, 0.589 in ²	

Drill string length is adjusted according to the well length

Well Path Parameters

